Radio Resource Management for Relay-Aided Device-to-Device Communication

by

Monowar Hasan

A Thesis submitted to The Faculty of Graduate Studies of

The University of Manitoba

in partial fulfillment of the requirements for the degree of

Master of Science

Department of Electrical and Computer Engineering

University of Manitoba

Winnipeg

May 2015

Quality is never an accident; it is always the result of high intention, sincere effort, intelligent direction and skillful execution; it represents the wise choice of many alternatives.

WILLIAM A. FOSTER

Abstract

In this thesis, performance of relay-assisted Device-to-device (D2D) communication is investigated where D2D traffic is carried through relay nodes. I develop resource management schemes to maximize end-to-end rate as well as conversing rate requirements for cellular and D2D UEs under total power constraint. I also develop a low-complexity distributed solution using the concept of message passing. Considering the uncertainties in wireless links (e.g., when interference from other relay nodes and the link gains are not exactly known), I extend the formulation using robust resource allocation techniques. In addition, a distributed solution approach using stable matching is developed to allocate radio resources in an efficient and computationally inexpensive way under the bounded channel uncertainties. Numerical results show that, there is a distance threshold beyond which relay-assisted D2D communication significantly improves network performance at the cost of small increase in end-to-end delay when compared to conventional approach.

Acknowledgements

At first I would like to acknowledge the blessings and guidance of Almighty "ALLAH". Throughout journey of pursuing M.Sc. degree, I have received tremendous support from a lot of people, which helps me to complete the thesis successfully.

I would like to sincerely thank my thesis supervisor, Prof. Ekram Hossain, for his invaluable guidance and support. His knowledge, integrity, dedication, diligence, and enthusiasm for research have always been an inspiration to me. I feel very fortunate to have Prof. Hossain as my supervisor, and would like to thank for giving me all the opportunities and freedoms to explore my favorite research topics. His flexibility, foresightedness, and encouragement have driven me far beyond my expectations. Prof. Hossain is an outstanding mentor, I really appreciate his precious advice which are motivational for me in various academic, professional, and personal aspects.

I appreciate the valuable advice from my thesis committee members, Prof. Pradeepa Yahampath, and Prof. Yang Wang. It was such a wonderful experience to collaborate with Prof. Dong Kim, Prof. Dusit Niyato, Prof. Long Li, Prof. Mehdi Rasti, and Prof. Sasitharan Balasubramaniam. Their selfless advice and feedback have significantly enhanced the quality of my research.

The current and past members of the *Wireless Communications, Networks, and Services Research Group* have contributed immensely to both my personal and professional experience at the University of Manitoba. I would like to thank all the colleagues in the our research group, for precious friendships that have supported me throughout the past few years. Special thanks to Dr. Hesham Elsawy – for his influencing guidelines not only in academic matters but also other aspects of life; Amr Adel – without his suggestions and programming codes on optimization models, I would not be able to complete this work; Madushan Thilina and Monjurul Islam Khan – for

being so supportive and being very good friend of mine; and Prabodini Semasinghe – for consistently tolerating and answering all my silly and annoying questions when we were working on 5G projects. It is worth mentioning that Prabodini's concept of 'transmission alignment' significantly helps me to contribute on several research projects.

I acknowledge the financial support from Prof. Hossain and Faculty of Graduate Studies, University of Manitoba. I would also like to thank Amy Dario for her kind assistance in each and every academic and administrative problem.

A very special and warm thank to my gorgeous wife Syeda Sumaiya for her patience and tolerance to the hurdles that a graduate student could bring. Without her unconditional love, support, and consideration, I would be a dropout in my first year of studies.

Lastly, I would like to thank my parents, my grandparents, my sister, and in-laws for their compassion, love, encouragement, and assistance. Thank you – without you people we are incomplete!

To my awesome grandmother,

without her I would not be here.

Table of Contents

List of Figures

List of Tables

List of Abbreviations

3GPP	3rd generation partnership project
Cellular user equipment	CUE
CSI	Channel state information
CQI	Channel quality indicator
eNB	Evolved node B
D2D	Device-to-device
L3	Layer 3
LTE-A	Long term evolution-advanced
M2M	Machine-to-machine
MAC	Medium access control
MP	Message passing
P2P	Peer-to-peer
QoS	Quality-of-service
RAP	Resource allocation problem
RB	Resource block
OFDMA	Orthogonal frequency division multiple access
SINR	Signal to interference plus noise ratio
UE	User equipment

List of Symbols

Notation	Physical interpretation	Usage
$\mathcal{N} = \{1, 2, \ldots, N\}$	Set of available RBs	Chapter 2, 3, 4, 5
$\mathcal{L} = \{1, 2, \ldots, L\}$	Set of relays	Chapter 2, 3, 4, 5
u_l	A UE served by relay l	Chapter 2, 3, 4, 5
$\mathcal{U}_l, \lvert\mathcal{U}_l\rvert$	Set of UEs and total number of UEs served by relay l, respectively	Chapter 2, 3, 4, 5
$h_{i,j,k}^{(n)}$	Direct link gain between the node i and j in hop $k \in \{1, 2\}$ over RB n	Chapter 2, 3, 4, 5
$\gamma_{u_l,l,1}^{(n)}, \gamma_{l,u_l,2}^{(n)}$	SINR for UE u_l over RB n is first and second hop, respectively	Chapter 2, 3, 4, 5
$R_{u_l}^{(n)}$	End-to-end data rate for u_l over RB n	Chapter 2, 3, 4, 5
Q_{u_l}	Data rate requirement for u_l	Chapter 2, 3, 4, 5
$x_{u_l}^{(n)}, S_{u_l,l}^{(n)}$	RB allocation indicator and actual transmit power for u_l over RB n, respectively	Chapter 2, 3, 4, 5
$\mathbf{x_l}, \mathbf{P_l}$	RB and power allocation vector	Chapter 2, 3, 4, 5
$\mathfrak{R}_{n,l}(\cdot), \mathfrak{W}_{u_l,l}(\cdot)$	Utility functions in factor graph dealing with optimization constraints	Chapter 3
$\delta_{\mathfrak{R}_{n,l}(\cdot)\to x_{u_l}^{(n)}}\left(x_{u_l}^{(n)}\right)$	Message from function node $\mathfrak{R}_{n,l}(\cdot)$ to variable node $x_{u_l}^{(n)}$	Chapter 3
$\delta_{\mathfrak{W}_{u_l,l}(\cdot)\to x_{u_l}^{(n)}}\left(x_{u_l}^{(n)}\right)$	Message from $\mathfrak{W}_{u_l,l}(\cdot)$ function node to any variable node $x_{u_l}^{(n)}$	Chapter 3
$\phi_{u_l}^{(n)}\left(x_{u_l}^{(n)}\right)$	Marginal at variable node $x_{u_l}^{(n)}$ in factor graph	Chapter 3

Notation	Physical interpretation	Usage
$\psi^{(n)}_{u_l,l}, \tilde{\psi}^{(n)}_{u_l,l}$	Normalize messages for UE u_l over RB n	Chapter 3
$\langle \upsilon^{(j)}_{u_l} \rangle_{z \setminus n}$	z-th sorted element of $\boldsymbol{\chi}_{\boldsymbol{u_l}}$ without considering the term $R^{(n)}_{u_l} + \tilde{\psi}^{(n)}_{u_l,l}$	Chapter 3
$\tau^{(n)}_{u_l,l}$	Node marginal for UE u_l over RB n	Chapter 3
κ_{u_l}	Required number RB(s) for u_l to satisfy the rate requirement Q_{u_l}	Chapter 3, 5
$\mathbf{abs}\{y\}$	Absolute value of variable y	Chapter 3
$\mathfrak{D}_{\text{2hop}}$	End-to-end delay for two hop relay-aided communication	Chapter 3
$I^{(n)}_{u_l,l}$	Aggregated interference experienced by u_l over RB n	Chapter 4
$\mathbf{g}^{(n)}_{l,i}$	Nominal link gain vector over RB n in hop i	Chapter 4
$\bar{\mathbf{g}}^{(n)}_{l,i}$, $\hat{\mathbf{g}}^{(n)}_{l,i}$	Estimated and uncertain (i.e., the bounded error) link gain vector, respectively, over RB n in hop i	Chapter 4
$\Re^{(n)}_{g_{l,i}}, \Delta^{(n)}_{g_{l,i}}$	Uncertainty set and protection function, respectively, for link gain over RB n in hop i	Chapter 4
$\Re^{(n)}_{I_{u_l,l}}, \Delta^{(n)}_{I_{u_l,l}}$	Uncertainty set and protection function of interference level, respectively, for u_l over RB n	Chapter 4
$\Psi^{(n)}_{l,i}$	Bound of uncertainty in link gain for hop i over RB n	Chapter 4
$\Upsilon^{(n)}_{u_l}$	Bound of uncertainty in interference level for u_l over RB n	Chapter 4
$\| \mathbf{y} \|_{\alpha}$	Linear norm of vector $\mathbf{y}$ with order α	Chapter 4
$\| \mathbf{y} \|^{*}$	Dual norm of $\| \mathbf{y} \|$	Chapter 4
$\mathbf{abs}\{y\}$	Absolute value of y	Chapter 4
$\mathbf{A}(j,:)$	j-th row of matrix $\mathbf{A}$	Chapter 4
$\Lambda^{(t)}_{\kappa}$	Step size for variable κ at iteration t	Chapter 4

Notation	**Physical interpretation**	**Usage**
$\mathcal{R}_{\Delta}$	Reduction of achievable sum-rate due to uncertainty	Chapter 4
$\Theta_{l,i}^{(n)}$	Threshold probability of violating interference constraint for RB n in hop i	Chapter 4
$\mathcal{S}_{\Theta_{l,i}^{(n)}}(\mathcal{R}_{\Delta})$	Sensitivity of $\mathcal{R}_{\Delta}$ in hop i over RB n	Chapter 4
$\bar{y}$, Δy	Nominal value and corresponding deviation in link gain parameter y	Chapter 5
$\xi_{3_{u_l}}^{(n)}, \xi_{2l}, \xi_{3_{u_l}}^{(n)}, \xi_{4_{u_l}}^{(n)}$	Uncertainty bounds in wireless links for UE u_l over RB n associated to relay l	Chapter 5
$\mathfrak{U}_l$	Utility matrix for the UEs over different RBs associated to relay l	Chapter 5
$\boldsymbol{\mathcal{P}}_{u_l}(\mathcal{N})$	Preference profile of a UE $u_l \in \mathcal{U}_l$ over the set of available RBs $\mathcal{N}$	Chapter 5
$\boldsymbol{\mathcal{P}}_n(\mathcal{U}_l)$	Preference profile of an RB n over set of UEs $\mathcal{U}_l$	Chapter 5
μ_l	The outcome (allocation) of matching at relay node l	Chapter 5
$\lvert y \rvert$	absolute value of variable y	Chapter 5
$\overline{\overline{\mathbf{y}}}$	Cardinality (length) of the set (vector) $\mathbf{y}$	Chapter 5

Chapter 1

Introduction

1.1 Overview and Motivation

Device-to-device (D2D) communication in cellular networks allows direct transmission between two cellular devices with local communication needs. In recent years, new applications such as content distribution and location-aware advertisement underlaying cellular networks have drawn much attention to end-users and network providers. The emergence of such new applications brings D2D communication under intensive discussions in academia, industry, and standardization bodies. The concept of D2D communication has been introduced to allow local peer-to-peer (P2P) transmission among user equipments (UEs) bypassing the base station (e.g., eNB in a Long Term Evolution Advanced [LTE-A] network) to cope with high data rate services (i.e., video sharing, online gaming, proximity-aware social networking). D2D communication was first proposed in [1] to enable multi-hop relaying in cellular networks. In addition to traditional local voice and data services, other potential D2D use-cases have been introduced in the literature such as P2P communication, local advertisement, multi-player gaming, data flooding [2–4], multicasting [5], [6], video dissemination [7–9],

and machine-to-machine (M2M) communication [10].

Using local data transmissions, D2D communication offers the following advantages: *i*) extended coverage [1]; *ii*) offloading users from cellular networks [11]; *iii*) increased throughput and spectrum efficiency as well as improved energy efficiency [12].

However, in a D2D-enabled network, a number of practical considerations may limit the advantages of D2D communication. In practice, setting up reliable direct links between the D2D UEs while satisfying the quality-of-service (QoS) requirements of both the traditional cellular UEs (CUEs) as well as the D2D UEs is challenging due to the following reasons:

i) *Large distance:* the potential D2D UEs may not be in near proximity;

ii) *Poor propagation condition:* the link quality between potential D2D UEs may not be favorable for direct communication;

iii) *Interference to and from CUEs:* in an underlay system, without an efficient power control mechanism, the D2D transmitters may cause severe interference to other receiving nodes. The D2D receivers may also experience interference from CUEs and/or eNB. One remedy to this problem is to partition the available spectrum (i.e., use overlay D2D communication). However, this can significantly reduce the spectrum utilization [13, 14].

In such cases, network-assisted transmissions through *relays* could efficiently enhance the performance of D2D communication when the D2D UEs are too far away from each other or the quality of the channel between the UEs is not good enough for direct communication.

Unlike most of the existing work on D2D communication, in this work, I consider relay-assisted D2D communication in LTE-A cellular networks where D2D pairs are

served by the relay nodes. In particular, I consider LTE-A Layer-3 (L3) relays[1]. I concentrate on scenarios in which the proximity and link condition between the potential D2D UEs may not be favorable for direct communication. Therefore, they may communicate via relays. The radio resources at the relays (e.g., resource blocks [RBs] and transmission power) are shared among the D2D communication links and the two-hop cellular links using these relays.

An use-case for such relay-aided D2D communication could be the M2M communication for smart cities. In such a communication scenario, automated sensors (i.e., UEs) are deployed within a macro-cell ranging a few city blocks; however, the link condition and/or proximity between devices may not be favorable. Due to the nature of applications, these UEs are required to periodically transmit data [16]. Relay-aided D2D communication could be an elegant solution to provide reliable transmission as well as improve overall network throughput in such a scenario.

1.2 Related Works and Contributions

Although resource allocation for D2D communication in orthogonal frequency-division multiple access (OFDMA)-based wireless networks is one of the active areas of research, only a very few work in the literature consider relays for D2D communication. In [17], a greedy heuristic-based resource allocation scheme is proposed for both uplink and downlink scenarios where a D2D pair shares the same resources with CUE only if the achieved signal-to-interference-plus-noise ratio (SINR) is greater than a given SINR requirement. A new spectrum sharing protocol for D2D communication overlaying a cellular network is proposed in [18], which allows the D2D users to com-

[1] An L3 relay performs the same operation as an eNB except that it has a lower transmit power and a smaller cell size. The relay transmits its own control signals and the UEs are able to receive scheduling information directly from the relay node [15]. The details of relaying mechanism in LTE-A systems is given in Section 2.1.2.

municate bi-directionally while assisting the two-way communications between the eNB and the CUE. In [14], the problem of mode selection and resource allocation for D2D communication underlaying cellular networks is investigated and the solution is obtained by particle swarm optimization. Through simulations, the authors show that the proposed scheme improves system performance compared to overlay D2D communication. In [6], D2D communication is proposed to improve the performance of multicast transmission among the members of a multicast group. A graph-based resource allocation method for cellular networks with underlay D2D communication is proposed in [19]. Due to the intractability of resource allocation problem, the authors propose a sub-optimal graph-based approach which accounts for interference and capacity of the network. A resource allocation scheme based on a column generation method is proposed in [13] to maximize the spectrum utilization by finding the minimum transmission length (i.e., time slots) for D2D links while protecting the cellular users from interference and guaranteeing QoS. A two-phase resource allocation scheme for cellular network with underlaying D2D communication is proposed in [20]. Due to NP-hardness of the optimal allocation problem, the author proposes a two-phase low-complexity sub-optimal solution where after performing optimal resource allocation for cellular users, a heuristic subchannel allocation scheme for D2D flows is applied which initiates the resource allocation from the flow with the minimum rate requirements. The above works, however, do not consider relays for D2D communication.

Although D2D communication was initially proposed to relay user traffic [1], not many work consider using relays in the context of D2D communication. To the best of my knowledge, relay-assisted D2D communication was first introduced in [21] where the relay selection problem for D2D communication underlaying cellular network was

studied. The authors propose a distributed relay selection method for relay assisted D2D communication system which firstly coordinates the interference caused by the coexistence of D2D system and cellular network and eliminates improper relays correspondingly. Afterwards, the best relay is chosen among the optional relays using a distributed method. In [22], the authors consider D2D communication for relaying UE traffic toward the eNB and deduce a relay selection rule based on the interference constraints. In [9], the authors propose an incremental relay mode for D2D communication where D2D transmitters multicast to both the D2D receiver and base station. In case the D2D transmission fails, the base station retransmits the multicast message to the D2D receiver. Although the base station receives a copy of the D2D message which is retransmitted in case of failure, this incremental relay mode of communication consumes part of the downlink resources for retransmission and reduces spectrum utilization. In [23, 24], the maximum ergodic capacity and outage probability of cooperative relaying is investigated in relay-assisted D2D communication considering power constraints at the eNB. The numerical results show that multi-hop relaying lowers the outage probability and improves cell edge capacity by reducing the effect of interference from the CUE.

It is worth noting that in [6,9,13,14,17–20,25,26], the effect of using relays in D2D communication is not studied. As a matter of fact, relaying mechanism explicitly in context of D2D communication has not been considered so far in the literature and most of the resource allocation schemes consider only one D2D link. Taking the advantage of L3 relays supported by the 3rd generation partnership project (3GPP) standard, in Chapter 2 I study the network performance of network-integrated D2D communication and show that relay-assisted D2D communication provides significant performance gain for long distance D2D links. However, the proposed solution in

Chapter 2 is obtained in a centralized manner by a central controller (i.e., L3 relay); which could be a bottleneck for a dense network with large number of UEs. To address this issue, in Chapter 3, I develop a *distributed solution* technique utilizing the *message passing* strategy on a factor graph. Factor graph and other graphical models have been used as powerful solution techniques to tackle a wide range of problems in various domains; however, they have not been commonly used in the context of resource allocation in cellular wireless networks. According to this message passing approach each UE sends and receives information messages to/from the relay node in an iterative manner with the goal of achieving an optimal allocation. Therefore, the computational effort is distributed among all the UEs and the corresponding relay node.

In all of the above cited work, it has generally been assumed that complete system information (e.g., channel state information [CSI]) is available to the network nodes, which is unrealistic for a practical system. To address this issue, in Chapter 4 I extend the work presented in Chapter 2 and Chapter 3 utilizing the theory of *worst-case robust optimization*. According to this approach, the interference link gain between UE and other relays (to which the UE is not associated) is modeled with ellipsoidal uncertainty sets.

One shortcoming of the approach presented in Chapter 4 is that the uncertainties in direct channel gain between relay (eNB) and the UE (relay) are not considered. To resolve this issue and to make the model more practical, in Chapter 5 I present a distributed resource allocation algorithm using *stable matching* considering the uncertainties in all the wireless channel gains. Matching theory, a sub-field of Economics, is a promising concept for distributed resource management in wireless networks. The matching theory allows low-complexity algorithmic manipulations to

provide a decentralized self-organizing solution to the resource allocation problems. In matching-based resource allocation, each of the agents (e.g., radio resources and UEs) ranks the opposite set using a preference relation. The solution of the matching is able to assign the resources with the UEs depending on the preferences.

A summary of the related work and comparison with my proposed approaches is presented in Table 1.1.

1.3 Scholastic Outputs and Achievements

This thesis includes some material previously published/submitted in peer-reviewed journals and conferences as summarized in Table 1.2. This work would not have been possible without the contribution of all co-authors of the above referenced publications. The copyright as well as all rights of those works (and therefore the parts of the thesis) are retained by the authors and/or by other copyright holders.

1.4 Organization of the Thesis

As can be seen from Fig. 1.1, I organize the major contents of the thesis into four chapters. The brief organization of the thesis is given below.

- In Chapter 2, I present the system model and the framework of the relay-aided communication scheme. To this end, an optimization-based radio resource allocation algorithm is proposed.

- Considering the computational complexity at the relay nodes, in Chapter 3 I propose a reduced complexity distributed solution using the concept of message passing. The convergence and optimality of the proposed distributed solution is analyzed.

Table 1.1: Summary of Related Work and Comparison with Proposed Schemes

Reference	Problem focus	Relay aided	Channel information	Solution approach	Solution type	Optimality
[17]	Resource allocation	No	Perfect	Proposed greedy heuristic	Centralized	Suboptimal
[18]	Resource allocation	No*	Perfect	Numerical optimization	Semi-distributed	Pareto optimal
[14]	Resource allocation, mode selection	No	Perfect	Particle swarm optimization	Centralized	Suboptimal
[6]	Theoretical analysis, spectrum utilization	No	Perfect	Iterative cluster partitioning	Centralized	Optimal
[19]	Resource allocation	No	Perfect	Interference graph coloring	Centralized	Suboptimal
[13]	Resource allocation	No	Perfect	Column generation based greedy heuristic	Centralized	Suboptimal
[20]	Resource allocation	No	Perfect	Two-phase heuristic	Centralized	Suboptimal
[21]	Resource allocation, mode selection	Yes	Perfect	Proposed heuristic	Distributed	Suboptimal
[22]	Performance evaluation, relay selection	Yes*	Perfect	KM algorithm and greedy heuristic	Centralized	N/A‡
[9]	Resource allocation	No	Perfect	Proposed heuristic	Centralized	Suboptimal
[23]	Theoretical analysis, performance evaluation	Yes	Perfect	Statistical analysis	Centralized	Optimal
[24]	Performance evaluation	Yes	Perfect	Heuristic, simulation	Centralized	N/A‡
Proposed schemes:						
Chapter 2	Resource allocation	Yes	Perfect	Numerical optimization	Semi-distributed	Asymptotically optimal
Chapter 3	Resource allocation	Yes	Perfect	Max-sum message passing	Distributed	Asymptotically optimal
Chapter 4	Resource allocation	Yes	Uncertain#	Robust optimization, gradient-based method	Distributed	Suboptimal
Chapter 5	Resource allocation	Yes	Uncertain	Matching theory (many-to-one matching)	Distributed	Weak Pareto optimal

*D2D UEs serve as relays to assist CUE-eNB communications.

‡No information is available.

#Uncertainty in direct link between UEs (relays) and relays (eNB) is not considered.

†Not applicable for the considered system model.

Table 1.2: Summary of Scholastic Outputs

	Publications*	**Appearance**
4.	**M. Hasan** and E. Hossain, "Distributed resource allocation for relay-aided device-to-device communication under channel uncertainties: A stable matching approach," submitted to the *IEEE Transactions on Communications* (under second round of revision).	Chapter 5
3.	**M. Hasan** and E. Hossain, "Distributed resource allocation for relay-aided device-to-device communication: A message passing approach," *IEEE Transactions on Wireless Communications*, vol. 13, no. 11, pp. 6326-6341, Nov. 2014.	Chapter 3
2.	**M. Hasan**, E. Hossain, and D. I. Kim, "Resource allocation under channel uncertainties for relay-aided device-to-device communications underlaying LTE-A cellular networks," *IEEE Transactions on Wireless Communications*, vol. 13, no. 4, pp. 2322-2338, Apr. 2014.	Chapter 4
1.	**M. Hasan** and E. Hossain, "Resource allocation for network-integrated device-to-device communications using smart relays," in Proc. of *IEEE Globecom Workshops (GC Wkshps)*, pp. 597-602, Dec. 2013.	Chapter 2

*According to reverse order of submission.

- Since in practical wireless systems the link gains are uncertain (e.g., imperfectly known), in Chapter 4 I reformulate the problem considering uncertainties in the interference links and propose a gradient-based solution. The robustness-optimality trade-off is discussed both analytically and numerically.

- Despite the fact the model presented in Chapter 4 captures the uncertainty in interference links, the direct link between the users and serving nodes (such as relay and eNB) assumes to be perfectly known. Hence, in Chapter 5, I extend the previous formulation considering uncertainties in both the direct and interference link gain. I use the theory of stable matching and proposed a distributed solution. The analytical properties (e.g., stability, optimality,

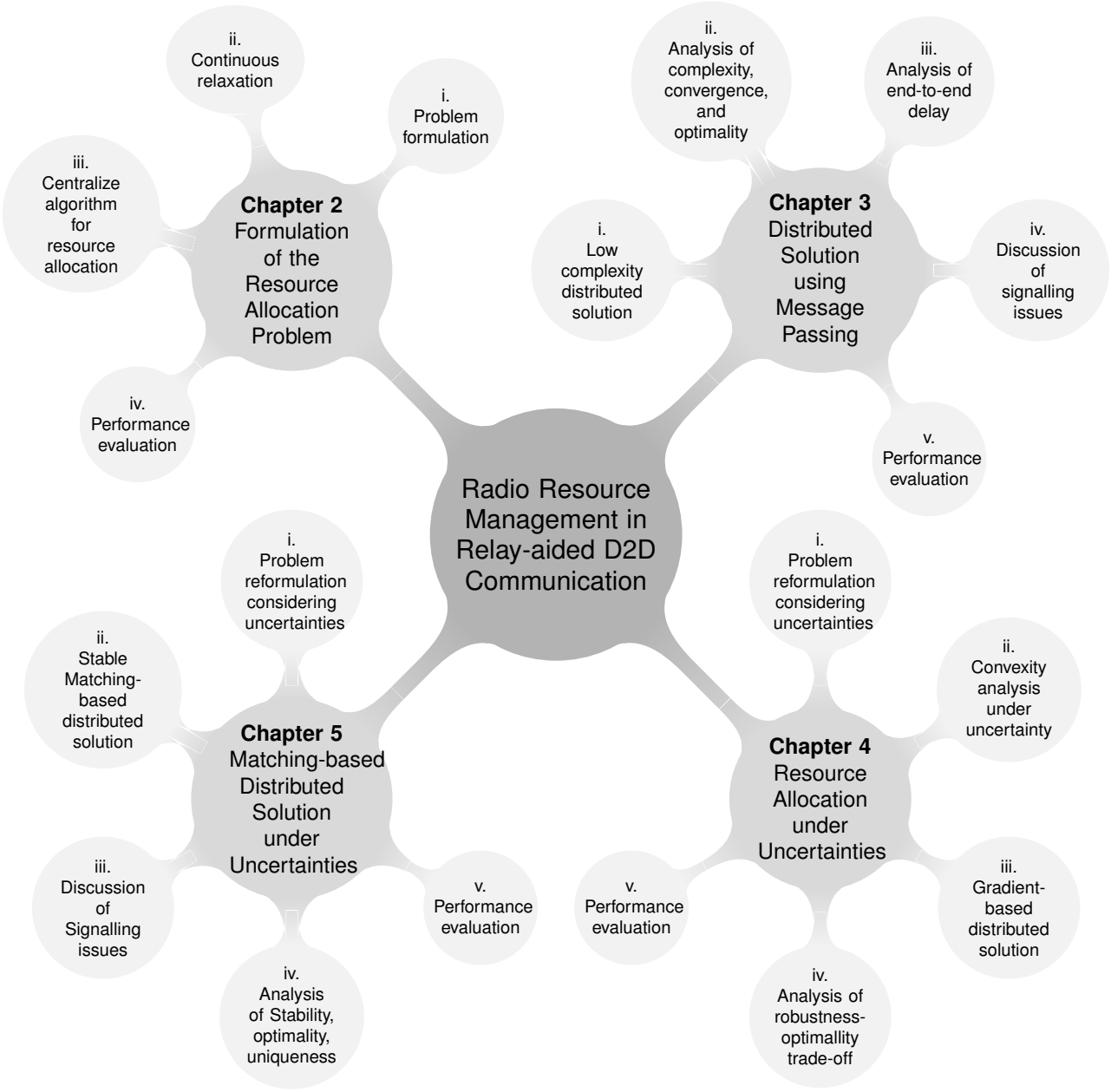

Figure 1.1: Organization of the thesis.

convergence etc.) are also discussed.

- I conclude the thesis in Chapter 6 highlighting the directions for future research.

Chapter 2

A Resource Allocation Framework for Relay-Aided D2D Communication

With increasing number of autonomous heterogeneous devices in future mobile networks, an efficient resource allocation scheme is required to maximize network throughput and achieve higher spectral efficiency. The goal of this work is to develop a resource allocation framework for relay-aided D2D communication. This framework will be used at the relays (specifically, at the L3 relays) for allocation of RBs and transmission power for cellular users as well as the D2D users served by the relays. The motivation of using relay-assisted D2D communication stems from the fact that relaying of D2D traffic may improve network performance when the D2D users are far apart. In my considered model, the presence of heterogeneous users (e.g., cellular and D2D) and multiple relays in the two-hop system with different destinations (e.g., eNB is the destination for cellular transmitters and D2D receivers are the destinations for D2D transmitters), and the combinatorial nature of the resource allocation problem

in multi-channel OFDMA systems make the formulation/analysis more challenging. The main contributions of this chapter can be summarized as follows:

- I model and analyze the performance of relay-assisted D2D communication in a multi-channel OFDMA-based cellular (e.g., LTE-A) network. The problem of RB and power allocation at the relay nodes for the CUEs and D2D UEs is formulated.
- As opposed to most of the resource allocation schemes in the literature where only a single D2D link is considered, I consider multiple D2D links along with multiple cellular links that are supported by the relay nodes.
- I compare the performance of my proposed method with an underlay D2D communication scheme where the D2D UEs communicate directly without the assistance of relays. The numerical results show that after a distance threshold for the D2D UEs, relaying D2D traffic provides significant gain in achievable data rate.

I organize the rest of the chapter as follows. Section 2.1 introduces LTE-A access methods and the relaying mechanisms. In Section 2.2, I present the system model and formulate the resource allocation problem (RAP). The permanence evaluation results are presented in Section 2.4 and I conclude the chapter in Section 2.5 outlining possible extensions.

2.1 Radio Access and Relaying in 3GPP LTE-A

2.1.1 Radio Access Methods in LTE-A Networks

In the LTE-A radio interface, two consecutive time slots create a subframe where each time slot spans 0.5 msec. Resources are allocated to UEs[1] in units of RBs over a subframe. Each RB occupies 1 slot (0.5 msec) in time domain and 180 KHz in frequency domain with subcarrier spacing of 15 KHz. The multiple access scheme for downlink (i.e., eNB/relay-to-UE) is OFDMA while the access scheme for uplink (i.e., UE-to-relay/eNB, relay-to-UE) is single carrier-FDMA (SC-FDMA). In general, SC-FDMA requires contiguous set of subcarrier allocation to UEs. Resource allocation in downlink supports both block-wise transmission *(localized allocation)* and transmission on non-consecutive subcarriers *(distributed allocation)*. For uplink transmission, current specification supports only localized resource allocation [27].

2.1.2 Relays in LTE-A Networks

Relay node in LTE-A is wirelessly connected to radio access network through a donor eNB and serves UEs. Depending on the function, different relaying mechanisms used in LTE-A [15]. *Layer 1* (L1) relays act as repeaters, amplifying the input signal without and decoding/re-encoding. The L1 relays can either use the same carrier frequency (i.e., in-band relaying) or an orthogonal carrier frequency (i.e., out-of-band relaying). The main advantages of L1 relays are simplicity, cost-effectiveness, and low delay. However, with L1 relaying, noise and interference are also amplified and retransmitted. Hence, the SINR of the signal may deteriorate.

Layer 2 (L2) relays are also known as decode and forward (DF) relay which in-

[1]By the term "UE", I refer to both cellular and D2D user equipments.

volves decoding the source signal at the relay node. The advantage of DF relays is that noise and interference do not propagate to the destination. However, a substantial delay occurs during the relaying operation. A L2 relay does not issue any scheduling information or any control signal (i.e., HARQ and channel feedback). Hence, an L2 relay cannot generate a complete cell and from a UE's perspective, it is only a part of donor cell.

Layer 3 (L3) relays with self-backhauling configuration performs the same operation as eNB except for lower transmit power and smaller cell size. It controls cell(s) and each cell has its own cell identity. The relay shall transmit its own control signals and UE shall receive scheduling information and HARQ feedback directly from the relay node.

When the link condition between D2D peers is poor or the distance is too far for direct communication, with the support of L3 relays, scheduling and resource allocation for D2D UE can be done in relay node and D2D traffic can be transmitted through relay. I refer to this scheme as *relay-aided D2D communication* which can be an alternative approach to provide higher data rate between distant D2D-links. In the next section, I describe the network configuration and present the formulation for resource allocation.

2.2 System Model

2.2.1 Network Model

Let $\mathcal{L} = \{1, 2, \ldots, L\}$ denote the set of fixed-location L3 relays in the network as shown in Fig. 2.1. The system bandwidth is divided into N orthogonal RBs denoted by $\mathcal{N} = \{1, 2, \ldots, N\}$ which are used by all the relays in a spectrum underlay

fashion. The set of CUEs and D2D pairs are denoted by $\mathcal{C} = \{1, 2, \ldots, C\}$ and $\mathcal{D} = \{1, 2, \ldots, D\}$, respectively. I assume that association of the UEs (both cellular and D2D) to the corresponding relays are performed before resource allocation. Prior to resource allocation, D2D pairs are also discovered and the D2D session is setup by transmitting known synchronization or reference signals [28].

I assume that the CUEs are outside the coverage region of the eNB and/or having bad channel condition, and therefore, the CUE-eNB communications need to be supported by the relays. Besides, direct communication between two D2D UEs requires the assistance of a relay node due to poor propagation condition. The UEs assisted by relay l are denoted by u_l. The set of UEs assisted by relay l is $\mathcal{U}_l = \{1, 2, \ldots, U_l\}$ such that $\mathcal{U}_l \subseteq \{\mathcal{C} \cup \mathcal{D}\}, \forall l \in \mathcal{L}$, $\bigcup_l \mathcal{U}_l = \{\mathcal{C} \cup \mathcal{D}\}$, and $\bigcap_l \mathcal{U}_l = \varnothing$.

In the second hop, there could be multiple relays transmitting to their associated D2D UEs. I assume that multiple relays transmit to the eNB (in order to forward CUEs' traffic) using orthogonal channels and this scheduling of relays is done by the eNB[2]. Note that, in the first hop, the transmission between a UE (i.e., either a CUE or a D2D UE) and a relay can be considered as an uplink transmission. In the second hop, the transmission between a relay and the eNB can be considered as an uplink transmission from the perspective of the eNB whereas the transmission from a relay to a D2D UE can be considered as a downlink transmission. In my system model, taking advantage of the capabilities of L3 relays, scheduling and resource allocation for the UEs is performed in the relay nodes to reduce the computational load at the eNB.

[2]Scheduling of relay nodes by the eNB is out of the scope of this work.

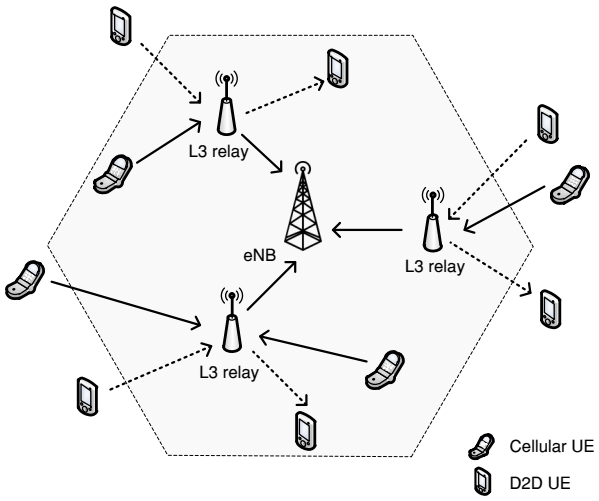

Figure 2.1: A schematic diagram of a single cell system with multiple relay nodes. I assume that the CUE-eNB links are unfavorable for direct communication and they need the assistance of relays. The D2D UEs are also supported by the relay nodes due to long distance and/or poor link condition between peers.

2.2.2 Achievable Data Rate

Let $\gamma^{(n)}_{u_l,l,1}$ denote the unit power SINR for the link between UE $u_l \in \mathcal{U}_l$ and relay l using RB n in the first hop and $\gamma^{(n)}_{l,u_l,2}$ be the unit power SINR for the second hop. Note that, in the second hop, when the relays transmit CUEs' traffic (i.e., $u_l \in \{\mathcal{C} \cap \mathcal{U}_l\}$), $\gamma^{(n)}_{l,u_l,2}$ denotes the unit power SINR for the link between relay l and the eNB. On the other hand, when a relay transmits to a D2D UE (i.e., $u_l \in \{\mathcal{D} \cap \mathcal{U}_l\}$), $\gamma^{(n)}_{l,u_l,2}$ refers to the unit power SINR for the link between relay l and the receiving D2D UE for the D2D-pair.

Let $P^{(n)}_{i,j} \geq 0$ denote the transmit power in the link between i and j over RB n and B_{RB} is the bandwidth of an RB. The achievable data rate[3] for u_l in the first hop can be expressed as $r^{(n)}_{u_l,1} = B_{RB} \log_2 \left(1 + P^{(n)}_{u_l,l} \gamma^{(n)}_{u_l,l,1}\right)$. Note that, this rate expression is valid under the assumption of Gaussian (and spectrally white) interference which holds for a large number of interferers. Similarly, the achievable data rate in the

[3]I will present the rate expressions in Section 2.3.1.

second hop is $r^{(n)}_{u_l,2} = B_{RB}\log_2\left(1 + P^{(n)}_{l,u_l}\gamma^{(n)}_{l,u_l,2}\right)$. Since I am considering a two-hop communication, the end-to-end data rate[4] for u_l on RB n is half of the minimum achievable data rate over two hops [29], i.e.,

$$R^{(n)}_{u_l} = \frac{1}{2}\min\left\{r^{(n)}_{u_l,1}, r^{(n)}_{u_l,2}\right\}. \tag{2.1}$$

2.3 Formulation of the RAP

In the following, I present the formulation of the RAP. For each relay, the objective of radio resource (i.e., RB and transmit power) allocation is to obtain the assignment of RB and power level to the UEs that maximizes the system capacity, which is defined as the minimum achievable data rate over two hops. Let the maximum allowable transmit power for UE (relay) is $P^{max}_{u_l}$ (P^{max}_{l}) and let the QoS (i.e., data rate) requirement for UE u_l be denoted by Q_{u_l}. The RB allocation indicator is a binary decision variable $x^{(n)}_{u_l} \in \{0, 1\}$, where

$$x^{(n)}_{u_l} = \begin{cases} 1, & \text{if RB } n \text{ is assigned to UE } u_l \\ 0, & \text{otherwise.} \end{cases} \tag{2.2}$$

2.3.1 Objective Function

Let $R_{u_l} = \sum_{n=1}^{N} x^{(n)}_{u_l} R^{(n)}_{u_l}$ denote the achievable sum-rate over allocated RB(s). I consider that the same RB(s) will be used by the relay in both the hops (i.e., for communication between relay and eNB and between relay and D2D UEs). The objective of RAP is

[4]In a conventional D2D communication approach where two D2D UEs communicate directly without a relay, the achievable data rate for D2D UE $u \in \mathcal{D}$ over RB n can be expressed as $\widetilde{R}^{(n)}_u = B_{RB}\log_2\left(1 + P^{(n)}_u \tilde{\gamma}^{(n)}_u\right)$, where $\tilde{\gamma}^{(n)}_u = \frac{h^{(n)}_{u,u}}{\sum_{\forall j \in \hat{\mathcal{U}}_u} P^{(n)}_j g^{(n)}_{u,j} + \sigma^2}$, $h^{(n)}_{u,u}$ is the channel gain of the link between the D2D UEs and $\hat{\mathcal{U}}_u$ denotes the set of UEs transmitting using the same RB(s) as u.

to maximize the end-to-end rate for each relay $l \in \mathcal{L}$ as follows:

$$\max_{x_{u_l}^{(n)}, P_{u_l,l}^{(n)}, P_{l,u_l}^{(n)}} \sum_{u_l \in \mathcal{U}_l} \sum_{n=1}^{N} x_{u_l}^{(n)} R_{u_l}^{(n)} \tag{2.3}$$

where the rate of UE u_l over RB n

$$R_{u_l}^{(n)} = \frac{1}{2} \min \left\{ B_{RB} \log_2 \left(1 + P_{u_l,l}^{(n)} \gamma_{u_l,l,1}^{(n)}\right), B_{RB} \log_2 \left(1 + P_{l,u_l}^{(n)} \gamma_{l,u_l,2}^{(n)}\right) \right\}.$$

In (2.3), the unit power SINR for the first hop,

$$\gamma_{u_l,l,1}^{(n)} = \frac{h_{u_l,l,1}^{(n)}}{\sum\limits_{\substack{\forall u_j \in \mathcal{U}_j, \\ j \neq l, j \in \mathcal{L}}} x_{u_j}^{(n)} P_{u_j,j}^{(n)} g_{u_j,l,1}^{(n)} + \sigma^2} \tag{2.4}$$

where $h_{i,j,k}^{(n)}$ denotes the direct link gain between node i and j over RB n for hop $k \in \{1, 2\}$, $\sigma^2 = N_0 B_{RB}$ in which N_0 denotes thermal noise. The interference link gain between relay (UE) i and UE (relay) j over RB n in hop k is denoted by $g_{i,j,k}^{(n)}$, where UE (relay) j is not associated with relay (UE) i. Similarly, the unit power SINR for the second hop[5],

$$\gamma_{l,u_l,2}^{(n)} = \begin{cases} \dfrac{h_{l,u_l,2}^{(n)}}{\sum\limits_{\substack{\forall u_j \in \{\mathcal{D} \cap \mathcal{U}_j\}, \\ j \neq l, j \in \mathcal{L}}} x_{u_j}^{(n)} P_{j,u_j}^{(n)} g_{j,eNB,2}^{(n)} + \sigma^2}, & u_l \in \{\mathcal{C} \cap \mathcal{U}_l\} \\ \dfrac{h_{l,u_l,2}^{(n)}}{\sum\limits_{\substack{\forall u_j \in \mathcal{U}_j, \\ j \neq l, j \in \mathcal{L}}} x_{u_j}^{(n)} P_{j,u_j}^{(n)} g_{j,u_l,2}^{(n)} + \sigma^2}, & u_l \in \{\mathcal{D} \cap \mathcal{U}_l\} \end{cases} \tag{2.5}$$

[5]According to LTE-A standard, the L3 relays are able to peform similar operation as an eNB. Besides, the relays in the network are interconnected through X2 interface for better interference management [30]. Since the relays can estimate the CQI values (and hence the interference level) using X2 interface, it is straightforward to account for interference in (2.4) and (2.5). Consequently, interference from other transmitter nodes (e.g., UEs associated to other relays in the first hop or other relays in the second hop) will appear as a constant term in (2.4) and (2.5).

where $h_{l,u_l,2}$ denotes the channel gain between relay-eNB link for CUEs (e.g., $u_l \in \{\mathcal{C} \cap \mathcal{U}_l\}$) or the channel gain between relay and receiving D2D UEs (e.g., $u_l \in \{\mathcal{D} \cap \mathcal{U}_l\}$). From (2.1), the maximum data rate for UE u_l over RB n is achieved when $P^{(n)}_{u_l,l}\gamma^{(n)}_{u_l,l,1} = P^{(n)}_{l,u_l}\gamma^{(n)}_{l,u_l,2}$. Therefore, in the second hop, the power P_{l,u_l} allocated for UE u_l, can be expressed as a function of power allocated for transmission in the first hop, $P_{u_l,l}$ as follows: $P^{(n)}_{l,u_l} = \frac{\gamma^{(n)}_{u_l,l,1}}{\gamma^{(n)}_{l,u_l,2}} P^{(n)}_{u_l,l}$. Hence the data rate for u_l over RB n can be expressed as $R^{(n)}_{u_l} = \frac{1}{2} B_{RB} \log_2 \left(1 + P^{(n)}_{u_l,l}\gamma^{(n)}_{u_l,l,1}\right)$. Considering the above, the objective function in (2.3) can be rewritten as

$$\max_{x^{(n)}_{u_l}, P^{(n)}_{u_l,l}} \sum_{u_l \in \mathcal{U}_l} \sum_{n=1}^{N} \tfrac{1}{2} x^{(n)}_{u_l} B_{RB} \log_2 \left(1 + P^{(n)}_{u_l,l}\gamma^{(n)}_{u_l,l,1}\right). \tag{2.6}$$

For each relay $l \in \mathcal{L}$ in the network, the objective of RAP is to obtain the RB and power allocation vectors, i.e., $\mathbf{x_l} = \left[x^{(1)}_1, \ldots, x^{(N)}_1, \ldots, x^{(1)}_{U_l}, \ldots, x^{(N)}_{U_l}\right]^\mathsf{T}$ and $\mathbf{P_l} = \left[P^{(1)}_{1,l}, \ldots, P^{(N)}_{1,l}, \ldots, P^{(1)}_{U_l,l}, \ldots, P^{(N)}_{U_l,l}\right]^\mathsf{T}$ respectively, which maximize the data rate.

2.3.2 Constraint Sets

In order to ensure the required data rate to the UEs while protecting all receiver nodes from harmful interference, I define the following set of constraints.

- The constraint in (2.7) ensures that each RB is assigned to only one UE, i.e.,

$$\sum_{u_l \in \mathcal{U}_l} x^{(n)}_{u_l} \leq 1, \ \forall n \in \mathcal{N}. \tag{2.7}$$

- The following constraints limit the transmit power in both the hops to the

maximum power budget:

$$\sum_{n=1}^{N} x_{u_l}^{(n)} P_{u_l,l}^{(n)} \leq P_{u_l}^{max}, \ \forall u_l \in \mathcal{U}_l \tag{2.8}$$

$$\sum_{u_l \in \mathcal{U}_l} \sum_{n=1}^{N} x_{u_l}^{(n)} P_{l,u_l}^{(n)} \leq \ P_l^{max}. \tag{2.9}$$

- Similar to [31], I assume that there is a maximum tolerable interference threshold limit for each allocated RB. The constraints in (2.10) and (2.11) limit the amount of interference introduced to the other relays and the receiving D2D UEs in the first and second hop, respectively, to be less than some threshold, i.e.,

$$\sum_{u_l \in \mathcal{U}_l} x_{u_l}^{(n)} P_{u_l,l}^{(n)} g_{u_l^*,l,1}^{(n)} \leq I_{th,1}^{(n)}, \quad \forall n \in \mathcal{N} \tag{2.10}$$

$$\sum_{u_l \in \mathcal{U}_l} x_{u_l}^{(n)} P_{l,u_l}^{(n)} g_{l,u_l^*,2}^{(n)} \leq I_{th,2}^{(n)}, \quad \forall n \in \mathcal{N}. \tag{2.11}$$

- The minimum data rate requirements for the CUE and D2D UEs is ensured by the following constraint:

$$R_{u_l} \geq Q_{u_l}, \ \forall u_l \in \mathcal{U}_l. \tag{2.12}$$

- The binary decision variable on RB allocation and non-negativity condition of transmission power is defined by

$$x_{u_l}^{(n)} \in \{0,1\}, \quad P_{u_l,l}^{(n)} \geq 0, \quad \forall u_l \in \mathcal{U}_l, \forall n \in \mathcal{N}. \tag{2.13}$$

Note that in constraint (2.10) and (2.11), I adopt the concept of reference user. For example, to allocate the power level considering the interference threshold in the first hop, each UE u_l associated with relay node l obtains the reference user u_l^* associated with the other relays and the corresponding channel gain $g^{(n)}_{u_l^*,l,1}$ for $\forall n$ according to the following equation:

$$u_l^* = \underset{j}{\operatorname{argmax}}\ g^{(n)}_{u_l,j,1}, \quad u_l \in \mathcal{U}_l, j \neq l, j \in \mathcal{L}. \tag{2.14}$$

Similarly, in the second hop, for each relay l, the transmit power will be adjusted accordingly considering interference introduced to the receiving D2D UEs (associated with other relays) considering the corresponding channel gain $g^{(n)}_{l,u_l^*,2}$ for $\forall n$, where the reference user is obtained by

$$u_l^* = \underset{u_j}{\operatorname{argmax}}\ g^{(n)}_{l,u_j,2}, \quad j \neq l, j \in \mathcal{L}, u_j \in \{\mathcal{D} \cap \mathcal{U}_j\}. \tag{2.15}$$

Based on the objective function (2.6) and the constraints given by Section 2.3.2, the RAP can be written as the following optimization problem.

(**P2.1**)

$$\max_{x_{u_l}^{(n)}, P_{u_l,l}^{(n)}} \sum_{u_l \in \mathcal{U}_l} \sum_{n=1}^{N} \tfrac{1}{2} x_{u_l}^{(n)} B_{RB} \log_2\Big(1 + P_{u_l,l}^{(n)} \gamma_{u_l,l,1}^{(n)}\Big)$$

$$\text{subject to} \quad \sum_{u_l \in \mathcal{U}_l} x_{u_l}^{(n)} \leq 1, \qquad \forall n \tag{2.16a}$$

$$\sum_{n=1}^{N} x_{u_l}^{(n)} P_{u_l,l}^{(n)} \leq P_{u_l}^{max}, \forall u_l \tag{2.16b}$$

$$\sum_{u_l \in \mathcal{U}_l} \sum_{n=1}^{N} x_{u_l}^{(n)} \frac{\gamma_{u_l,l,1}^{(n)}}{\gamma_{l,u_l,2}^{(n)}} P_{u_l,l}^{(n)} \leq P_l^{max} \tag{2.16c}$$

$$\sum_{u_l \in \mathcal{U}_l} x_{u_l}^{(n)} P_{u_l,l}^{(n)} g_{u_l^*,l,1}^{(n)} \leq I_{th,1}^{(n)}, \ \forall n \tag{2.16d}$$

$$\sum_{u_l \in \mathcal{U}_l} x_{u_l}^{(n)} \frac{\gamma_{u_l,l,1}^{(n)}}{\gamma_{l,u_l,2}^{(n)}} P_{u_l,l}^{(n)} g_{l,u_l^*,2}^{(n)} \leq I_{th,2}^{(n)}, \ \forall n \tag{2.16e}$$

$$\sum_{n=1}^{N} \tfrac{1}{2} x_{u_l}^{(n)} B_{RB} \log_2\Big(1 + P_{u_l,l}^{(n)} \gamma_{u_l,l,1}^{(n)}\Big) \geq Q_{u_l}, \quad \forall u_l \tag{2.16f}$$

$$P_{u_l,l}^{(n)} \geq 0, \quad \forall n, u_l. \tag{2.16g}$$

2.3.3 Continious Relaxation and Reformulation

As mentioned in the following corollary, the optimization problem **P2.1** is a mixed-integer non-linear program (MINLP) which is computationally intractable.

Corollary 2.1. *The objective function in (2.6) and the set of constraints in (2.7)-(2.13) turn the optimization problem* **P2.1** *to a MINLP with non-convex feasible set. MINLP problems have the difficulties of both of their sub-classes, i.e., the combinatorial nature of mixed integer programs (MIPs) and the difficulty in solving nonlinear programs (NLPs). Since MIPs and NLPs are NP-complete, the RAP* **P2.1** *is strongly NP-hard.*

A well-known approach to solve the above problem is to relax the constraint that an RB is used by only one UE by using the *time-sharing* strategy [32]. In particular,

I relax the optimization problem by replacing the non-convex constraint $x_{u_l}^{(n)} \in \{0,1\}$ with the convex constraint $0 < x_{u_l}^{(n)} \leq 1$. Thus $x_{u_l}^{(n)}$ represents the sharing factor where each $x_{u_l}^{(n)}$ denotes the portion of time that RB n is assigned to UE u_l and satisfies the constraint $\sum_{u_l \in \mathcal{U}_l} x_{u_l}^{(n)} \leq 1, \ \forall n$. Besides, I introduce a new variable $S_{u_l,l}^{(n)} = x_{u_l}^{(n)} P_{u_l,l}^{(n)} \geq 0$, which denotes the actual transmit power of UE u_l on RB n [33]. Then the relaxed problem can be stated as follows:

(**P2.2**)

$$\max_{x_{u_l}^{(n)}, S_{u_l,l}^{(n)}} \sum_{u_l \in \mathcal{U}_l} \sum_{n=1}^{N} \tfrac{1}{2} x_{u_l}^{(n)} B_{RB} \log_2 \left(1 + \frac{S_{u_l,l}^{(n)} \gamma_{u_l,l,1}^{(n)}}{x_{u_l}^{(n)}}\right) \tag{2.17a}$$

$$\text{subject to} \sum_{u_l \in \mathcal{U}_l} x_{u_l}^{(n)} \leq 1, \qquad \forall n \tag{2.17b}$$

$$\sum_{n=1}^{N} S_{u_l,l}^{(n)} \leq P_{u_l}^{max}, \ \forall u_l \tag{2.17c}$$

$$\sum_{u_l \in \mathcal{U}_l} \sum_{n=1}^{N} \frac{\gamma_{u_l,l,1}^{(n)}}{\gamma_{l,u_l,2}^{(n)}} S_{u_l,l}^{(n)} \leq P_l^{max} \tag{2.17d}$$

$$\sum_{u_l \in \mathcal{U}_l} S_{u_l,l}^{(n)} g_{u_l^*,l,1}^{(n)} \leq I_{th,1}^{(n)}, \quad \forall n \tag{2.17e}$$

$$\sum_{u_l \in \mathcal{U}_l} \frac{\gamma_{u_l,l,1}^{(n)}}{\gamma_{l,u_l,2}^{(n)}} S_{u_l,l}^{(n)} g_{l,u_l^*,2}^{(n)} \leq I_{th,2}^{(n)}, \quad \forall n \tag{2.17f}$$

$$\sum_{n=1}^{N} \tfrac{1}{2} x_{u_l}^{(n)} B_{RB} \log_2 \left(1 + \frac{S_{u_l,l}^{(n)} \gamma_{u_l,l,1}^{(n)}}{x_{u_l}^{(n)}}\right) \geq Q_{u_l}, \quad \forall u_l \tag{2.17g}$$

$$0 < x_{u_l}^{(n)} \leq 1, \ S_{u_l,l}^{(n)} \geq 0, \qquad \forall n, u_l \tag{2.17h}$$

where $\gamma_{u_l,l,1}^{(n)} = \dfrac{h_{u_l,l}^{(n)}}{\sum\limits_{\substack{\forall u_j \in \mathcal{U}_j, \\ j \neq l, j \in \mathcal{L}}} S_{u_j,j}^{(n)} g_{u_j,l,1}^{(n)} + \sigma^2}$.

Corollary 2.2. *The objective function in (2.17a) is concave, the constraint in (2.17g) is convex, and the remaining constraints in (2.17b), (2.17c)-(2.17h) are affine. Therefore, the optimization problem* **P2.2** *is convex.*

The duality gap of any optimization problem satisfying the time-sharing condition becomes negligible as the number of RBs becomes significantly large. Since **P2.2** is a non-linear convex problem, each relay can solve the optimization problem using standard algorithms such as interior point method [34, Chapter 11]. Note that, the optimization problem **P2.2** satisfies the time-sharing condition. Therefore, the solution of the relaxed problem is asymptotically optimal [35].

2.3.4 Algorithm for Resoruce Allocation

Each relay in the network independently allocates resources to its associated UEs. Based on the mathematical formulation in the previous section, the overall resource allocation algorithm is shown in **Algorithm 1**.

Algorithm 1 Joint RB and power allocation algorithm

1: UEs measure interference level from previous time slot and inform the respective relays.
2: Each relay $l \in \mathcal{L}$ obtains the channel state information among all relays $j; j \neq l, j \in \mathcal{L}$ and to its scheduled UEs $\forall u_j \in \mathcal{U}_j; j \neq l, j \in \mathcal{L}$.
3: For each relay and its associated UEs, obtain the reference node for the first and second hops according to (2.14) and (2.15).
4: Solve the optimization problem **P2.2** for each relay independently to obtain RB and power allocation vectors, e.g., $\mathbf{x_l}, \mathbf{P_l}$ for $\forall l \in \mathcal{L}$.
5: Allocate resources (i.e., RB and transmit power) to associated UEs for each relay and calculate average achievable data rate.

The proposed solution can be referred to as a *semi-distributed* approach in a sense that instead of solving the resource allocation globally by the eNB, the computational load is distributed among the relays. Hence, these relays perform the resource allocation locally. It is worth mentioning that at each relay l, solving **P2.2** by using the interior point method incurs a complexity of $\mathcal{O}\left(\left(|\mathbf{x_l}| + |\mathbf{S_l}|\right)^3\right)$ [34, Chapter 11], [36] where $\mathbf{x_l} = \left[x_1^{(1)}, \cdots, x_1^{(N)}, \cdots, x_{U_l}^{(1)}, \cdots, x_{U_l}^{(N)}\right]^\mathsf{T}$ and $\mathbf{S_l} =$

$\left[S_{1,l}^{(1)}, \cdots, S_{1,l}^{(N)}, \cdots, S_{U_l,l}^{(1)}, \cdots, S_{U_l,l}^{(N)}\right]^{\mathsf{T}}$.

Since the L3 relays can perform the same operation as an eNB, these relays can communicate using the X2 interface [30] defined in the 3GPP LTE-A standard. Therefore, in the proposed algorithm, the relays can obtain the channel state information through inter-relay message passing without increasing signalling overhead at the eNB.

2.4 Performance Evaluation

The performance results for the resource allocation schemes obtained by a simulator written in MATLAB[6]. In order to study network performance in presence of the L3 relay, I compare the performance of the proposed scheme with a *reference scheme* [17] in which an RB allocated to CUE can be shared with at most one D2D-link. D2D UE shares the same RB(s) (allocated to CUE by solving optimization problem) and communicate directly between peers without relay only if the QoS requirements for both CUE and D2D UE are satisfied.

2.4.1 Numerical Results

Achievable data rate vs. distance between D2D-links

In Fig. 2.2, I illustrate the average achievable data rate $\bar{R}$ for D2D UEs which is calculated as $\bar{R} = \frac{\sum_{u \in \mathcal{D}} R_u^{\text{ach}}}{|\mathcal{D}|}$, where R_u^{ach} is the achievable data rate for UE u and $|\cdot|$ denotes set cardinality. Although the reference scheme outperforms when the distance between D2D-link is closer (i.e., $d < 60$m); my proposed algorithm can greatly increase the data rate especially when the distance increases. This is due to

[6]For details of the simulator and the parameters used in the simulation refer to **Appendix A**.

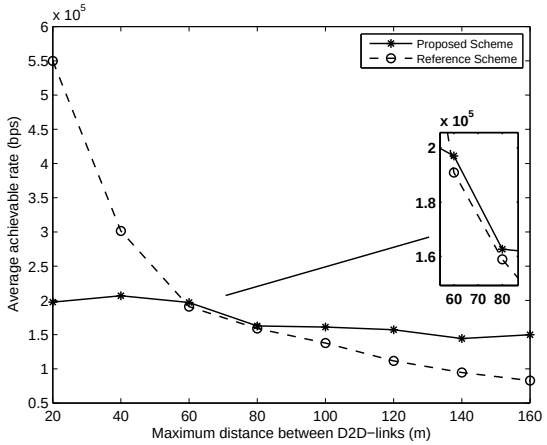

Figure 2.2: Average achievable data rate with varying distance; number of CUE, $|\mathcal{C}| = 15$ (i.e., 5 CUEs assisted by each relay), number of D2D-pair, $|\mathcal{D}| = 9$ (i.e., 3 D2D-pair assisted by each relay) and interference threshold -70 dBm.

the fact that when the distance is higher, the performance of direct communication deteriorates due to poor propagation medium. Besides, when the D2D UEs share resources with only one CUE, the spectrum may not utilize efficiently and decreases the achievable rate. Consequently, the gap between the achievable rate of my proposed algorithm and that of the reference scheme becomes wider when the distance increases.

Rate gain vs. distance between D2D-links

Fig. 2.3(a) depicts the rate gain in terms of aggregated achievable rate for the UEs. I calculate the gain as follows:

$$R_{\text{gain}} = \frac{R_{\text{prop}} - R_{\text{ref}}}{R_{\text{ref}}} \times 100\%, \tag{2.18}$$

where R_{prop} and R_{ref} denote the aggregate data rate for the D2D UEs in the proposed scheme and the reference scheme, respectively. It is observed from the figure that, with the increasing distance between D2D-links my proposed scheme provides significant

gain in terms of achievable data rate. To observe the effect of gain in different network realization I vary the number of D2D UE in Fig. 2.3(b). It is clear from figure that irrespective of the number of D2D UEs in the network, my proposed scheme provides considerable rate gain for distant D2D-pairs.

2.5 Summary and Discussions

I have provided a mathematical formulation for radio resource allocation and analyzed the performance of relay-assisted D2D communication. The performance evaluation results have shown that relay-assisted D2D communication is beneficial to provide higher rate for distant D2D-links. However, when the number of UEs is large, solving the optimization problem **P2.2** centrally could be bottleneck for the relay nodes. Besides when the perfect channel knowledge is not available, the effects of uncertainties in the system parameter need to be considered by using a robust optimization formulation. These issues will be discussed in the following chapters.

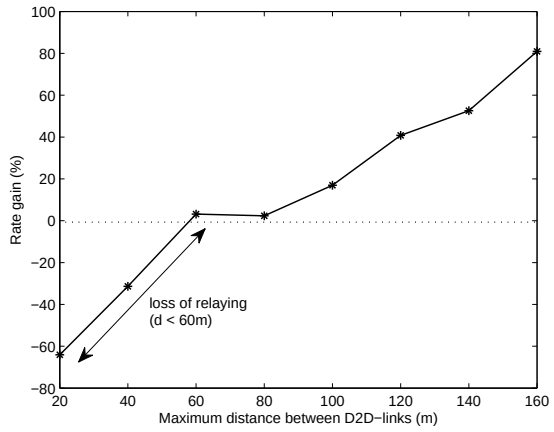

(a)

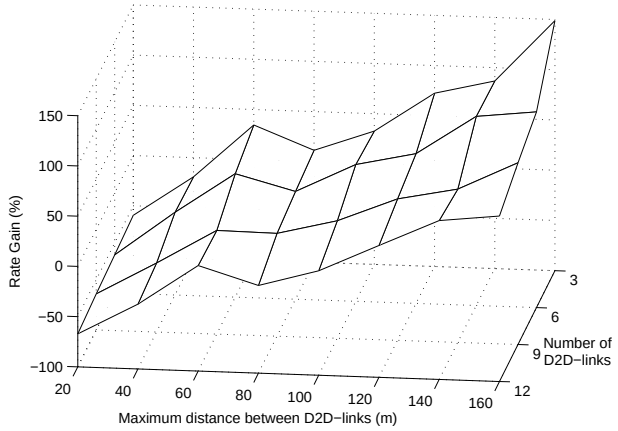

(b)

Figure 2.3: Gain in aggregated achievable data rate with varying distance (for $|\mathcal{C}| = 15$, interference threshold -70 dBm): (a) 3 D2D-pairs assisted by each relay (i.e., $|\mathcal{D}| = 9$); (b) number of D2D-pairs varies from 1 to 4 UE(s)/relay (i.e., $|\mathcal{D}| = 3, 6, 9, 12$). There is a critical distance d (i.e., $d \approx 60$m here), beyond which relaying provides significant performance gain.

Chapter 3

Distributed Solution for Relay-Aided D2D Communication : A Message Passing Approach

As I have shown in **Corollary 2.1**, the RAP **P2.1** is NP-hard. Instead of solving **P2.1** in a centralized manner using relaxation techniques as presented in Chapter 2, in this chapter I present a distributed approach. The centralize solutions for wireless radio resource allocation problems generally not scalable, and also incur huge computational and signaling overheads. Therefore, goal of this chapter is to design a practical resource allocation algorithm for relay-aided D2D communications. I show that the RAP can be converted to a *max-sum message passing* (MP) problem over a graphical model. The MP algorithms have been recognized as powerful tools that can be used to solve many problems in signal processing, coding theory, machine learning, natural language processing, and computer vision. When MP is applied to solve a problem, the messages represent probabilities (i.e., beliefs) exchanged with the goal of achieving optimal decisions. Analogously, in the context of the resource

allocation for relay-aided D2D communication, the MP strategy can be applied to pass messages between UEs and relays until a global allocation is obtained. The advantage of applying MP strategy in resource allocation is that it provides a low-complexity distributed solution and reduces the computation burden at the controller node. Motivated by the above fact, in this chapter, I apply the max-sum variation of the message passing technique to represent the resource allocation problem by a *factor graph*. To this end, I propose a distributed solution approach with polynomial time-complexity and low signaling overhead. The main contributions of this chapter can be summarized as follows:

- I provide a novel solution technique using message passing. Utilizing message passing strategy, I develop a low-complexity distributed solution by which RBs and transmission power can be allocated in a distributed fashion.

- I analyze the complexity and the optimality of the solution. To this end, I compare the performance of my relay-based D2D communication scheme with a direct D2D communication method and observe that relaying improves network performance for distant D2D peers without increasing the end-to-end delay significantly.

The remainder of this chapter is organized as follows. I introduce the message passing strategy to solve the RAP in Section 3.1. A distributed solution is proposed in Section 3.2 and the performance evaluation results are presented in Section 3.3. I summarize and conclude the chapter in Section 3.4.

3.1 Message Passing Approach to Solve the RAP

3.1.1 MP Strategy for the Max-sum Problem

Given the RAP formulation **P2.1**, I focus on the max-sum variant [37] of MP paradigm. Let me consider a generic function $f(y_1, y_2, \ldots, y_J) : \mathfrak{D}_{\mathbf{y}} \rightarrow \mathbb{R}$ where each variable y_j corresponds to a finite alphabet $\mathfrak{a}$, i.e., $\mathfrak{D}_{\mathbf{y}} = \mathfrak{a}^J$. I concentrate on maximizing the function $f(\cdot)$, i.e.,

$$\tilde{Z} = \max_{\mathbf{y}} f(\mathbf{y}). \tag{3.1}$$

That is, $\tilde{Z}$ represents the maximization over all possible combinations of the vector $\mathbf{y} \in \mathfrak{a}^J$ where $\mathbf{y} = [y_1, y_2, \ldots, y_J]^{\mathsf{T}}$. The *marginal* of $\tilde{Z}$ with respect to variable y_j is given by

$$\phi_j(y_j) = \max_{\sim(y_j)} f(\mathbf{y}) \tag{3.2}$$

where $\max_{\sim(\alpha)} f(\cdot)$ denotes the maximization over all variables in $f(\cdot)$ except variable α. Let me decompose $f(\mathbf{y})$ into the summation of K functions $f_k(\cdot) : \mathfrak{D}_{\widehat{y}_k} \rightarrow \mathbb{R}, k \in \{1, 2, \ldots, K\}$, i.e., $f(\mathbf{y}) = \sum_{k=1}^{K} f_k(\widehat{y}_k)$, where $\widehat{y}_k$ is a subset of elements of $\mathbf{y}$ and $\mathfrak{D}_{\widehat{y}_k} \subset \mathfrak{D}_{\mathbf{y}}$. Besides, let $\mathbf{f(\cdot)} = [f_1(\cdot), f_2(\cdot), \ldots, f_K(\cdot)]^{\mathsf{T}}$ denote the vector of K functions and $\mathfrak{f}_j$ represent the subset of functions in $\mathbf{f(\cdot)}$ where the variable y_j appears. Hence, (3.2) can be rewritten as

$$\phi_j(y_j) = \max_{\sim(y_j)} \sum_{k=1}^{K} f_k(\widehat{y}_k). \tag{3.3}$$

Utilizing any MP algorithm, the computation of marginals involves passing messages between nodes represented by a specific graphical model. Among different graphical models, in this work, I consider factor graph [38] to capture the structure of generic function $f(\cdot)$. The factor graph consists of two different types of nodes,

namely, function (or factor) nodes and variable nodes. A function node is connected with a variable node if and only if the variable appears in the corresponding function. Consequently, a factor graph contains two types of messages, i.e., message from factor nodes to variable nodes and vice-versa. According to the max-sum MP strategy, the message passed by any variable node $y_j,\ j \in \{1, 2, \ldots, J\}$, to any generic function node $f_k(\cdot),\ k \in \{1, 2, \ldots, K\}$, is given as

$$\delta_{y_j \to f_k(\cdot)}(y_j) = \sum_{\substack{i \in \mathfrak{f}_j, \\ i \neq k}} \delta_{f_i(\cdot) \to y_j}(y_j). \tag{3.4}$$

Likewise, the message from factor node $f_k(\cdot)$ to variable node y_j is given as follows:

$$\delta_{f_k(\cdot) \to y_j}(y_j) = \max_{\sim(y_j)} \left(f_k(y_1, \ldots, y_J) + \sum_{\substack{i \in \widehat{y}_k, \\ i \neq j}} \delta_{y_i \to f_k(\cdot)}(y_i) \right). \tag{3.5}$$

When the factor graph is cycle free, it is represented as a tree (i.e., there is a unique path connecting any two nodes); hence, all the variable nodes can compute the marginals as

$$\phi_j(y_j) = \sum_{k=1}^{K} \delta_{f_k(\cdot) \to y_j}(y_j). \tag{3.6}$$

By invoking the general distributive law (i.e., $\max \sum = \sum \max$) [39], the maximization in (3.1) can be computed as

$$\tilde{Z} = \sum_{j=1}^{J} \max_{y_j} \phi_j(y_j). \tag{3.7}$$

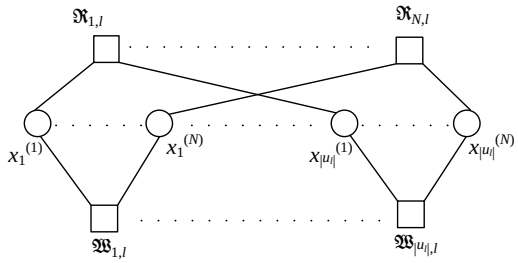

Figure 3.1: An arbitrary factor graph representing MP formulation of the RAP. For ease of representation, the variables are denoted by circular nodes whereas the functions are denoted by square nodes. A variable node $x_{u_l}^{(n)}$ is connected to the function nodes $\mathfrak{R}_{n,l}(\cdot)$ and $\mathfrak{W}_{u_l,l}(\cdot)$ if and only if the variable appears in the corresponding function.

3.1.2 Utility Functions

In the following, I develop a joint RB and power allocation mechanism that leverages the dynamics of MP strategy. Compared to centralized optimization solutions, MP allows to distribute the computational burden of achieving a feasible resource allocation by exchanging information among UEs and the corresponding relay.

Let me consider the original optimization problem **P2.1** as presented in Page 22. In order to solve RAP **P2.1** using the MP scheme, I reformulate it as a utility maximization (i.e., cost minimization) problem and define the utility functions as in (3.8) and (3.9) where unfulfilled constraints result in infinite cost. Per RB constraints [i.e., (2.16a), (2.16c), (2.16d), (2.16e)] are incorporated in the utility function $\mathfrak{R}_{n,l}(\cdot)$

as follows:

$$\mathfrak{R}_{n,l}(\cdot) = \begin{cases} 0, & \text{if } \sum_{u_l \in \mathcal{U}_l} x_{u_l}^{(n)} \leq 1 \\ & \sum_{u_l \in \mathcal{U}_l} x_{u_l}^{(n)} \frac{\gamma_{u_l,l,1}^{(n)}}{\gamma_{l,u_l,2}^{(n)}} P_{u_l,l}^{(n)} \leq {P_l^{(n)}}^{max} \\ & \sum_{u_l \in \mathcal{U}_l} x_{u_l}^{(n)} P_{u_l,l}^{(n)} g_{u_l^*,l,1}^{(n)} \leq I_{th,1}^{(n)} \\ & \sum_{u_l \in \mathcal{U}_l} x_{u_l}^{(n)} \frac{\gamma_{u_l,l,1}^{(n)}}{\gamma_{l,u_l,2}^{(n)}} P_{u_l,l}^{(n)} g_{l,u_l^*,2}^{(n)} \leq I_{th,2}^{(n)} \\ -\infty, & \text{otherwise} \end{cases} \tag{3.8}$$

where ${P_l^{(n)}}^{max} = \frac{P_l^{max}}{N}$. On the other hand, per UE constraints are incorporated in the utility function $\mathfrak{W}_{u_l,l}(\cdot)$ which is the achievable rate of each UE only if the constraints in (2.16b) and (2.16f) are satisfied, i.e.,

$$\mathfrak{W}_{u_l,l}(\cdot) = \begin{cases} \sum_{n=1}^{N} x_{u_l}^{(n)} R_{u_l}^{(n)}, & \text{if } \sum_{n=1}^{N} x_{u_l}^{(n)} P_{u_l,l}^{(n)} \leq P_{u_l}^{max} \\ & \sum_{n=1}^{N} x_{u_l}^{(n)} R_{u_l}^{(n)} \geq Q_{u_l} \\ -\infty, & \text{otherwise.} \end{cases} \tag{3.9}$$

3.1.3 MP Formulation for the RAP

Using the utility functions above, the RAP for each relay l can be rewritten as

$$\mathbf{x}_l^* = \max_{\mathbf{x}} \left(\sum_{n=1}^{N} \mathfrak{R}_{n,l}(\cdot) + \sum_{u_l \in \mathcal{U}_l} \mathfrak{W}_{u_l,l}(\cdot) \right). \tag{3.10}$$

By exploiting the concept described in Section 3.1.1, let me associate (3.10) with a factor graph as shown in Fig. 3.1. Following an MP strategy, the variable and function nodes exchange messages along their connecting edges until the values of

$x_{u_l}^{(n)}$ are determined for $\forall u_l, n$. Let $\phi_{u_l}^{(n)}$ be the marginalization of (3.10) with respect to $x_{u_l}^{(n)}$ and given as

$$\phi_{u_l}^{(n)}\left(x_{u_l}^{(n)}\right) = \max_{\sim\left(x_{u_l}^{(n)}\right)} \left(\sum_{n=1}^{N} \mathfrak{R}_{n,l}(\cdot) + \sum_{u_l \in \mathcal{U}_l} \mathfrak{W}_{u_l,l}(\cdot) \right). \tag{3.11}$$

Let $\delta_{\mathfrak{R}_{n,l}(\cdot)\to x_{u_l}^{(n)}}\left(x_{u_l}^{(n)}\right)$ and $\delta_{x_{u_l}^{(n)}\to\mathfrak{R}_{n,l}(\cdot)}\left(x_{u_l}^{(n)}\right)$ denote the message exchanged between function nodes $\mathfrak{R}_{n,l}(\cdot)$ and the connected variable nodes for $\forall u_l, n$. Similarly, $\delta_{\mathfrak{W}_{u_l,l}(\cdot)\to x_{u_l}^{(n)}}\left(x_{u_l}^{(n)}\right)$ and $\delta_{x_{u_l}^{(n)}\to\mathfrak{W}_{u_l,l}(\cdot)}\left(x_{u_l}^{(n)}\right)$ denote the exchanged messages between function nodes $\mathfrak{W}_{u_l,l}(\cdot)$ and variable nodes for $\forall u_l, n$. Let me consider a generic RB n in the factor graph. The square node in Fig. 3.1 corresponding to $\mathfrak{R}_{n,l}(\cdot)$ which is connected to all variable nodes $x_{u_l}^{(n)}$ for $\forall u_l \in \mathcal{U}_l$. Hence from (3.5), the message to be delivered to the particular variable node $x_{u_l}^{(n)}$ is obtained as follows:

$$\begin{aligned}
\delta_{\mathfrak{R}_{n,l}(\cdot)\to x_{u_l}^{(n)}}\left(x_{u_l}^{(n)}\right) = \max \sum_{j\in\mathcal{U}_l, j\neq u_l} \delta_{x_j^{(n)}\to\mathfrak{R}_{n,l}(\cdot)}\left(x_j^{(n)}\right) \\
\text{subject to } \sum_{u_l\in\mathcal{U}_l} x_{u_l}^{(n)} \leq 1 \\
\sum_{u_l\in\mathcal{U}_l} x_{u_l}^{(n)} \frac{\gamma_{u_l,l,1}^{(n)}}{\gamma_{l,u_l,2}^{(n)}} P_{u_l,l}^{(n)} \leq {P_l^{(n)}}^{max} \\
\sum_{u_l\in\mathcal{U}_l} x_{u_l}^{(n)} P_{u_l,l}^{(n)} g_{u_l^*,l,1}^{(n)} \leq I_{th,1}^{(n)} \\
\sum_{u_l\in\mathcal{U}_l} x_{u_l}^{(n)} \frac{\gamma_{u_l,l,1}^{(n)}}{\gamma_{l,u_l,2}^{(n)}} P_{u_l,l}^{(n)} g_{l,u_l^*,2}^{(n)} \leq I_{th,2}^{(n)}.
\end{aligned} \tag{3.12}$$

Let me consider a generic user u_l. As illustrated in Fig. 3.1, the square nodes corresponding to function $\mathfrak{W}_{u_l,l}(\cdot)$ in factor graph are connected to all variable nodes $x_{u_l}^{(n)}$ for $\forall n \in \mathcal{N}$. Using (3.5) and (3.9), the message from function node $\mathfrak{W}_{u_l,l}(\cdot)$ to any variable node $x_{u_l}^{(n)}$ is given by (3.13).

$$\delta_{\mathfrak{W}_{u_l,l}(\cdot)\to x_{u_l}^{(n)}}\left(x_{u_l}^{(n)}\right) = x_{u_l}^{(n)} R_{u_l}^{(n)} + \max\left(\sum_{\substack{j=1,\\ j\neq n}}^{N} x_{u_l}^{(j)} R_{u_l}^{(j)} + \delta_{x_{u_l}^{(j)}\to\mathfrak{W}_{u_l,l}(\cdot)}\left(x_{u_l}^{(j)}\right)\right)$$

$$\text{subject to } \sum_{n=1}^{N} x_{u_l}^{(n)} P_{u_l,l}^{(n)} \leq P_{u_l}^{max}, \qquad \sum_{n=1}^{N} x_{u_l}^{(n)} R_{u_l}^{(n)} \geq Q_{u_l}. \tag{3.13}$$

From (3.12) and (3.13), the marginal $\phi_{u_l}^{(n)}\left(x_{u_l}^{(n)}\right)$ can be obtained as

$$\phi_{u_l}^{(n)}\left(x_{u_l}^{(n)}\right) = \delta_{\mathfrak{R}_{n,l}(\cdot)\to x_{u_l}^{(n)}}\left(x_{u_l}^{(n)}\right) + \delta_{\mathfrak{W}_{u_l,l}(\cdot)\to x_{u_l}^{(n)}}\left(x_{u_l}^{(n)}\right). \tag{3.14}$$

Consequently, the RB allocation indicator for UE u_l over RB n is given by

$$x_{u_l}^{(n)^*} = \underset{x_{u_l}^{(n)}}{\text{argmax}}\left[\phi_{u_l}^{(n)}\left(x_{u_l}^{(n)}\right)\right]. \tag{3.15}$$

From (3.12) and (3.13), it can be noted that both the messages, i.e., $\delta_{\mathfrak{R}_{n,l}(\cdot)\to x_{u_l}^{(n)}}\left(x_{u_l}^{(n)}\right)$ and $\delta_{\mathfrak{W}_{u_l,l}(\cdot)\to x_{u_l}^{(n)}}\left(x_{u_l}^{(n)}\right)$ solve a local optimization problem with respect to the allocation variable $x_{u_l}^{(n)}$. It is worth noting that, in my system model, each function node $\mathfrak{W}_{u_l,l}(\cdot)$ and corresponding variable nodes are located at the UE u_l, while all $\delta_{\mathfrak{R}_{n,l}}(\cdot)$ nodes are located at the relay. Hence, sending messages $\delta_{\mathfrak{R}_{n,l}}(\cdot)$ from variable nodes to function nodes (and vice-versa) requires actual transmission on the radio channel. However, the message exchanges between variable nodes and function nodes $\mathfrak{W}_{u_l,l}(\cdot)$ are performed locally at the UEs without actual transmission on the radio channel.

3.1.4 An Effective Implementation of MP Strategy

In a practical LTE-A system, since the exchange of messages actually involves effective transmissions over the channel, the MP scheme described in the preceding section might be limited by the signaling overhead due to transfer of messages between relay and UEs. In the following, I observe that the amount of message signaling can be significantly reduced by some algebraic manipulations. Note that, the message $\delta_{\mathfrak{W}_{u_l,l}(\cdot)\to x_{u_l}^{(n)}}(1)$ carries information regarding the use of RB n by UE u_l with transmission power $P_{u_l,l}^{(n)}$, while $\delta_{\mathfrak{W}_{u_l,l}(\cdot)\to x_{u_l}^{(n)}}(0)$ carries information regarding the lack of transmission on RB n by UE u_l, i.e., $P_{u_l,l}^{(n)}=0$. Hence, each UE eventually delivers a real-valued vector of two elements, i.e.,

$$\boldsymbol{\Delta}_{\boldsymbol{\mathfrak{W}_{u_l,l}(\cdot)\to x_{u_l}^{(n)}}}=\left[\delta_{\mathfrak{W}_{u_l,l}(\cdot)\to x_{u_l}^{(n)}}(1),\delta_{\mathfrak{W}_{u_l,l}(\cdot)\to x_{u_l}^{(n)}}(0)\right]^{\mathsf{T}}.$$

Let κ_{u_l} denote the required number of RB(s)[1] to satisfy the data rate requirement Q_{u_l} for UE u_l. Therefore, the constraint in (2.16f) can be rewritten as

$$\sum_{n=1}^{N}x_{u_l}^{(n)}\geq\kappa_{u_l},\quad\forall u_l. \tag{3.16}$$

Now, replacing the constraint in (3.13) with that in (3.16) and subtracting the constant term $\sum_{\substack{j=1;\\ j\neq n}}^{N}\delta_{x_{u_l}^{(j)}\to\mathfrak{W}_{u_l,l}(\cdot)}(0)$ from both sides of (3.13), I obtain (3.17). Let me introduce the normalized messages $\tilde{\psi}_{u_l,l}^{(n)}=\delta_{x_{u_l}^{(n)}\to\mathfrak{W}_{u_l,l}(\cdot)}(1)-\delta_{x_{u_l}^{(n)}\to\mathfrak{W}_{u_l,l}(\cdot)}(0)=\delta_{\mathfrak{R}_{n,l}(\cdot)\to x_{u_l}^{(n)}}(1)-\delta_{\mathfrak{R}_{n,l}(\cdot)\to x_{u_l}^{(n)}}(0)$. It can be observed that the terms within the summation in (3.17) are either 0 or $R_{u_l}^{(n)}+\tilde{\psi}_{u_l,l}^{(n)}$ depending on whether the RB allocation indicator variable $x_{u_l}^{(n)}$ is 0 or 1.

[1]The calculation of κ_{u_l} is given in **Appendix B.1**.

$$\delta_{\mathfrak{W}_{u_l,l}(\cdot)\to x_{u_l}^{(n)}}\left(x_{u_l}^{(n)}\right)-\sum_{\substack{j=1;\\ j\neq n}}^{N}\delta_{x_{u_l}^{(j)}\to\mathfrak{W}_{u_l,l}(\cdot)}\left(0\right)=x_{u_l}^{(n)}R_{u_l}^{(n)}$$

$$+\max\left(\sum_{\substack{j=1,\\ j\neq n}}^{N}x_{u_l}^{(j)}R_{u_l}^{(j)}+\delta_{x_{u_l}^{(j)}\to\mathfrak{W}_{u_l,l}(\cdot)}\left(x_{u_l}^{(j)}\right)-\delta_{x_{u_l}^{(j)}\to\mathfrak{W}_{u_l,l}(\cdot)}\left(0\right)\right)$$

$$\text{subject to }\sum_{n=1}^{N}x_{u_l}^{(n)}P_{u_l,l}^{(n)}\leq P_{u_l}^{max},\qquad\sum_{n=1}^{N}x_{u_l}^{(n)}\geq\kappa_{u_l}. \tag{3.17}$$

Given the above, the maximization is straightforward. For instance, consider the vector

$$\boldsymbol{\chi_{u_l}}=\left[R_{u_l}^{(1)}+\tilde{\psi}_{u_l,l}^{(1)},\ldots,R_{u_l}^{(j)}+\tilde{\psi}_{u_l,l}^{(j)},\ldots,R_{u_l}^{(N)}+\tilde{\psi}_{u_l,l}^{(N)}\right]^{\mathsf{T}}$$

and $\langle\upsilon_{u_l}^{(j)}\rangle_{z\backslash n}$ be the z-th sorted element of $\boldsymbol{\chi_{u_l}}$ without considering the term $R_{u_l}^{(j)}+\tilde{\psi}_{u_l,l}^{(j)}$ so that

$$\langle\upsilon_{u_l}^{(j)}\rangle_{(z-1)\backslash n}\geq\langle\upsilon_{u_l}^{(j)}\rangle_{z\backslash n}\geq\langle\upsilon_{u_l}^{(j)}\rangle_{(z+1)\backslash n}$$

for $\forall j\in\mathcal{N}, j\neq n$. Hence, for $x_{u_l}^{(n)}=1$, the maximum rate will be achieved if [40]

$$\delta_{\mathfrak{W}_{u_l,l}(\cdot)\to x_{u_l}^{(n)}}\left(1\right)-\sum_{\substack{j=1,\\ j\neq n}}^{N}\delta_{x_{u_l}^{(j)}\to\mathfrak{W}_{u_l,l}(\cdot)}\left(0\right)$$

$$=\ R_{u_l}^{(n)}+\sum_{z=1}^{\kappa_{u_l}-1}\langle\upsilon_{u_l}^{(j)}\rangle_{z\backslash n}. \tag{3.18}$$

Similarly, for $x_{u_l}^{(n)}=0$, the maximum is given by [40]

$$\delta_{\mathfrak{W}_{u_l,l}(\cdot)\to x_{u_l}^{(n)}}\left(0\right)-\sum_{\substack{j=1;\\ j\neq n}}^{N}\delta_{x_{u_l}^{(j)}\to\mathfrak{W}_{u_l,l}(\cdot)}\left(0\right)=\sum_{z=1}^{\kappa_{u_l}}\langle\upsilon_{u_l}^{(j)}\rangle_{z\backslash n}. \tag{3.19}$$

Since by definition

$$\psi_{u_l,l}^{(n)} = \delta_{\mathfrak{W}_{u_l,l}(\cdot)\to x_{u_l}^{(n)}}(1) - \delta_{\mathfrak{W}_{u_l,l}(\cdot)\to x_{u_l}^{(n)}}(0),$$

from (3.18) and (3.19), the normalized messages can be derived as follows:

$$\begin{aligned}\psi_{u_l,l}^{(n)} &= R_{u_l}^{(n)} - \langle \upsilon_{u_l}^{(j)} \rangle_{\kappa_{u_l}\setminus n} \\ &= R_{u_l}^{(n)} - \langle R_{u_l}^{(j)} + \tilde{\psi}_{u_l,l}^{(j)} \rangle_{\kappa_{u_l}\setminus n} \end{aligned} \tag{3.20}$$

where $j \in \mathcal{N}$ and $j \neq n$. Note that the messages sent from UE u_l to RB n in factor graph is a scalar quantity. Similarly, the normalized messages from RB n to UE u_l, i.e., $\tilde{\psi}_{u_l,l}^{(n)} = \delta_{\mathfrak{R}_{n,l}(\cdot)\to x_{u_l}^{(n)}}(1) - \delta_{\mathfrak{R}_{n,l}(\cdot)\to x_{u_l}^{(n)}}(0)$ becomes [40]

$$\tilde{\psi}_{u_l,l}^{(n)} = -\max_{\substack{i\in\mathcal{U}_l,\\ i\neq u_l}} \psi_{i,l}^{(n)}. \tag{3.21}$$

Note that, for any arbitrary graph, the allocation variables may keep oscillating and might not converge to any fixed point. In the context of loopy graphical models, by introducing a suitable weight, the messages in (3.20) and (3.21) perturb to a fixed point. Accordingly, (3.20) and (3.21) can be rewritten as [41]

$$\psi_{u_l,l}^{(n)} = R_{u_l}^{(n)} - \omega \left\langle R_{u_l}^{(j)} + \psi_{u_l,l}^{(j)} \right\rangle_{\kappa_{u_l}\setminus n} + (1-\omega)\left(R_{u_l}^{(n)} + \tilde{\psi}_{u_l,l}^{(n)}\right) \tag{3.22a}$$

$$\tilde{\psi}_{u_l,l}^{(n)} = -\omega \max_{\substack{i\in\mathcal{U}_l,\\ i\neq u_l}} \psi_{i,l}^{(n)} - (1-\omega)\psi_{u_l,l}^{(n)}. \tag{3.22b}$$

Note that, when $\omega = 1$, (3.22a) and (3.22b) reduce to the original formulation, i.e., (3.20) and (3.21), respectively. Thus the solution $x_{u_l}^{(n)^*}$ can be easily obtained by calculating the node marginals for each UE-RB pair, i.e., for all $u_l \in \mathcal{U}_l, n \in \mathcal{N}$ pair

as follows:

$$\tau_{u_l,l}^{(n)} = \psi_{u_l,l}^{(n)} + \tilde{\psi}_{u_l,l}^{(n)}. \tag{3.23}$$

Hence, from (3.15), the optimal RB allocation can be computed as

$$x_{u_l}^{(n)*} = \begin{cases} 0, & \text{if } \tau_{u_l,l}^{(n)} < 0 \\ 1, & \text{otherwise.} \end{cases} \tag{3.24}$$

3.2 Distributed Solution for the Resource Allocation Problem

3.2.1 Algorithm Development

Once the optimal RB allocation is obtained, the transmission power of the UEs on assigned RB(s) is obtained as follows. I couple the classical generalized distributed constrained power control scheme (GDCPC) [42] with an autonomous power control method [43] which considers the data rate requirements of UEs while protecting other receiving nodes from interference. More specifically, at each iteration, the transmission power is updated using (3.26) where $P_{u_l}^{(n)^{max}} = \frac{P_{u_l}^{max}}{\sum_{n=1}^{N} x_{u_l}^{(n)}}$ and $\hat{P}_{u_l,l}^{(n)}$ is obtained as

$$\hat{P}_{u_l,l}^{(n)} = \min\left(\tilde{P}_{u_l,l}^{(n)},\ \min\left(P_{u_l}^{(n)^{max}}, \varpi_{u_l,l}^{(n)}\right)\right). \tag{3.25}$$

$$P_{u_l,l}^{(n)}(t+1) = \begin{cases} \frac{2^{Q_{u_l}}-1}{2^{R_{u_l}(t)}-1} P_{u_l,l}^{(n)}(t), & \text{if } \frac{2^{Q_{u_l}}-1}{2^{R_{u_l}(t)}-1} P_{u_l,l}^{(n)}(t) \leq {P_{u_l}^{(n)}}^{max} \\ \hat{P}_{u_l,l}^{(n)}, & \text{otherwise} \end{cases} \tag{3.26}$$

In (3.25), $\tilde{P}_{u_l,l}^{(n)}$ is chosen arbitrarily within the range of $0 \leq \tilde{P}_{u_l,l}^{(n)} \leq {P_{u_l}^{(n)}}^{max}$ and $\varpi_{u_l,l}^{(n)}$ is given by

$$\varpi_{u_l,l}^{(n)} = \min\left(\frac{I_{th,1}^{(n)}}{g_{u_l^*,l,1}^{(n)}}, \frac{\gamma_{l,u_l,2}^{(n)}}{\gamma_{u_l,l,1}^{(n)}} \cdot \frac{I_{th,2}^{(n)}}{g_{l,u_l^*,2}^{(n)}} \right). \tag{3.27}$$

Each relay independently performs the resource allocation and allocates resources to the associated UEs. For completeness, the distributed joint RB and power allocation algorithm is summarized in **Algorithm 2**.

Algorithm 2 Allocation of RB and transmission power using message passing

1: Estimate channel quality indicator (CQI) matrices from previous time slot.
2: Initialize $t := 0, P_{u_l,l}^{(n)}(0) := \frac{P_{u_l}^{max}}{N}, \psi_{u_l,l}^{(n)}(0) := 0, \tilde{\psi}_{u_l,l}^{(n)}(0) := 0$ for $\forall u_l \in \mathcal{U}_l, n \in \mathcal{N}$.
3: **repeat**
4: Each UE u_l sends messages $\psi_{u_l,l}^{(n)}(t+1) = R_{u_l}^{(n)}(t) - \omega \left\langle R_{u_l}^{(j)}(t) + \psi_{u_l,l}^{(j)}(t) \right\rangle_{\kappa_{u_l} \setminus n} + (1-\omega)\left(R_{u_l}^{(n)}(t) + \tilde{\psi}_{u_l,l}^{(n)}(t) \right)$ to the relay $l \in \mathcal{L}$ for each RB $n \in \mathcal{N}$.
5: The relay $l \in \mathcal{L}$ sends messages $\tilde{\psi}_{u_l,l}^{(n)}(t+1) = -\omega \max_{\substack{i \in \mathcal{U}_l, \\ i \neq u_l}} \psi_{i,l}^{(n)}(t) - (1-\omega)\psi_{u_l,l}^{(n)}(t)$ to each associated UE $u_l \in \mathcal{U}_l$ for $\forall n \in \mathcal{N}$.
6: Each UE u_l computes the marginals as $\tau_{u_l,l}^{(n)}(t+1) = \psi_{u_l,l}^{(n)}(t) + \tilde{\psi}_{u_l,l}^{(n)}(t)$ for $\forall n \in \mathcal{N}$ and reports to the corresponding relay.
7: Each relay l calculates the RB and power allocation vector for each UE according to (3.24) and (3.26), respectively.
8: Calculate the aggregated achievable network rate as $R_l(t+1) := \sum_{u_l \in \mathcal{U}_l} R_{u_l}(t+1)$.
9: Update $t := t+1$.
10: **until** $t = T_{max}$ or the convergence criterion met (i.e., $\mathbf{abs}\{R_l(t+1) - R_l(t)\} < \varepsilon$, where ε is the tolerance for convergence).
11: Allocate resources (i.e., RB and transmit power) to the associated UEs for each relay.

Remark 3.1. *Since* $\mathbf{x_l}^*$ *satisfies the binary constraints, and the optimal allocation* $(\mathbf{x_l}^*, \mathbf{P_l}^*)$ *satisfies all the constraints in* **P2***, for a sufficient number of available RBs, the solution obtained by* **Algorithm 2** *gives a lower bound on the solution of the original RAP* **P2.1**.

3.2.2 Complexity Analysis

If the algorithm requires T iterations to converge, it is easy to verify that the time complexity at each relay $l \in \mathcal{L}$ is of $\mathcal{O}(T|\mathcal{U}_l|N)$. Similarly, considering a standard sorting algorithm (e.g., merge sort, heap sort) to generate the outputs $\langle v_{u_l}^{(j)} \rangle_{z \setminus n}$ for $\forall n$ with a worst-case complexity of $\mathcal{O}(N \log N)$, the overall time complexity at each UE is $\mathcal{O}\left(TN^2 \log N\right)$.

3.2.3 Convergence of the Algorithm and Optimality of the Solution

Proposition 3.1. *If the algorithm converges to a fixed point message, this point follows the slackness condition of* **P2.1***, and hence it becomes the optimal solution for the original RAP.*

Proof. See **Appendix B.2**. □

Proposition 3.2. *The message passing algorithm converges to a solution with zero duality gap as the number of resource blocks goes to infinity, i.e., dual problem of* **P2.1** *[e.g.,* $\mathcal{D}_l$*, given by (B.7)] has the same optimal objective function value [44].*

Proof. See **Appendix B.3**. □

3.2.4 End-to-End Delay for the Proposed Solution

I measure the total end-to-end delay due to relaying for the proposed framework as follows [45]:

$$\mathfrak{D}_{\text{2hop}} = \mathfrak{t}_{\text{schedule}} + \mathfrak{t}^{[1]}_{\text{delivery}} + \mathfrak{t}_{\text{decode}} + \mathfrak{t}^{[2]}_{\text{delivery}} \tag{3.28}$$

where $\mathfrak{t}_{\text{schedule}}$ is the time required to schedule the UEs and perform resource allocation, $\mathfrak{t}_{\text{decode}}$ is the decoding time at relay nodes before data packets are forwarded in second hop, and $\mathfrak{t}^{[j]}_{\text{delivery}} = \mathfrak{t}^{[j]}_{\text{transmit}} + \mathfrak{t}^{[j]}_{\text{pd}}$ is the sum of packet transmission time and propagation delay for hop $j \in \{1, 2\}$. While calculating delay using (3.28), I assume that each scheduled UE is ready to transmit data and the waiting time before transmission is zero (i.e., there is no queuing delay).

3.2.5 Implementation of Proposed Solution in a Practical LTE-A Scenario

Let $\boldsymbol{\psi}_{\boldsymbol{u_l}} = \left[\psi^{(1)}_{u_l}, \psi^{(2)}_{u_l}, \ldots, \psi^{(N)}_{u_l}\right]^{\mathsf{T}}$ and $\tilde{\boldsymbol{\psi}}_{\boldsymbol{u_l}} = \left[\tilde{\psi}^{(1)}_{u_l}, \tilde{\psi}^{(2)}_{u_l}, \ldots, \tilde{\psi}^{(N)}_{u_l}\right]^{\mathsf{T}}$ denote the message vectors for UE u_l. These messages can be mapped into standard LTE-A scheduling control messages as illustrated in Fig. 3.2. In an LTE-A system, UEs periodically sense the physical uplink control channel (PUCCH) and transmit known sequences using sounding reference signal (SRS). After reception of scheduling request (SR) from UEs, an L3 relay performs scheduling and resource allocation. After scheduling, the L3 relay allocates RB(s) and informs to the UEs by sending scheduling grant (SG) through physical downlink control channel (PDCCH). Once the allocation of RB(s) is received, the UEs periodically send the buffer status report (BSR) using PUCCH to the relay in order to update the resource requirement, and in response, the relay sends back an acknowledgment (ACK) in physical hybrid-ARQ indicator

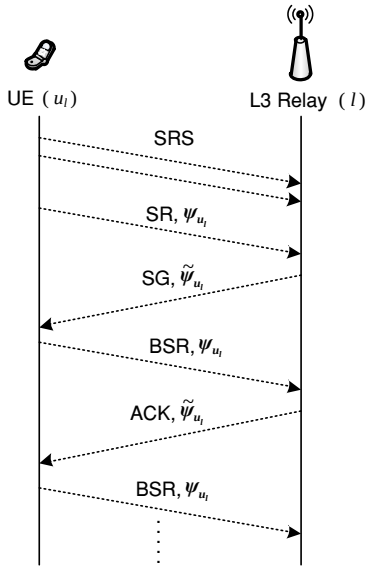

Figure 3.2: Possible implementation of the MP scheme in an LTE-A system.

channel (PHICH). Considering the above scenario, my proposed message passing approach can be implemented by incorporating $\boldsymbol{\psi_{u_l}}$ messages in SR and BSR, and $\tilde{\boldsymbol{\psi}}_{\boldsymbol{u_l}}$ messages in SG and ACK control signals, respectively.

3.3 Results

3.3.1 Convergence

In Fig. 3.3, I depict the convergence behavior of the proposed algorithm. In particular, I show the average achievable data rate versus the number of iterations. The average achievable rate R_{avg} for UEs is calculated as $R_{\text{avg}} = \frac{\sum_{u \in \{\mathcal{C} \cup \mathcal{D}\}} R_u^{\text{ach}}}{C+D}$ where R_u^{ach} is the achievable data rate for UE u. Note that the higher the number of users, the lower the average data rate.

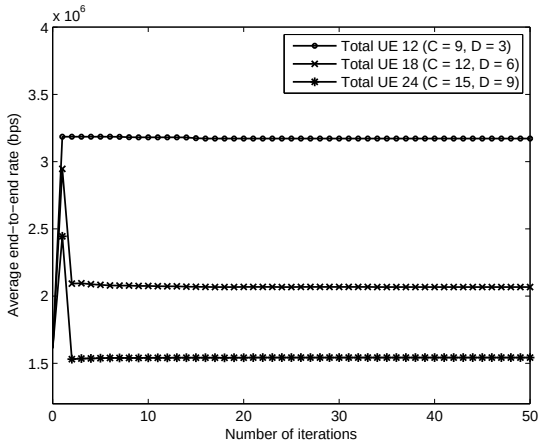

Figure 3.3: Convergence behavior of the proposed algorithm with different number of UEs: $D_{r,d} = 80$ meter, $D_{d,d} = 140$ meter.

3.3.2 Performance of Relay-aided D2D Communication

Average achievable data rate vs. distance between D2D UEs:

The average achievable data rate of D2D UEs for both the proposed and reference schemes is illustrated in Fig. 3.4. I find the similar trends in performance evaluation results with those observed in Chapter 2. For example, although the reference scheme outperforms when the distance between D2D UEs is small (i.e., $d < 70$ m), my proposed approach using MP scheme, which uses relays for D2D traffic, can greatly improve the data rate especially when the distance increases. This is due to the fact that when the distance increases, the performance of direct communication deteriorates due to increased signal attenuation. Besides, when the D2D UEs share resources with only one CUE, the spectrum may not be utilized efficiently, and therefore, the achievable rate decreases. As a result, the gap between the achievable rate with my proposed algorithm and that with the reference scheme becomes wider when the distance increases.

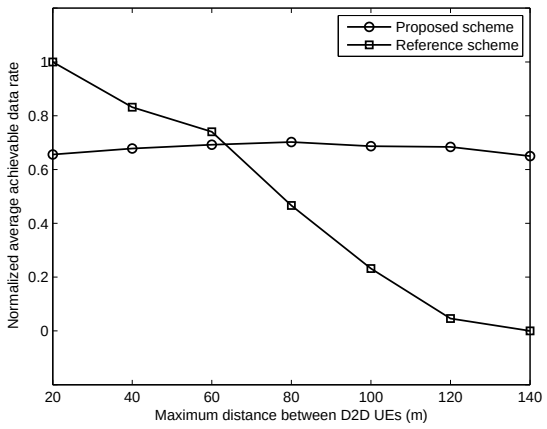

Figure 3.4: Average achievable data rate for both the proposed and reference schemes with varying distance between D2D UEs: number of CUE, $|\mathcal{C}| = 15$ and number of D2D pairs, $|\mathcal{D}| = 9$ (i.e., 5 CUE and 3 D2D-pairs are assisted by each relay, and hence $|\mathcal{U}_l| = 8$ for each relay). $D_{r,d}$ is considered 80 meter.

Gain in aggregated achievable data vs. varying distance between D2D UEs:

The gain in terms of aggregated achievable data rate is shown in Fig. 3.5(a). Similar to previous chapter, I calculate the rate gain using (2.18). In Fig. 3.5(b), I compare the rate gain with the asymptotic upper bound[2]. The figures show that, compared to direct communication, with the increasing distance between D2D UEs, relaying provides considerable gain in terms of achievable data rate and hence spectrum utilization. In addition, my proposed distributed solution performs nearly close to the upper bound.

[2]The asymptotic upper bound is obtained by solving the optimization problem **P2.2**, e.g., relaxing the constraint that an RB is used by only one UE by using the time-sharing factor [32]. Thus $x_{u_l}^{(n)} \in (0, 1]$ represents the sharing factor where each $x_{u_l}^{(n)}$ denotes the portion of time that RB n is assigned to UE u_l and satisfies the constraint $\sum_{u_l \in \mathcal{U}_l} x_{u_l}^{(n)} \leq 1, \ \forall n$.

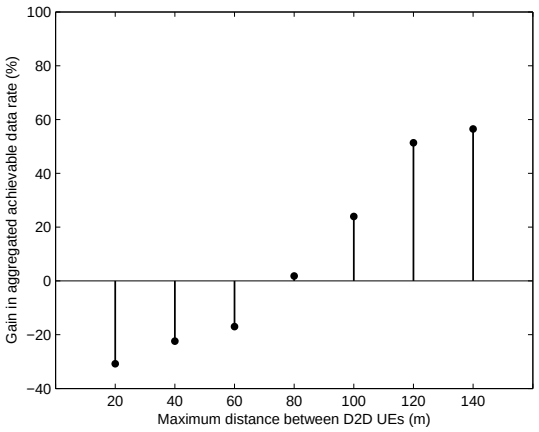

(a)

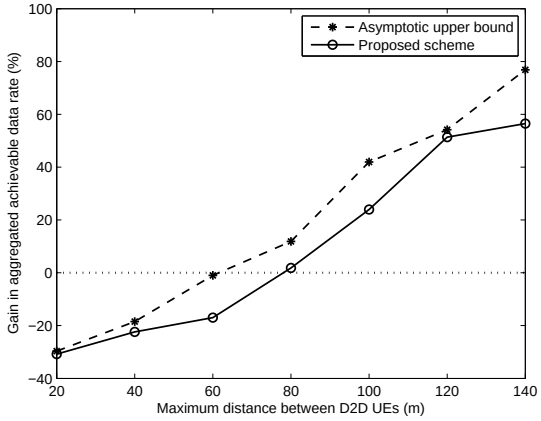

(b)

Figure 3.5: (a) Gain in aggregated achievable data rate and (b) Comparing gain with asymptotic upper bound using the similar setup of Fig. 3.4. There is a critical distance, beyond which relaying of D2D traffic provides significant performance gain.

Effect of relay-UE distance and distance between D2D UEs on rate gain:

The performance gain in terms of the achievable aggregated data rate under different relay-D2D UE distance is shown in Fig. 3.6. It is clear from the figure that, even for relatively large relay-D2D UE distances, e.g., $D_{r,d} \geq 80$ m, relaying D2D traffic provides considerable rate gain for distant D2D UEs.

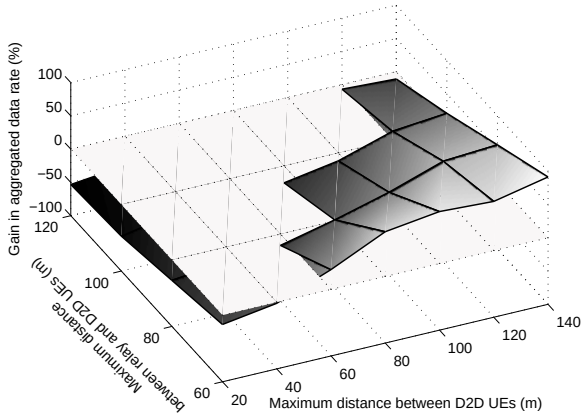

Figure 3.6: Effect of relay distance on rate gain: $|\mathcal{C}| = 15$, $|\mathcal{D}| = 9$. For every $D_{r,d}$, there is a distance threshold (i.e., upper side of the lightly shaded surface) beyond which relaying provides significant gain in terms of aggregated achievable rate.

Effect of number of D2D UEs and distance between D2D UEs on rate gain:

I vary the number of D2D UEs and plot the rate gain in Fig. 3.7 to observe the performance of my proposed scheme in a dense network. The figure suggests that even in a moderately dense situation (e.g., $|\mathcal{C}| + |\mathcal{D}| = 15 + 12 = 27$) my proposed method provides a higher rate compared to direct communication between distant D2D UEs.

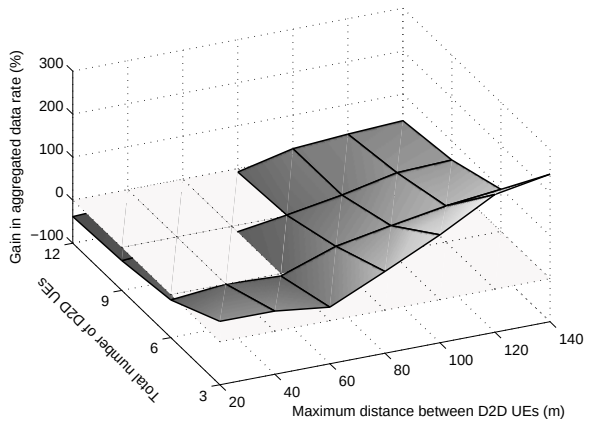

Figure 3.7: Effect of number of D2D UEs on rate gain: $|\mathcal{C}| = 15$, $D_{r,d} = 80$ meter. The upper position of lightly shaded surface illustrates the positive gain in terms of aggregated achievable rate.

Impact of relaying on delay:

In Fig. 3.8, I show results on the delay performance of the proposed relay-aided D2D communication approach. In particular, I observe the empirical complementary cumulative distribution function (CCDF)[3] for both the proposed scheme (which uses relay for D2D communication) and reference scheme (where D2D UEs communicate without relay). Note that in the reference scheme, the delay for one hop communication is given by $\mathfrak{D}_{1\text{hop}} = \mathfrak{t}_{\text{schedule}} + \mathfrak{t}_{\text{delivery}}$. The variation in end-to-end delay is experienced due to variation in achievable data rate and propagation delay at different values of $D_{r,d}$ and $D_{d,d}$. From this figure it can be observed that the relay-aided D2D communication increases the end-to-end delay. However, this increase (e.g., $0.431 - 0.189 = 0.242$ msec) of delay would be acceptable for many D2D applications.

[3]The empirical CCDF of delay is defined as $\widehat{\mathfrak{D}}_\eta(\mathtt{t}) = \frac{1}{\eta}\sum_{i=1}^{\eta}\mathbb{I}_{[\text{delay}_i > \mathtt{t}]}$ where η is the total number of distance observations (e.g., UE-relay distance for the proposed scheme and the distance between D2D UEs for the reference scheme, respectively) used in the simulation, delay_i is the end-to-end delay at i-th distance observation, and $\mathtt{t}$ represents the x-axis values in Fig. 3.8. The indicator function $\mathbb{I}_{[\cdot]}$ outputs 1 if the condition $[\cdot]$ is satisfied and 0 otherwise.

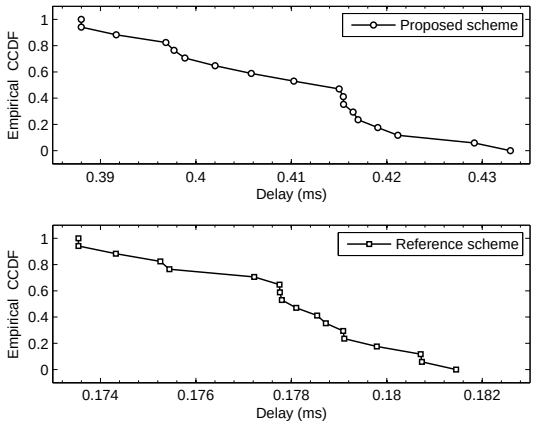

Figure 3.8: End-to-end delay for the proposed and reference scheme where $|\mathcal{C}| = 15$, $|\mathcal{D}| = 9$. I vary the distances $D_{r,d}$ and $D_{d,d}$ from 60 to 140 meter with 5 meter interval. The decoding delay at a relay node is assumed to be 0.173 millisecond (obtained from [45]).

3.4 Summary and Discussions

This chapter presented a comprehensive resource allocation framework for relay-assisted D2D communication. Due to the NP-hardness of original RAP, I have utilized the max-sum message passing strategy and presented a low-complexity distributed solution based on the message passing approach. The convergence and optimality of the proposed scheme have been proved. The performance of the proposed method has been evaluated through simulations and I have observed that after a distance margin, relaying of D2D traffic improves system performance and provides a better data rate to the D2D UEs at the cost of a small increase in end-to-end delay.

In the following chapters, I reformulate the RAP considering the uncertainties in the channel gains. Due to random nature of wireless channels, resource allocation schemes considering the link gain uncertainties in such relay-aided D2D communication is worth investigating for practical implementations.

Chapter 4

Resource Allocation Under Channel Uncertainties

In the previous two chapters, I have studied the performance of network-assisted D2D communications assuming the availability of perfect CSI and showed that relay-aided D2D communication provides significant performance gain for long distance D2D links. However, the assumption of perfect information availability is unrealistic for a practical wireless communication system. Considering the time-varying and random nature of wireless channel, in this chapter I extend the previous work utilizing the theory of *worst-case robust optimization*. To be specific, I formulate a robust RAP with an objective to maximizing the end-to-end rate (i.e., minimum achievable rate over two hops) for the UEs while maintaining the QoS (i.e., rate) requirements for cellular and D2D UEs under total power constraint at the relay node. The link gains, the interference among relay nodes, and interference at the receiving D2D UEs are not exactly known (i.e., estimated with an additive error). The robust problem formulation is observed to be convex, and therefore, I apply a gradient-based method to solve the problem distributively at each relay node with polynomial complexity.

I demonstrate that introducing robustness to deal with channel uncertainties affects the achievable network sum-rate. To reduce the cost of robustness defined as the corresponding reduction of achievable sum-rate, I utilize the *chance constraint approach* to achieve a trade-off between robustness and optimality by adjusting some protection functions.

The main contributions of this chapter can be summarized as follows:

- I analyze the performance of relay-assisted D2D communication under uncertain system parameters. The problem of RB and power allocation at the relay nodes for the CUEs and D2D UEs is formulated and solved for the globally optimal solution when perfect channel gain information for the different links is available.

- Assuming that the perfect channel information is unavailable, I formulate a robust RAP for relay-assisted D2D communication under uncertain channel information in both the hops and show that the convexity of the robust formulation is maintained. I propose a distributed algorithm with a polynomial time complexity.

- The cost of robust resource allocation is analyzed. In order to achieve a balance between the network performance and robustness, I provide a trade-off mechanism.

The rest of this chapter is organized as follows. In Section 4.2, I formulate the RB and power allocation problem for the nominal (i.e., non-robust) case. The robust RAP is formulated in Section 4.3. In order to allocate resources efficiently, I propose a robust distributed algorithm and discuss the robustness-optimality trade-off in Section 4.4. The performance evaluation results are presented in Section 4.5 and finally I conclude the chapter in Section 4.6.

4.1 Modeling the Channel Uncertainties in Wireless Systems

Uncertainty in the CSI (in particular the channel quality indicator [CQI] in an LTE-A system) can be modeled by sum of estimated CSI (i.e., the nominal value) and some additive error (the uncertain element). Accordingly, by using robust optimization theory, the nominal optimization problem (i.e., the optimization problem without considering uncertainty) is mapped to another optimization problem (i.e., the robust problem). To tackle uncertainty, two approaches have commonly been used in robust optimization theory. First, the *Bayesian approach* (Chapter 6.4 in [34]) considers the statistical knowledge of errors and satisfies the optimization constraints in a probabilistic manner. Second, the *worst-case approach* (Chapter 6.4 in [34], [46]) assumes that the error (i.e., uncertainty) is bounded in a closed set called the *uncertainty set* and satisfies the constraints for all realizations of the uncertainty in that set. Although the Bayesian approach has been widely used in the literature (e.g., in [47], [48]), the worst-case approach is more appropriate due to the fact that it satisfies the constraints in all error instances. By applying the worst-case approach, the size of the uncertainty set can be obtained from the statistics of error. As an example, the uncertainty set can be defined by a probability distribution function of uncertainty in such a way that all realizations of uncertainty remain within the uncertainty set with a given probability.

Applying robustness brings in new variables in the optimization problem, which may change the nominal formulation to a non-convex optimization problem and require excessive calculations to solve. To avoid this difficulty, the robust problem is converted to a convex optimization problem and solved in a traditional way.

4.2 Reformulation of the RAP : The Nominal Problem

In order to model the uncertainties in my model, I first modify some of the constraints the optimization problem **P2.2**. The resource optimization problem (given in Page 55) is known as *nominal problem* since no uncertainties is considered. In Section 4.3.1 I will extend this formulation to introduce the channel uncertainties.

Let the variable $I^{(n)}_{u_l,l,1}$ and $I^{(n)}_{l,u_l,2}$ denote the interference received by u_l over RB n in the first and second hop, respectively, and are given as follows:

$$I^{(n)}_{u_l,l,1} = \sum_{\forall u_j \in \mathcal{U}_j, j \neq l, j \in \mathcal{L}} x^{(n)}_{u_j} P^{(n)}_{u_j,j} g^{(n)}_{u_j,l,1} \tag{4.1}$$

$$I^{(n)}_{l,u_l,2} = \begin{cases} \sum\limits_{\forall u_j \in \{\mathcal{D} \cap \mathcal{U}_j\}, j \neq l, j \in \mathcal{L}} x^{(n)}_{u_j} P^{(n)}_{j,u_j} g^{(n)}_{j,eNB,2}, & u_l \in \{\mathcal{C} \cap \mathcal{U}_l\} \\ \sum\limits_{\forall u_j \in \mathcal{U}_j, j \neq l, j \in \mathcal{L}} x^{(n)}_{u_j} P^{(n)}_{j,u_j} g^{(n)}_{j,u_l,2}, & u_l \in \{\mathcal{D} \cap \mathcal{U}_l\}. \end{cases} \tag{4.2}$$

Using (4.1) and (4.2) I can express the unit power SINR for the first hop,

$$\gamma^{(n)}_{u_l,l,1} = \frac{h^{(n)}_{u_l,l,1}}{I^{(n)}_{u_l,l,1} + \sigma^2} \tag{4.3}$$

and the unit power SINR for the second hop,

$$\gamma^{(n)}_{l,u_l,2} = \begin{cases} \frac{h^{(n)}_{l,eNB,2}}{I^{(n)}_{l,u_l,2} + \sigma^2}, & u_l \in \{\mathcal{C} \cap \mathcal{U}_l\} \\ \frac{h^{(n)}_{l,u_l,2}}{I^{(n)}_{l,u_l,2} + \sigma^2}, & u_l \in \{\mathcal{D} \cap \mathcal{U}_l\} \end{cases} \tag{4.4}$$

Hence the data rate of u_l over RB n is given by

$$R^{(n)}_{u_l} = \frac{1}{2} \min \left\{ B_{RB} \log_2 \left(1 + P^{(n)}_{u_l,l} \gamma^{(n)}_{u_l,l,1}\right), B_{RB} \log_2 \left(1 + P^{(n)}_{l,u_l} \gamma^{(n)}_{l,u_l,2}\right) \right\}$$

which can be equivalently expressed as expressed as

$$R_{u_l}^{(n)} = \frac{1}{2} B_{RB} \log_2 \left(1 + P_{u_l,l}^{(n)} \gamma_{u_l,l,1}^{(n)}\right). \tag{4.5}$$

4.2.1 Formulation of the Nominal RAP

Utilizing the time-sharing concept (e.g., $x_{u_l}^{(n)} \in (0,1]$ denotes the portion of time that RB n is assigned to UE u_l and satisfies the constraint $\sum_{u_l \in \mathcal{U}_l} x_{u_l}^{(n)} \leq 1,\ \forall n.$) introduced in Section 2.3.3, I can state the nominal problem as follows:

(**P4.1**)

$$\max_{x_{u_l}^{(n)}, S_{u_l,l}^{(n)}, \omega_{u_l}^{(n)}} \sum_{u_l \in \mathcal{U}_l} \sum_{n=1}^{N} \frac{1}{2} x_{u_l}^{(n)} B_{RB} \log_2 \left(1 + \frac{S_{u_l,l}^{(n)} h_{u_l,l,1}^{(n)}}{x_{u_l}^{(n)} \omega_{u_l}^{(n)}}\right)$$

$$\text{subject to} \quad \sum_{u_l \in \mathcal{U}_l} x_{u_l}^{(n)} \leq 1, \quad \forall n \tag{4.6a}$$

$$\sum_{n=1}^{N} S_{u_l,l}^{(n)} \leq P_{u_l}^{max}, \forall u_l \tag{4.6b}$$

$$\sum_{u_l \in \mathcal{U}_l} \sum_{n=1}^{N} \frac{h_{u_l,l,1}^{(n)}}{h_{l,u_l,2}^{(n)}} S_{u_l,l}^{(n)} \leq P_l^{max} \tag{4.6c}$$

$$\sum_{u_l \in \mathcal{U}_l} S_{u_l,l}^{n} g_{u_l^*,l,1}^{(n)} \leq I_{th,1}^{(n)}, \quad \forall n \tag{4.6d}$$

$$\sum_{u_l \in \mathcal{U}_l} \frac{h_{u_l,l,1}^{(n)}}{h_{l,u_l,2}^{(n)}} S_{u_l,l}^{(n)} g_{l,u_l^*,2}^{(n)} \leq I_{th,2}^{(n)}, \quad \forall n \tag{4.6e}$$

$$\sum_{n=1}^{N} \frac{1}{2} x_{u_l}^{(n)} B_{RB} \log_2 \left(1 + \frac{S_{u_l,l}^{(n)} h_{u_l,l,1}^{(n)}}{x_{u_l}^{(n)} \omega_{u_l}^{(n)}}\right) \geq Q_{u_l}, \quad \forall u_l \tag{4.6f}$$

$$S_{u_l,l}^{(n)} \geq 0, \quad \forall n, u_l \tag{4.6g}$$

$$I_{u_l,l}^{(n)} + \sigma^2 \leq \omega_{u_l}^{(n)}, \forall n, u_l \tag{4.6h}$$

where $\omega_{u_l}^{(n)}$ is an auxiliary variable for u_l over RB n and let $I_{u_l,l}^{(n)} = \max\left\{I_{u_l,l,1}^{(n)}, I_{l,u_l,2}^{(n)}\right\}$. Since the objective function is concave, the constraint in (4.6f) is convex, and all the

remaining constraints are affine, the optimization problem **P4.1** is convex. Due to convexity of the optimization problem **P4.1**, there exists a unique optimal solution.

Statement 4.1. *(a) The power allocation for UE u_l over RB n is given by*

$$P_{u_l,l}^{(n)*} = \frac{S_{u_l,l}^{(n)*}}{x_{u_l}^{(n)*}} = \left[\delta_{u_l,l}^{(n)} - \frac{\omega_{u_l}^{(n)}}{h_{u_l,l,1}^{(n)}}\right]^+ \tag{4.7}$$

where $\delta_{u_l,l}^{(n)} = \frac{\frac{1}{2}B_{RB}\frac{(1+\lambda_{u_l})}{\ln 2}}{\rho_{u_l} + \frac{h_{u_l,l,1}^{(n)}}{h_{l,u_l,2}^{(n)}}\nu_l + g_{u_l^*,l,1}^{(n)}\psi_n + \frac{h_{u_l,l,1}^{(n)}}{h_{l,u_l,2}^{(n)}}g_{l,u_l^*,2}^{(n)}\varphi_n}$ *and* $[\epsilon]^+ = \max\{\epsilon, 0\}$.

(b) The RB allocation is determined as follows:

$$x_{u_l}^{(n)*} = \begin{cases} 1, & \mu_n \leq \chi_{u_l,l}^{(n)} \\ 0, & \mu_n > \chi_{u_l,l}^{(n)} \end{cases} \tag{4.8}$$

and $\chi_{u_l,l}^{(n)}$ *is defined as*

$$\chi_{u_l,l}^{(n)} = \tfrac{1}{2}(1+\lambda_{u_l})B_{RB}\left[\log_2\left(1 + \frac{S_{u_l,l}^{(n)}h_{u_l,l,1}^{(n)}}{x_{u_l}^{(n)}\omega_{u_l}^{(n)}}\right) - \theta_{u_l,l}^{(n)}\right] \tag{4.9}$$

where $\theta_{u_l,l}^{(n)} = \frac{S_{u_l,l}^{(n)}\gamma_{u_l,l,1}^{(n)}}{\left(x_{u_l}^{(n)}\omega_{u_l}^{(n)} + S_{u_l,l}^{(n)}\gamma_{u_l,l,1}^{(n)}\right)\ln 2}$.

Proof. See **Appendix C.1**. □

In the above problem formulation it is assumed that each of the relays and D2D UEs has the perfect information about the experienced interference. Also, the channel gains between the relay and the other UEs (associated with neighbouring relays) are known to the relay. However, estimating the exact values of link gains is not easy in practice. To deal with the uncertainties in the estimated values, in the following I apply the worst-case robust optimization method [49].

4.3 Robust Resource Allocation

4.3.1 Formulation of Robust Problem

Let the vector of link gains between relay l and other transmitting UEs (associated with other relays, i.e., for $\forall j \in \mathcal{L}, j \neq l$) in the first hop over RB n be denoted by $\mathbf{g}_{l,1}^{(n)} = \left[g_{1^*,l,1}^{(n)},\ g_{2^*,l,1}^{(n)}, \cdots,\ g_{|\mathcal{U}_l|^*,l,1}^{(n)}\right]$, where $|\mathcal{U}_l|$ is the total number of UEs associated with relay l. Similarly, the vector of link gains between relay l and receiving D2D UEs (associated with other relays) in the second hop over RB n is given by $\mathbf{g}_{l,2}^{(n)} = \left[g_{l,1^*,2}^{(n)},\ g_{l,2^*,2}^{(n)}, \cdots,\ g_{l,|\mathcal{U}_l|^*,2}^{(n)}\right]$.

I assume that the link gains and the aggregated interference (i.e., $I_{u_l,l}^{(n)}, \forall n, u_l$ and elements of $\mathbf{g}_{l,1}^{(n)}, \mathbf{g}_{l,2}^{(n)}, \forall n$) are unknown but are bounded in a region (i.e., uncertainty set) with a given probability. For example, the channel gain in the first hop is bounded in $\Re_{g_{l,1}}^{(n)}$, with estimated value $\bar{\mathbf{g}}_{l,1}^{(n)}$ and the bounded error $\hat{\mathbf{g}}_{l,1}^{(n)}$, i.e., $\mathbf{g}_{l,1}^{(n)} = \bar{\mathbf{g}}_{l,1}^{(n)} + \hat{\mathbf{g}}_{l,1}^{(n)}$, and $\mathbf{g}_{l,1}^{(n)} \in \Re_{g_{l,1}}^{(n)}, \forall n \in \mathcal{N}$, where $\Re_{g_{l,1}}^{(n)}$ is the uncertainty set for $\mathbf{g}_{l,1}^{(n)}$. Similarly, let $\Re_{g_{l,2}}^{(n)},\ \forall n$ be the uncertainty set for the link gains in the second hop and $\Re_{I_{u_l,l}}^{(n)},\ \forall n, u_l$ be the uncertainty set for interference level.

In the formulation of robust problem, I utilize a similar rate expression [i.e., equation (4.5)] as the one used in the nominal problem formulation. Although dealing with similar utility function (i.e., rate equation) for both nominal and robust problems is quite common in literature (e.g., in [50–52]), when perfect channel information is not available to receiver nodes, the rate obtained by (4.5) actually approximates the achievable rate[1]. The solution to **P4.12** is robust against uncertainties if and only if for any realization of $\mathbf{g}_{l,1}^{(n)} \in \Re_{g_{l,1}}^{(n)}, \mathbf{g}_{l,2}^{(n)} \in \Re_{g_{l,2}}^{(n)}$, and $I_{u_l,l}^{(n)} \in \Re_{I_{u_l,l}}^{(n)}$, the optimal

[1]According to information-theoretic capacity analysis, in presence of channel uncertainties at the receiver, the lower and upper bounds of the rate are given by equations (46) and (49) in [53], respectively. However, for mathematical tractability, I resort to (4.5) to calculate the achievable data rate in both the nominal and robust problem formulations.

solution satisfies the constraints in (4.6d), (4.6e), and (4.6h). Therefore, the robust counterpart of **P4.1** is represented as

(**P4.2**)

$$\max_{x_{u_l}^{(n)}, S_{u_l,l}^{(n)}, \omega_{u_l}^{(n)}} \sum_{u_l \in \mathcal{U}_l} \sum_{n=1}^{N} \frac{1}{2} x_{u_l}^{(n)} B_{RB} \log_2 \left(1 + \frac{S_{u_l,l}^{(n)} h_{u_l,l,1}^{(n)}}{x_{u_l}^{(n)} \omega_{u_l}^{(n)}} \right)$$

subject to (4.6a), (4.6b), (4.6c), (4.6d),

(4.6e), (4.6f), (4.6g), (4.6h)

$$\text{and} \quad \mathbf{g}_{l,1}^{(n)} \in \Re_{g_{l,1}}^{(n)}, \quad \mathbf{g}_{l,2}^{(n)} \in \Re_{g_{l,2}}^{(n)}, \quad \forall n \tag{4.10a}$$

$$I_{u_l,l}^{(n)} \in \Re_{I_{u_l,l}}^{(n)}, \ \forall n, \forall u_l \tag{4.10b}$$

where the constraints in (4.10a) and (4.10b) represent the requirements for the robustness of the solution.

Proposition 4.1. *When $\Re_{g_{l,1}}^{(n)}, \Re_{g_{l,2}}^{(n)}$, and $\Re_{I_{u_l,l}}$ are compact and convex sets,* **P4.2** *is a convex optimization problem.*

Proof. See **Appendix C.2**. □

The problem **P4.1** is the nominal problem of **P4.2** where it is assumed that the perfect channel state information is available, i.e., the estimated values are considered as exact values. With the inclusion of uncertainty in (4.6d), (4.6e), and (4.6h), the constraints in the optimization problem **P4.2** are still affine. In order to express the constraints in closed-form (i.e., to avoid using the uncertainty set), in the following, I utilize the notion of protection function [49, 54] instead of uncertainty set.

4.3.2 Uncertainty Set and Protection Function

From **P4.2**, the optimization problem is impacted by the uncertainty sets $\Re_{g_{l,1}}^{(n)}, \Re_{g_{l,2}}^{(n)}$, and $\Re_{I_{u_l,l}}^{(n)}$. To obtain the robust formulation, I consider that the uncertainty sets

for the uncertain parameters are based on the differences between the actual (i.e., uncertain) and nominal (i.e., without considering uncertainty) values. These differences can be mathematically represented by general norms [54]. For example, the uncertainty sets for channel gain in the first and second hops for $\forall n \in \mathcal{N}$ are given by

$$\Re_{g_{l,1}}^{(n)} = \left\{ \mathbf{g}_{l,1}^{(n)} | \parallel \mathbf{M}_{g_{l,1}}^{(n)} \cdot \left(\mathbf{g}_{l,1}^{(n)} - \bar{\mathbf{g}}_{l,1}^{(n)} \right)^{\mathsf{T}} \parallel \leq \Psi_{l,1}^{(n)} \right\} \tag{4.11a}$$

$$\Re_{g_{l,2}}^{(n)} = \left\{ \mathbf{g}_{l,2}^{(n)} | \parallel \mathbf{M}_{g_{l,2}}^{(n)} \cdot \left(\mathbf{g}_{l,2}^{(n)} - \bar{\mathbf{g}}_{l,2}^{(n)} \right)^{\mathsf{T}} \parallel \leq \Psi_{l,2}^{(n)} \right\} \tag{4.11b}$$

where $\| \cdot \|$ denotes the general norm, $\Psi_{l,1}^{(n)}$ and $\Psi_{l,2}^{(n)}$ represent the bound on the uncertainty set; $\mathbf{g}_{l,1}^{(n)}$, $\mathbf{g}_{l,2}^{(n)}$ are the actual and $\bar{\mathbf{g}}_{l,1}^{(n)}$, $\bar{\mathbf{g}}_{l,2}^{(n)}$ are the estimated (i.e., nominal) channel gain vectors; $\mathbf{M}_{g_{l,1}}^{(n)}$ and $\mathbf{M}_{g_{l,2}}^{(n)}$ are the invertible $\Re^{|\mathcal{U}_l| \times |\mathcal{U}_l|}$ weight matrices for the first and second hop, respectively. Likewise, the uncertainty set for the experienced interference is expressed as

$$\Re_{I_{u_l,l}}^{(n)} = \left\{ I_{u_l,l}^{(n)} | \parallel M_{I_{u_l,l}}^{(n)} \cdot \left(I_{u_l,l}^{(n)} - \bar{I}_{u_l,l}^{(n)} \right) \parallel \leq \Upsilon_{u_l}^{(n)} \right\} \tag{4.12}$$

where $I_{u_l,l}^{(n)}$ and $\bar{I}_{u_l,l}^{(n)}$ are the actual and estimated interference levels, respectively; the variable $M_{I_{u_l,l}}^{(n)}$ denotes weight and $\Upsilon_{u_l}^{(n)}$ is the upper bound on the uncertainty set.

In the proof of **Proposition 4.1** (refer to Page 125), the terms

$$\Delta_{g_{l,1}}^{(n)} = \max_{\mathbf{g}_{l,1}^{(n)} \in \Re_{g_{l,1}}^{(n)}} \sum_{u_l \in \mathcal{U}_l} S_{u_l,l}^{(n)} \left(g_{u_l^*,l,1}^{(n)} - \bar{g}_{u_l^*,l,1}^{(n)} \right) \tag{4.13a}$$

$$\Delta_{g_{l,2}}^{(n)} = \max_{\mathbf{g}_{l,2}^{(n)} \in \Re_{g_{l,2}}^{(n)}} \sum_{u_l \in \mathcal{U}_l} \frac{h_{u_l,l,1}^{(n)}}{h_{l,u_l,2}^{(n)}} S_{u_l,l}^{(n)} \left(g_{l,u_l^*,2}^{(n)} - \bar{g}_{l,u_l^*,2}^{(n)} \right) \tag{4.13b}$$

$$\Delta_{I_{u_l,l}}^{(n)} = \max_{I_{u_l,l}^{(n)} \in \Re_{I_{u_l,l}}^{(n)}} \left(I_{u_l,l}^{(n)} - \bar{I}_{u_l,l}^{(n)} \right) \tag{4.13c}$$

are called protection functions for constraint (4.6d), (4.6e), and (4.6h), respectively, whose value (i.e., protection value) depends on the uncertain parameters. Using the protection function, the optimization problem can be rewritten as (**P4.3**)

$$\max_{x_{u_l}^{(n)}, S_{u_l,l}^{(n)}, \omega_{u_l}^{(n)}} \sum_{u_l \in \mathcal{U}_l} \sum_{n=1}^{N} \frac{1}{2} x_{u_l}^{(n)} B_{RB} \log_2 \left(1 + \frac{S_{u_l,l}^{(n)} h_{u_l,l,1}^{(n)}}{x_{u_l}^{(n)} \omega_{u_l}^{(n)}} \right)$$

subject to (4.6a), (4.6b), (4.6c), (4.6f), (4.6g) and

$$\sum_{u_l \in \mathcal{U}_l} S_{u_l,l}^{(n)} \bar{g}_{u_l^*,l,1}^{(n)} + \Delta_{g_{l,1}}^{(n)} \leq I_{th,1}^{(n)}, \quad \forall n \tag{4.14a}$$

$$\sum_{u_l \in \mathcal{U}_l} \frac{h_{u_l,l,1}^{(n)}}{h_{l,u_l,2}^{(n)}} S_{u_l,l}^{(n)} \bar{g}_{l,u_l^*,2}^{(n)} + \Delta_{g_{l,2}}^{(n)} \leq I_{th,2}^{(n)}, \quad \forall n \tag{4.14b}$$

$$\bar{I}_{u_l,l}^{(n)} + \Delta_{I_{u_l,l}}^{(n)} + \sigma^2 \leq \omega_{u_l}^{(n)}, \forall n, u_l \tag{4.14c}$$

where $\Delta_{g_{l,1}}^{(n)}, \Delta_{g_{l,2}}^{(n)}$, and $\Delta_{I_{u_l,l}}^{(n)}$ are defined by (4.13a), (4.13b), and (4.13c), respectively.

Proposition 4.2. *The protection functions for the uncertainty sets represented by general norms [i.e., by (4.11a), (4.11b), and (4.12)] are*

$$\Delta_{g_{l,1}}^{(n)} = \Psi_{l,1}^{(n)} \parallel \mathbf{M}_{g_{l,1}}^{(n)\,-1} \cdot \left(\mathbf{S}_{l,1}^{(n)} \right)^{\mathsf{T}} \parallel^* \tag{4.15a}$$

$$\Delta_{g_{l,2}}^{(n)} = \Psi_{l,2}^{(n)} \parallel \mathbf{M}_{g_{l,2}}^{(n)\,-1} \cdot \left(\mathbf{H}_{l}^{(n)} \cdot \mathbf{S}_{l,1}^{(n)} \right)^{\mathsf{T}} \parallel^* \tag{4.15b}$$

$$\Delta_{I_{u_l,l}}^{(n)} = \Upsilon_{u_l}^{(n)} \parallel M_{I_{u_l,l}}^{(n)\,-1} \cdot I_{u_l,l}^{(n)} \parallel^* \tag{4.15c}$$

where $\mathbf{S}_{l,1}^{(n)} = \left[S_{1,l}^{(n)},\ S_{2,l}^{(n)}, \cdots,\ S_{|\mathcal{U}_l|,l}^{(n)} \right]$, $\mathbf{H}_{l}^{(n)} = \left[\frac{h_{1,l,1}^{(n)}}{h_{l,1,2}^{(n)}},\ \frac{h_{2,l,1}^{(n)}}{h_{l,2,2}^{(n)}}, \cdots,\ \frac{h_{|\mathcal{U}_l|,l,1}^{(n)}}{h_{l,|\mathcal{U}_l|,2}^{(n)}} \right]$ *and* $\| \cdot \|^*$ *is the dual norm of* $\| \cdot \|$.

Proof. See **Appendix C.3**. □

Since the dual norm is a convex function, the convexity of **P4.3** is preserved. In addition, when the uncertainty set for any vector $\mathbf{y}$ is a linear norm defined by $\| \mathbf{y} \|_\alpha = (\sum \mathbf{abs}\{y\}^\alpha)^{\frac{1}{\alpha}}$ with order $\alpha \geq 2$, where $\mathbf{abs}\{y\}$ is the absolute value of y and

the dual norm is a linear norm with order $\beta = 1 + \frac{1}{\alpha - 1}$. In such cases, the protection function can be defined as a linear norm of order β. Therefore, the protection function becomes a deterministic function of the optimization variables (i.e., $x_{u_l}^{(n)}, S_{u_l,l}^{(n)}$, and $\omega_{u_l}^{(n)}$), and the non-linear max function is eliminated from the protection functions [i.e., from constraint (4.14a), (4.14b), and (4.14c)]. Consequently, the RAP turns out to be a standard form of convex optimization problem as presented below

(**P4.4**)

$$\max_{x_{u_l}^{(n)}, S_{u_l,l}^{(n)}, \omega_{u_l}^{(n)}} \sum_{u_l \in \mathcal{U}_l} \sum_{n=1}^{N} \frac{1}{2} x_{u_l}^{(n)} B_{RB} \log_2 \left(1 + \frac{S_{u_l,l}^{(n)} h_{u_l,l,1}^{(n)}}{x_{u_l}^{(n)} \omega_{u_l}^{(n)}} \right)$$

$$\text{subject to} \quad \sum_{u_l \in \mathcal{U}_l} x_{u_l}^{(n)} \leq 1, \qquad \forall n \quad (4.16a)$$

$$\sum_{n=1}^{N} S_{u_l,l}^{(n)} \leq P_{u_l}^{max}, \ \forall u_l \quad (4.16b)$$

$$\sum_{u_l \in \mathcal{U}_l} \sum_{n=1}^{N} \frac{h_{u_l,l,1}^{(n)}}{h_{l,u_l,2}^{(n)}} S_{u_l,l}^{(n)} \leq P_l^{max} \quad (4.16c)$$

$$\sum_{u_l \in \mathcal{U}_l} S_{u_l,l}^{(n)} \bar{g}_{u_l^*,l,1}^{(n)} + \Psi_{l,1}^{(n)} \left(\sum_{k=1}^{|\mathcal{U}_l|} \left({\mathbf{M}_{g_{l,1}}^{(n)}}^{-1}(k,:) \cdot \mathbf{S}_{l,1}^{(n)} \right)^{\beta} \right)^{\frac{1}{\beta}} \leq I_{th,1}^{(n)}, \quad \forall n \quad (4.16d)$$

$$\sum_{u_l \in \mathcal{U}_l} \frac{h_{u_l,l,1}^{(n)}}{h_{l,u_l,2}^{(n)}} S_{u_l,l}^{(n)} \bar{g}_{l,u_l^*,2}^{(n)} + \Psi_{l,2}^{(n)} \left(\sum_{k=1}^{|\mathcal{U}_l|} \left({\mathbf{M}_{g_{l,2}}^{(n)}}^{-1}(k,:) \cdot \left(\mathbf{H}_l^{(n)} \cdot \mathbf{S}_{l,1}^{(n)} \right) \right)^{\beta} \right)^{\frac{1}{\beta}} \leq I_{th,2}^{(n)}, \quad \forall n \quad (4.16e)$$

$$\sum_{n=1}^{N} \frac{1}{2} x_{u_l}^{(n)} B_{RB} \log_2 \left(1 + \frac{S_{u_l,l}^{(n)} h_{u_l,l,1}^{(n)}}{x_{u_l}^{(n)} \omega_{u_l}^{(n)}} \right) \geq Q_{u_l}, \quad \forall u_l \quad (4.16f)$$

$$S_{u_l,l}^{(n)} \geq 0, \qquad \forall n, u_l \quad (4.16g)$$

$$\bar{I}_{u_l,l}^{(n)} + \Delta_{I_{u_l,l}}^{(n)} + \sigma^2 \leq \omega_{u_l}^{(n)}, \quad \forall n, u_l \quad (4.16h)$$

where $\Delta_{I_{u_l,l}}^{(n)} = \Upsilon_{u_l}^{(n)} \| \ {M_{I_{u_l,l}}^{(n)}}^{-1} \cdot I_{u_l,l}^{(n)} \ \|_{\beta}$ and $\mathbf{A}(j,:)$ denotes the j-th row of matrix $\mathbf{A}$.

In the LTE-A system, which exploits orthogonal frequency-division multiplexing (OFDM) for radio access, fading can be considered uncorrelated across RBs [55, Chapter 1]; hence, it can be assumed that uncertainty and channel gain in each

element of $\mathbf{g}_{l,1}^{(n)}$ and $\mathbf{g}_{l,2}^{(n)}$ are i.i.d. random variables [56]. Therefore, $\mathbf{M}_{g_{l,1}}^{(n)}$ and $\mathbf{M}_{g_{l,2}}^{(n)}$ become a diagonal matrix. Note that for any diagonal matrix $\mathbf{A}$ with j-th diagonal element a_{jj}, the vector $\mathbf{A}^{-1}(j,:)$ contains only non-zero elements $\frac{1}{a_{jj}}$. In addition, since the channel uncertainties are random, a commonly used approach is to represent the uncertainty set by an ellipsoid, i.e., the linear norm with $\alpha = 2$ so that the dual norm is a linear norm with $\beta = 2$ [57, 58]. Hence, problem **P4.4** turns to a conic quadratic programming problem [59]. In order to solve **P4.4** efficiently, a distributed gradient-aided algorithm is developed in the following section.

4.4 Robust Distributed Algorithm

4.4.1 Algorithm Development

Statement 4.2. *(a) The optimal power allocation for u_l over RB n is given by the following water-filling equation:*

$$P_{u_l,l}^{(n)*} = \frac{S_{u_l,l}^{(n)*}}{x_{u_l}^{(n)*}} = \left[\delta_{u_l,l}^{(n)} - \frac{\omega_{u_l}^{(n)}}{h_{u_l,l,1}^{(n)}}\right]^+ \tag{4.17}$$

where $\delta_{u_l,l}^{(n)}$ is given by

$$\delta_{u_l,l}^{(n)} = \frac{\frac{1}{2}B_{RB}\frac{(1+\lambda_{u_l})}{\ln 2}}{\rho_{u_l} + \nu_l \frac{h_{u_l,l,1}^{(n)}}{h_{l,u_l,2}^{(n)}} + \psi_n\left(\bar{g}_{u_l^*,l,1}^{(n)} + \Psi_{l,1}^{(n)} m_{u_l u_{l g_{l,1}}}^{(n)}\right) + \varphi_n \frac{h_{u_l,l,1}^{(n)}}{h_{l,u_l,2}^{(n)}}\left(\bar{g}_{l,u_l^*,2}^{(n)} + \Psi_{l,2}^{(n)} m_{u_l u_{l g_{l,2}}}^{(n)}\right)}. \tag{4.18}$$

(b) The RB allocation for u_l over RB n is obtained by (4.8).

Proof. See **Appendix C.4**. □

Based on **Statement 4.2**, I utilize a gradient-based method (given in **Appendix**

C.5) to update the variables. Each relay independently performs the resource allocation and allocates resources to the associated UEs. For completeness, the distributed joint RB and power allocation algorithm is summarized in **Algorithm 3**.

Algorithm 3 Joint RB and power allocation algorithm

1: Each relay $l \in \mathcal{L}$ estimates the reference gain $\bar{g}^{(n)}_{u_l^*,l,1}$ and $\bar{g}^{(n)}_{u_l^*,l,2}$ from previous time slot $\forall u_l \in \mathcal{U}_l$ and $n \in \mathcal{N}$.
2: Initialize Lagrange multipliers to some positive value and set $t := 0$, $S^{(n)}_{u_l,l} := \frac{P^{max}_{u_l}}{N}$ $\forall u_l, n$.
3: **repeat**
4: Set $t := t + 1$.
5: Calculate $x^{(n)}_{u_l}$ and $S^{(n)}_{u_l,l}$ for $\forall u_l, n$ using (4.8) and (4.17).
6: Update the Lagrange multipliers by (C.7a)–(C.7h) (see Page 128) and calculate the aggregated achievable network rate as $R_l(t) := \sum_{u_l \in \mathcal{U}_l} R_{u_l}(t)$.
7: **until** $t = T_{max}$ or the convergence criterion met (i.e., $\mathbf{abs}\{R_l(t) - R_l(t-1)\} < \varepsilon$, where ε is the tolerance for convergence).
8: Allocate resources (i.e., RB and transmit power) to associated UEs for each relay and calculate the average achievable data rate.

As I have mentioned in Chapter 2, the L3 relays are able to perform their own scheduling (unlike L1 and L2 relays in [15]) as an eNB. These relays can obtain information such as the transmission power allocation at the other relays, channel gain information, etc. by using the X2 interface [30, Section 7] defined in the 3GPP specifications. In particular, a separate load indication procedure is used over the X2 interface for interface management (for details refer to [30] and references therein). As a result, the relays can obtain the channel state information without increasing signaling overhead at the eNB.

4.4.2 Complexity Analysis

Proposition 4.3. *Using a small step size in gradient-based updating, the proposed algorithm achieves a sum-rate such that the difference in the sum rate in successive*

iterations is less than an arbitrary $\varepsilon > 0$ with a polynomial computation complexity in $|\mathcal{U}_l|$ and N.

Proof. See **Appendix C.6**. □

4.4.3 Cost of Robust Resource Allocation

An important issue in robust resource allocation is the substantial reduction in the achievable network sum-rate. Reduction of achievable sum-rate due to introducing robustness is measured by $\mathcal{R}_\Delta = \| R^* - R^*_\Delta \|_2$, where R^* and R^*_Δ are the optimal achievable sum-rates obtained by solving the nominal and the robust problem, respectively.

Proposition 4.4. *Let $\boldsymbol{\psi}^*$, $\boldsymbol{\varphi}^*$, $\boldsymbol{\varrho}^*$ be the optimal values of Lagrange multipliers for constraint (4.6d), (4.6e), and (4.6h) in* **P4.1**, *respectively. For all values of $\Delta^{(n)}_{g_{l,1}}, \Delta^{(n)}_{g_{l,2}}$, and $\Delta^{(n)}_{I_{u_l,l}}$ the reduction of achievable sum rate can be approximated as*

$$\mathcal{R}_\Delta \approx \sum_{n=1}^{N} \psi^*_n \Delta^{(n)}_{g_{l,1}} + \sum_{n=1}^{N} \varphi^*_n \Delta^{(n)}_{g_{l,2}} + \sum_{u_l \in \mathcal{U}_l} \sum_{n=1}^{N} \varrho^{n*}_{u_l} \Delta^{(n)}_{I_{u_l,l}}. \tag{4.19}$$

Proof. See **Appendix C.7**. □

From **Proposition 4.4**, the value of $\mathcal{R}_\Delta$ depends on the uncertainty set and by adjusting the size of $\Delta^{(n)}_{g_{l,1}}$ and $\Delta^{(n)}_{g_{l,2}}$, $\mathcal{R}_\Delta$ can be controlled.

4.4.4 Trade-off Between Robustness and Achievable Sum-rate

The robust worst-case resource allocation dealing with channel uncertainties is very conservative and often leads to inefficient utilization of resources. In practice, uncertainty does not always correspond to its worst-case and in many instances the robust

worst-case resource allocation may not be necessary. In such cases, it is desirable to achieve a trade-off between robustness and network sum-rate. This can be achieved through modifying the worst-case approach, where the uncertainty set is chosen in such a way that the probability of violating the interference threshold in both the hops is kept below a predefined level, and the network sum-rate is kept close to optimal value of nominal case. Therefore, I modify the constraints (4.6d) and (4.6e) in **P4.1** as

$$\mathbb{P}\left(\sum_{u_l\in\mathcal{U}_l} S_{u_l,l}^{(n)} g_{u_l^*,l,1}^{(n)} \geq I_{th,1}^{(n)}\right) \leq \Theta_{l,1}^{(n)}, \quad \forall n \tag{4.20a}$$

$$\mathbb{P}\left(\sum_{u_l\in\mathcal{U}_l} \frac{h_{u_l,l,1}^{(n)}}{h_{l,u_l,2}^{(n)}} S_{u_l,l}^{(n)} g_{l,u_l^*,2}^{(n)} \geq I_{th,2}^{(n)}\right) \leq \Theta_{l,2}^{(n)}, \quad \forall n \tag{4.20b}$$

where $\Theta_{l,1}^{(n)}$ and $\Theta_{l,2}^{(n)}$ are given probabilities of violation of constraints (4.6d) and (4.6e) for any n in the first hop and second hop, respectively. By changing $\Theta_{l,1}^{(n)}$ and $\Theta_{l,2}^{(n)}$, the trade-off between robustness and optimality will be achieved. By reducing $\Theta_{l,1}^{(n)}$ and $\Theta_{l,2}^{(n)}$, the network becomes more robust against uncertainty, while by increasing $\Theta_{l,1}^{(n)}$ and $\Theta_{l,2}^{(n)}$, the network sum-rate is increased.

To deal with this trade-off I use the *chance constrained approach*. When the constraints are affine functions, for i.i.d. values of uncertain parameters, (4.6d) and (4.6e) can be replaced by convex functions as their safe approximations [49]. Applying this approach I obtain

$$\sum_{u_l\in\mathcal{U}_l} S_{u_l,l}^{(n)} g_{u_l^*,l,1}^{(n)} = \sum_{u_l\in\mathcal{U}_l} S_{u_l,l}^{(n)} \bar{g}_{u_l^*,l,1}^{(n)} + \sum_{u_l\in\mathcal{U}_l} \xi_{u_l,l,1}^{(n)} S_{u_l,l}^{(n)} \hat{g}_{u_l^*,l,1}^{(n)}$$

$$\sum_{u_l\in\mathcal{U}_l} \frac{h_{u_l,l,1}^{(n)}}{h_{l,u_l,2}^{(n)}} S_{u_l,l}^{(n)} g_{l,u_l^*,2}^{(n)} = \sum_{u_l\in\mathcal{U}_l} \frac{h_{u_l,l,1}^{(n)}}{h_{l,u_l,2}^{(n)}} S_{u_l,l}^{(n)} \bar{g}_{l,u_l^*,2}^{(n)} + \sum_{u_l\in\mathcal{U}_l} \xi_{l,u_l,2}^{(n)} \frac{h_{u_l,l,1}^{(n)}}{h_{l,u_l,2}^{(n)}} S_{u_l,l}^{(n)} \hat{g}_{l,u_l^*,2}^{(n)}$$

$$\tilde{\Delta}_{g_{l,1}}^{(n)} = \sum_{u_l \in \mathcal{U}_l} \eta_{\mathcal{P}_{u_l,l,1}^{(n)}}^{+} S_{u_l,l}^{(n)} \hat{g}_{u_l^*,l,1}^{(n)} + \sqrt{2\ln\frac{1}{\Theta_{l,1}^{(n)}}} \left(\sum_{u_l \in \mathcal{U}_l} \tau_{\mathcal{P}_{u_l,l,1}^{(n)}}^{2} \left(S_{u_l,l}^{(n)} \hat{g}_{u_l^*,l,1}^{(n)} \right)^2 \right)^{\frac{1}{2}}, \forall n \quad (4.23a)$$

$$\tilde{\Delta}_{g_{l,2}}^{(n)} = \sum_{u_l \in \mathcal{U}_l} \eta_{\mathcal{P}_{l,u_l,2}^{(n)}}^{+} S_{u_l,l}^{(n)} \hat{g}_{l,u_l^*,2}^{(n)} + \sqrt{2\ln\frac{1}{\Theta_{l,2}^{(n)}}} \left(\sum_{u_l \in \mathcal{U}_l} \tau_{\mathcal{P}_{l,u_l,2}^{(n)}}^{2} \left(\frac{h_{u_l,l,1}^{(n)}}{h_{l,u_l,2}^{(n)}} S_{u_l,l}^{(n)} \hat{g}_{l,u_l^*,2}^{(n)} \right)^2 \right)^{\frac{1}{2}}, \forall n \quad (4.23b)$$

---

where $\xi_j^{(n)} = \frac{g_j^{(n)} - \bar{g}_j^{(n)}}{\hat{g}_j^{(n)}}, \forall n$ is varied within the range $[-1, +1]$. Under the assumption of uncorrelated fading channels, all values of $\xi_{u_l,l,1}^{(n)}$ and $\xi_{l,u_l,2}^{(n)}$ are independent of each other and belong to a specific class of probability distribution $\mathcal{P}_{u_l,l,1}^{(n)}$ and $\mathcal{P}_{l,u_l,2}^{(n)}$, respectively. Now the constraints in (4.6d) and (4.6e) can be replaced by Bernstein approximations of chance constraints [49] as follows:

$$\sum_{u_l \in \mathcal{U}_l} S_{u_l,l}^{(n)} \bar{g}_{u_l^*,l,1}^{(n)} + \tilde{\Delta}_{g_{l,1}}^{(n)} \leq I_{th,1}^{(n)}, \quad \forall n \quad (4.22a)$$

$$\sum_{u_l \in \mathcal{U}_l} \frac{h_{u_l,l,1}^{(n)}}{h_{l,u_l,2}^{(n)}} S_{u_l,l}^{(n)} \bar{g}_{l,u_l^*,2}^{(n)} + \tilde{\Delta}_{g_{l,2}}^{(n)} \leq I_{th,2}^{(n)}, \quad \forall n \quad (4.22b)$$

where the protection functions $\tilde{\Delta}_{g_{l,1}}^{(n)}$ and $\tilde{\Delta}_{g_{l,2}}^{(n)}$ are given by (4.23a) and (4.23a), respectively. The variables $-1 \leq \eta_{\mathcal{P}_j}^{+} \leq +1$ and $\tau_{\mathcal{P}_j} \geq 0$ are used for safe approximation of chance constraints and depend on the probability distribution $\mathcal{P}_j$. For a fixed value of $\mathcal{P}_j$ the values of these parameters are listed in Table C.1 (see **Appendix C.8**). The constraints in (4.22a) and (4.22b) turn the RAP into a conic quadratic programming problem [59] and using the inequality $\| \mathbf{y} \|_2 \leq \| \mathbf{y} \|_1$, the optimal RB and power allocation can be obtained in a distributed manner similar to that in **Algorithm 3**. Note that in (4.23a) and (4.23b), the protection functions depend on $\Theta_{l,1}^{(n)}$ and $\Theta_{l,2}^{(n)}$. By adjusting $\Theta_{l,1}^{(n)}$ and $\Theta_{l,2}^{(n)}$, a trade-off between rate and robustness can be achieved.

4.4.5 Sensitivity Analysis

In the previous section I have showed that the protection functions depend on $\Theta_{l,1}^{(n)}$ and $\Theta_{l,2}^{(n)}$. In the following, I analyze the sensitivity of $\mathcal{R}_\Delta$ to the values of the trade-off parameters. Using the protections functions (4.23a) and (4.23b), $\mathcal{R}_\Delta$ is given by

$$\mathcal{R}_\Delta \approx \sum_{n=1}^{N} \psi_n^* \tilde{\Delta}_{g_{l,1}}^{(n)} + \sum_{n=1}^{N} \varphi_n^* \tilde{\Delta}_{g_{l,2}}^{(n)} + \sum_{u_l \in \mathcal{U}_l} \sum_{n=1}^{N} \varrho_{u_l}^{n*} \Delta_{I_{u_l,l}}^{(n)}. \tag{4.24}$$

Differentiating (4.24) with respect the to trade-off parameters $\Theta_{l,1}^{(n)}$ and $\Theta_{l,2}^{(n)}$, the sensitivity of $\mathcal{R}_\Delta$, i.e., $\mathcal{S}_{\Theta_{l,i}^{(n)}}(\mathcal{R}_\Delta) = \frac{\partial \mathcal{R}_\Delta}{\partial \Theta_{l,i}^{(n)}}$ is obtained as follows:

$$\mathcal{S}_{\Theta_{l,1}^{(n)}}(\mathcal{R}_\Delta) = -\frac{\psi_n^* \left(\sum_{u_l \in \mathcal{U}_l} \tau^2_{\mathcal{P}_{u_l,l,1}^{(n)}} \left(S_{u_l,l}^{(n)} \hat{g}_{u_l^*,l,1}^{(n)} \right)^2 \right)^{\frac{1}{2}}}{\Theta_{l,1}^{(n)} \sqrt{2 \ln\left(\frac{1}{\Theta_{l,1}^{(n)}} \right)}} \tag{4.25a}$$

$$\mathcal{S}_{\Theta_{l,2}^{(n)}}(\mathcal{R}_\Delta) = -\frac{\varphi_n^* \left(\sum_{u_l \in \mathcal{U}_l} \tau^2_{\mathcal{P}_{l,u_l,2}^{(n)}} \left(\frac{h_{u_l,l,1}^{(n)}}{h_{l,u_l,2}^{(n)}} S_{u_l,l}^{(n)} \hat{g}_{l,u_l^*,2}^{(n)} \right)^2 \right)^{\frac{1}{2}}}{\Theta_{l,2}^{(n)} \sqrt{2 \ln\left(\frac{1}{\Theta_{l,2}^{(n)}} \right)}}. \tag{4.25b}$$

4.5 Performance Evaluation

In my simulations, I express the uncertainty bounds $\Psi_{l,1}^{(n)}$, $\Psi_{l,2}^{(n)}$, and $\Upsilon_{u_l}^{(n)}$ in percentage as $\Psi_{l,1}^{(n)} = \frac{\|\mathbf{g}_{l,1}^{(n)} - \bar{\mathbf{g}}_{l,1}^{(n)}\|_2}{\|\bar{\mathbf{g}}_{l,1}^{(n)}\|_2}$, $\Psi_{l,2}^{(n)} = \frac{\|\mathbf{g}_{l,2}^{(n)} - \bar{\mathbf{g}}_{l,2}^{(n)}\|_2}{\|\bar{\mathbf{g}}_{l,2}^{(n)}\|_2}$, and $\Upsilon_{u_l}^{(n)} = \frac{\|I_{u_l,l}^{(n)} - \bar{I}_{u_l,l}^{(n)}\|_2}{\|\bar{I}_{u_l,l}^{(n)}\|_2}$. As an example, for any relay node l, if $\Psi_{l,1}^{(n)} = 0.5$, the error in the channel gain over RB n for the first hop is not more than 50% of its nominal value. I assume that the estimated interference experienced at relay node and receiving D2D UEs is $\bar{I}_{u_l,l}^{(n)} = 2\sigma^2$ for all the RBs. The

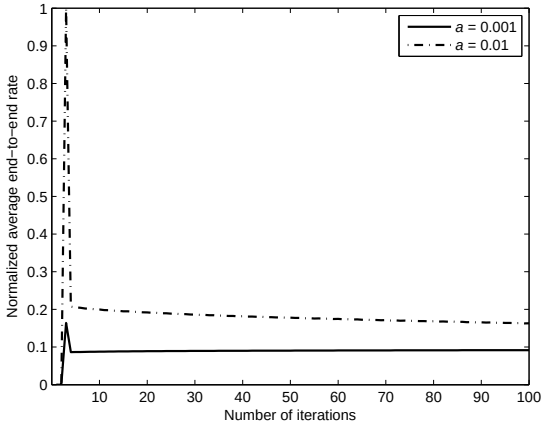

Figure 4.1: Convergence behavior of the proposed algorithm: number of CUE, $|\mathcal{C}| = 15$ (i.e., 5 CUEs assisted by each relay), number of D2D pairs, $|\mathcal{D}| = 9$ (i.e., 3 D2D pairs are assisted by each relay), and hence $|\mathcal{U}_l| = 8$ for each relay. The average end-to-end-rate is calculated by $\frac{R_l}{|\mathcal{U}_l|}$, the maximum distance between relay-D2D UE, $D_{r,d} = 60$ meter, and the interference threshold for both hops is -70 dBm. The errors (in link gain and experienced interference) are considered to be not more than 50% in each RB.

matrices $\mathbf{M}_{g_{l,1}}^{(n)}$ and $\mathbf{M}_{g_{l,2}}^{(n)}$ are considered to be identity matrices and $M_{I_{u_l,l}}^{(n)}$ is set to 1 for all the RBs. The results are obtained by averaging over 250 realizations of the simulation scenarios (i.e., UE locations and link gains).

4.5.1 Results

Convergence of the proposed algorithm

I consider the same step size for all the Lagrange multipliers, i.e., for any Lagrange multiplier κ, step size at iteration t is calculated as $\Lambda_{\kappa}^{(t)} = \frac{a}{\sqrt{t}}$, where a is a small constant. Fig. 4.1 shows the convergence behavior of the proposed algorithm when $a = 0.001$ and $a = 0.01$. For convergence, the step size should be selected carefully. It is clear from this figure that when a is sufficiently small, the algorithm converges very quickly (i.e., in less than 20 iterations) to the optimal solution.

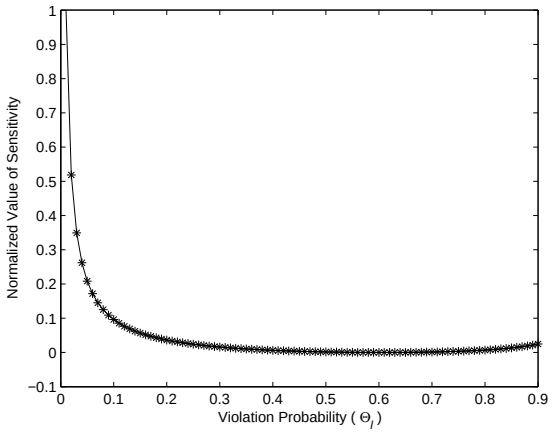

Figure 4.2: Sensitivity of $\mathcal{R}_\Delta$ vs. trade-off parameter using a setup similar to that of Fig. 4.1. I consider $\hat{g}_{l,1}^{(n)} = 0.5 \times \bar{g}_{l,1}^{(n)}$, $\hat{g}_{l,2}^{(n)} = 0.5 \times \bar{g}_{l,2}^{(n)}$ and $\Theta_{l,1}^{(n)} = \Theta_{l,2}^{(n)} = \Theta_l$ for all the RBs.

Sensitivity of $\mathcal{R}_\Delta$ to the trade-off parameter

The absolute sensitivity of $\mathcal{R}_\Delta$ considering $\Theta_l = \Theta_{l,1}^{(n)} = \Theta_{l,2}^{(n)}$ for $\forall n$ is shown in Fig. 4.2. For all the RBs, I assume that the probability density function of $\hat{g}_{l,1}^{(n)}$ and $\hat{g}_{l,2}^{(n)}$ is Gaussian; hence, $\mathcal{P}_{u_l,l,1}^{(n)}$ and $\mathcal{P}_{l,u_l,2}^{(n)}$ correspond to the last row of Table C.1. For a given uncertainty set and interference threshold, when $\Theta_l < 0.2$, the value of $\mathcal{S}_{\Theta_l}(\mathcal{R}_\Delta)$ is very sensitive to Θ_l. However, for higher values of Θ_l, the sensitivity of $\mathcal{R}_\Delta$ is relatively independent of Θ_l. From (4.24), increasing Θ_l proportionally decreases $\mathcal{R}_\Delta$ which increases network sum-rate. Small values of Θ_l make the system more robust against uncertainty, while higher values of Θ_l increase the network sum-rate. Therefore, by adjusting Θ_l within the range of 0.2 a trade-off between optimality and robustness can be attained.

Effect of relaying

In Fig. 4.3, I compare the performance of **Algorithm 3** with asymptotic upper bound. In order to obtain the upper bound, I solve **P4.1** using interior point method

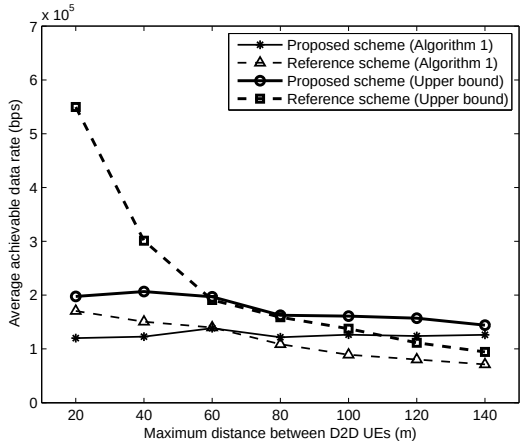

Figure 4.3: Average achievable data rates for D2D UEs in both the proposed and reference schemes compared to the asymptotic upper bound (for $|\mathcal{C}| = 15$, $|\mathcal{D}| = 9$, $D_{r,d} = 80$ meter and interference threshold $= -70$ dBm).

(Chapter 11 in [34]). Note that solving **P4.1** by using the interior point method incurs a complexity of $\mathcal{O}\left((|\mathbf{x_l}| + |\mathbf{S_l}| + |\omega_l|)^3\right)$ [34, Chapter 11], [36] where $\mathbf{x_l} = \left[x_1^{(1)}, \cdots, x_1^{(N)}, \cdots, x_{|\mathcal{U}_l|}^{(1)}, \cdots, x_{|\mathcal{U}_l|}^{(N)}\right]^{\mathsf{T}}$, $\mathbf{S_l} = \left[S_{1,l}^{(1)}, \cdots, S_{1,l}^{(N)}, \cdots, S_{|\mathcal{U}_l|,l}^{(1)}, \cdots, S_{|\mathcal{U}_l|,l}^{(N)}\right]^{\mathsf{T}}$ and $\boldsymbol{\omega_l} = \left[\omega_1^{(1)}, \cdots, \omega_1^{(N)}, \cdots, \omega_{|\mathcal{U}_l|}^{(1)}, \cdots, \omega_{|\mathcal{U}_l|}^{(N)}\right]^{\mathsf{T}}$. From Fig. 4.3 it can be observed that my proposed approach, which uses relays for D2D traffic, can greatly improve the data rate in particular when the distance increases. In addition, proposed algorithm performs close to upper bound with significantly less complexity.

The rate gains for both perfect CSI and under uncertainties are depicted in Fig. 4.4. As expected, under uncertainties, the gain is reduced compared to the case when perfect channel information is available. Although the reference scheme outperforms when the distance between D2D-link is closer, my proposed approach of relay-aided D2D communication can greatly increase the data rate especially when the distance increases. When the distance between D2D becomes higher, the performance of direct communication deteriorates.

The performance gain in terms of the achievable aggregated data rate under dif-

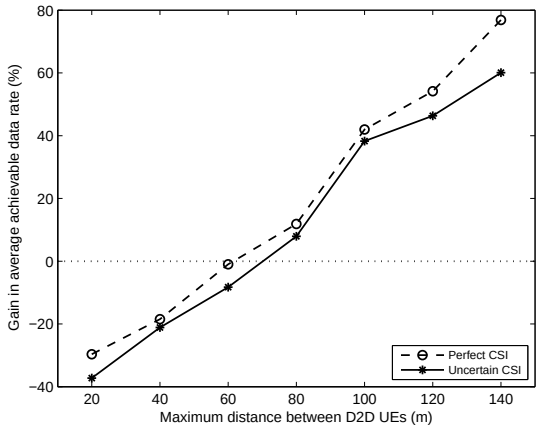

Figure 4.4: Gain in average achievable data rate for D2D UEs (for $|\mathcal{C}| = 15$, $|\mathcal{D}| = 9$, $D_{r,d} = 80$ meter and interference threshold $= -70$ dBm). For uncertain CSI, the bound on the uncertainty set for channel gain and interference (i.e., $\Psi_{l,1}^{(n)}$, $\Psi_{l,2}^{(n)}$, and $\Upsilon_{u_l}^{(n)}$) is considered 20% for all the RBs.

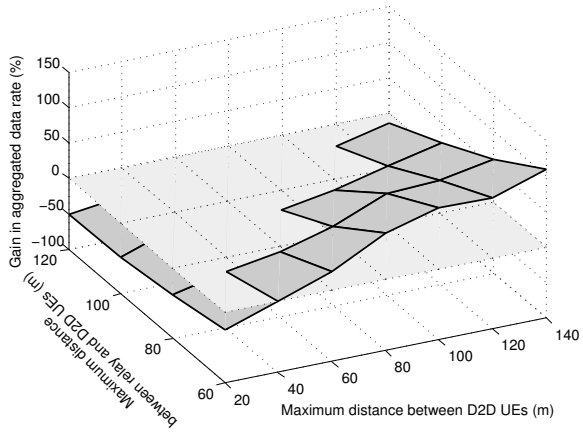

Figure 4.5: Gain in aggregated data rate with different distance between relay and D2D UEs, $D_{r,d}$ where $|\mathcal{C}| = 15$, $|\mathcal{D}| = 9$, interference threshold $= -70$ dBm, $\Psi_{l,1}^{(n)}$, $\Psi_{l,2}^{(n)}$, and $\Upsilon_{u_l}^{(n)}$ are considered 20% for all the RBs. For different values of $D_{r,d}$, there is a distance margin beyond which relaying D2D traffic improves network performance (i.e., the upper portion the of shaded surface where rate gain is positive).

ferent relay-D2D UE distance is shown in Fig. 4.5. It can be observed that, even for relatively large relay-D2D UE distances, e.g., $D_{r,d} \geq 80$ m, relaying D2D traffic provides considerable rate gain for distant D2D UEs. To observe the performance of

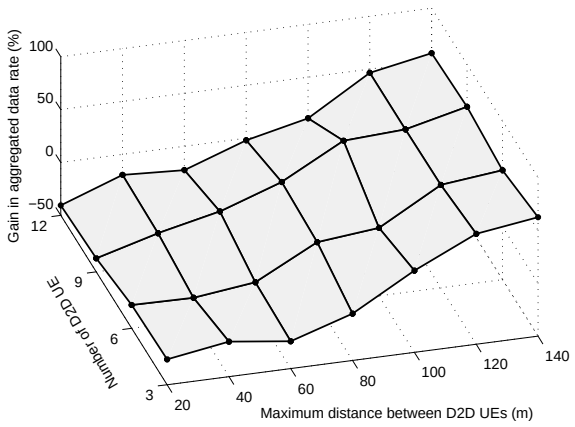

Figure 4.6: Gain in aggregated data rate with varying number of D2D UEs (for $|\mathcal{C}| = 15$, $D_{r,d} = 80$ meter, interference threshold $= -70$ dBm, $\Psi_{l,1}^{(n)}, \Psi_{l,2}^{(n)}$, and $\Upsilon_{u_l}^{(n)}$ is considered 20% for all the RBs).

my proposed scheme in a dense network, I vary the number of D2D UEs and plot the rate gain in Fig. 4.6. As can be seen from this figure, even in a moderately dense situation (e.g., $|\mathcal{C}| + |\mathcal{D}| = 15 + 12 = 27$) my proposed method provides a higher rate compared to that for direct communication between distant D2D UEs.

4.6 Chapter Summary

I have investigated the radio resource management problem in a relay-aided D2D network considering uncertainties in wireless channels. Considering two major sources of uncertainty, namely, the link gain between neighboring relay nodes in both hops and the experienced interference at each receiving network node, the uncertainty has been modeled as a bounded difference between actual and nominal values. By modifying the protection functions in the robust problem, I have shown that the convexity of the problem is maintained. In order to allocate radio resources efficiently, I have proposed a polynomial time distributed algorithm and to balance the cost of

robustness defined as the reduction of achievable network sum-rate, I have provided a trade-off mechanism.

It is worth noting that the formulation of this chapter only considers the uncertainties in interference links (e.g., the experienced interference at each receiving network node in both hops) and assumes the direct link gains (e.g., between UE and relay in first hop and relay-eNB/receiving D2D UE in second hop) is perfectly known. However, in practical systems, both the direct and interfering links could be time-varying and random, and hence may not be perfectly estimated. Considering this fact, in the following chapter I reformulate the RAP to capture the uncertainties in both the direct and interference channel gains.

Chapter 5

Distributed Resource Allocation Under Channel Uncertainties: A Stable Matching Approach

The RAP formation given by **P4.2**-**P4.4** do not consider the uncertainties in the direct channel gains (e.g., the link gain between the UEs-relay and relay-eNB/receiving D2D UEs for the first and second hop, respectively). To be specific, the previous formulation assumes that the perfect information about the direct link gains (e.g., $h^{(n)}_{u_l,l,1}$ and $h^{(n)}_{l,u_l,2}$ for $\forall l, u_l, n$) is available to the network nodes. In this chapter I extend the previous model to consider the uncertainties in both the direct and interference link gains. I utilize time-sharing strategy and the reformulate the problem using worst-case robust optimization theory. The uncertainties in channel gains (e.g., both the direct and interference links) are modeled using ellipsoidal uncertainty sets. Each relay node can centrally solve the RAP taking channel uncertainty into consideration. However, considering the high (e.g., cubic to the number of UEs and RBs) computational overhead at the relay nodes, I provide a *distributed* solution based on

stable matching theory which is computationally inexpensive (e.g., linear with the number of UEs and RBs). I also analyze the stability, uniqueness, and optimality of the proposed solution.

Considering the computational and signaling overheads and lack of scalability of the centralized solutions, game theoretical models have been widely used for wireless radio resource allocation problems. However, the analytical tractability of equilibrium in such game-theoretical models requires special properties for the objective functions, such as convexity, which may not be satisfied for many practical cases [60]. In this context, resource allocation using matching theory has several beneficial properties [60,61]. For example, the stable matching algorithm terminates for every given preference profile. The outcome of matching provides suitable solutions in terms of stability and optimality, which can accurately reflect different system objectives. Besides, with suitable data structures, a Pareto optimal stable matching (e.g., allocation of resources to the UEs) can be obtained quickly for online implementation.

The main contributions of this work can be summarized as follows:

- I model and analyze the RAP for relay-aided D2D communication underlaying an OFDMA cellular network considering the uncertainties in link gains. I show that the convexity of the optimization problem is conserved under bounded channel uncertainty.

- I provide a distributed iterative solution using stable matching considering bounded channel uncertainty. The stability, uniqueness, optimality, and complexity of the proposed solution are analyzed.

- Numerical results show that the proposed distributed solution performs close to the upper bound of the optimal solution obtained in a centralized manner; however it incurs a lower (e.g., linear compared to cubic) computational complexity.

Similar to previous chapters, I also compare the performance of the proposed approach with a traditional underlay D2D communication scheme and observe that after a distant margin, relaying of D2D traffic improves network performance.

I organize the rest of the chapter as follows. Followed by the formulation of the nominal RAP in Section 5.1, I reformulate the RAP considering the wireless link uncertainties in Section 5.2. I develop the stable matching-based distributed resource allocation algorithm in Section 5.3. Theoretical analysis of the proposed solution is presented in Section 5.4. In Section 5.5 I present the performance evaluation results before I conclude the chapter in Section 5.6.

5.1 Resource Allocation: Formulation of the Nominal Problem

As I have mentioned in Section 2.3.1 the end-to-end data rate for UE u_l over RB n given by (2.1) can be written is achieved when $P^{(n)}_{u_l,l}\gamma^{(n)}_{u_l,l,1} = P^{(n)}_{l,u_l}\gamma^{(n)}_{l,u_l,2}$. Hence in the second hop, the power P_{l,u_l} allocated for UE u_l, can be expressed as a function of power allocated for transmission in the first hop, $P_{u_l,l}$ as follows

$$P^{(n)}_{l,u_l} = \frac{\gamma^{(n)}_{u_l,l,1}}{\gamma^{(n)}_{l,u_l,2}} P^{(n)}_{u_l,l} \approx \frac{h^{(n)}_{u_l,l,1}}{h^{(n)}_{l,u_l,2}} P^{(n)}_{u_l,l}. \tag{5.1}$$

Using (5.1), the relaxed problem can be stated as follows:

(**P5.1**)

$$\max_{x_{u_l}^{(n)}, S_{u_l,l}^{(n)}} \sum_{u_l \in \mathcal{U}_l} R_{u_l}$$

$$\text{subject to} \sum_{u_l \in \mathcal{U}_l} x_{u_l}^{(n)} \leq 1, \quad \forall n \tag{5.2a}$$

$$\sum_{n=1}^{N} S_{u_l,l}^{(n)} \leq P_{u_l}^{max}, \ \forall u_l \tag{5.2b}$$

$$\sum_{u_l \in \mathcal{U}_l} \sum_{n=1}^{N} H_{u_l,l}^{(n)} S_{u_l,l}^{(n)} \leq P_l^{max} \tag{5.2c}$$

$$\sum_{u_l \in \mathcal{U}_l} S_{u_l,l}^{(n)} g_{u_l^*,l,1}^{(n)} \leq I_{th,1}^{(n)}, \quad \forall n \tag{5.2d}$$

$$\sum_{u_l \in \mathcal{U}_l} H_{u_l,l}^{(n)} S_{u_l,l}^{(n)} g_{l,u_l^*,2}^{(n)} \leq I_{th,2}^{(n)}, \quad \forall n \tag{5.2e}$$

$$\sum_{n=1}^{N} \tfrac{1}{2} x_{u_l}^{(n)} B_{RB} \log_2 \left(1 + P_{u_l,l}^{(n)} \gamma_{u_l,l,1}^{(n)}\right) \geq Q_{u_l}, \quad \forall u_l \tag{5.2f}$$

$$0 < x_{u_l}^{(n)} \leq 1, \ S_{u_l,l}^{(n)} \geq 0, \quad \forall n, u_l \tag{5.2g}$$

where $\gamma_{u_l,l,1}^{(n)} = \frac{h_{u_l,l}^{(n)}}{\sum_{\substack{\forall u_j \in \mathcal{U}_j, \\ j \neq l, j \in \mathcal{L}}} S_{u_j,j}^{(n)} g_{u_j,l,1}^{(n)} + \sigma^2}$, $H_{u_l,l}^{(n)} = \frac{h_{u_l,l,1}^{(n)}}{h_{l,u_l,2}^{(n)}}$ and $R_{u_l} = \sum_{n=1}^{N} \frac{1}{2} x_{u_l}^{(n)} B_{RB} \log_2 \left(1 + \frac{S_{u_l,l}^{(n)} \gamma_{u_l,l,1}^{(n)}}{x_{u_l}^{(n)}}\right)$.

5.2 Resource Allocation Under Channel Uncertainty

In this section, I consider the uncertainty of the channel gains in RAP and use ellipsoid sets to describe the uncertainty. For worst-case robust resource optimization problems, the channel state information is assumed to have a bounded uncertainty of unknown distribution. An ellipsoid is often used (e.g., [62–64]) to approximate such an uncertainty region.

5.2.1 Uncertainty Sets

Let the variable $F^{(n)}_{u_l,u_j,l}$ denote the normalized channel gain which is defined as follows:

$$F^{(n)}_{u_l,u_j,l} \triangleq \frac{g^{(n)}_{u_j,l,1}}{h^{(n)}_{u_l,l,1}}, \quad \forall u_j \in \mathcal{U}_j, j \neq l, j \in \mathcal{L}. \tag{5.3}$$

In addition, let $\mathcal{F}^{(n)}_{u_l,l}$ denote the uncertainty set that describes the perturbation of link gains for u_l over RB n. The normalized gain is then denoted by

$$F^{(n)}_{u_l,u_j,l} = \bar{F}^{(n)}_{u_l,u_j,l} + \Delta F^{(n)}_{u_l,u_j,l} \tag{5.4}$$

where $\bar{F}^{(n)}_{u_l,u_j,l}$ is the nominal value and $\Delta F^{(n)}_{u_l,u_j,l}$ is the perturbation part. The uncertainty in the CQI values of each user is modeled under an ellipsoidal approximation as follows:

$$\mathcal{F}^{(n)}_{u_l,l} = \left\{ \bar{F}^{(n)}_{u_l,u_j,l} + \Delta F^{(n)}_{u_l,u_j,l} : \sum_{\substack{\forall u_j \in \mathcal{U}_j, \\ j \neq l, j \in \mathcal{L}}} |\Delta F^{(n)}_{u_l,u_j,l}|^2 \leq \xi^{(n)}_{1_{u_l}}; \forall u_l, n \right\} \tag{5.5}$$

where $\xi^{(n)}_{1_{u_l}} \geq 0$ is the uncertainty bound in each RB. Using (5.3) I rewrite the rate expression for u_l over RB n as

$$R^{(n)}_{u_l} = \tfrac{1}{2} B_{RB} \log_2 \left(1 + \frac{P^{(n)}_{u_l,l}}{\sum\limits_{\substack{\forall u_j \in \mathcal{U}_j, \\ j \neq l, j \in \mathcal{L}}} F^{(n)}_{u_l,u_j,l} P^{(n)}_{u_j,j} + \tilde{\sigma}^{(n)}_{u_l}} \right) \tag{5.6}$$

where $\tilde{\sigma}^{(n)}_{u_l} \triangleq \frac{\sigma^2}{h^{(n)}_{u_l,l,1}}$ and $F^{(n)}_{u_l,u_j,l}$ is given by (5.4).

5.2.2 Reformulation of the Optimization Problem Considering Channel Uncertainty

Utilizing uncertainty sets similar to (5.5) in the constraints (5.2c)-(5.2e), the optimization problem **P5.1** can be equivalently represented under channel uncertainty as follows:

(**P5.2**)

$$\max_{x_{u_l}^{(n)}, S_{u_l,l}^{(n)}} \min_{\substack{\Delta F_{u_l,u_j,l}^{(n)}, \Delta g_{u_l^*,l,1}^{(n)}, \\ \Delta H_{u_l,l}^{(n)}, \Delta H_{u_l,l}^{(n)} g_{l,u_l^*,2}^{(n)}}} \sum_{u_l \in \mathcal{U}_l} R_{u_l}$$

$$\text{subject to} \quad \text{(5.2a), (5.2f), (5.2b), (5.2g)} \quad \text{and}$$

$$\sum_{u_l \in \mathcal{U}_l} \sum_{n=1}^{N} \left(\bar{H}_{u_l,l}^{(n)} + \Delta H_{u_l,l}^{(n)} \right) S_{u_l,l}^{(n)} \leq P_l^{max} \tag{5.7}$$

$$\sum_{u_l \in \mathcal{U}_l} \left(\bar{g}_{u_l^*,l,1}^{(n)} + \Delta g_{u_l^*,l,1}^{(n)} \right) S_{u_l,l}^{(n)} \leq I_{th,1}^{(n)}, \quad \forall n \tag{5.8}$$

$$\sum_{u_l \in \mathcal{U}_l} \left(\bar{H}_{u_l,l}^{(n)} \bar{g}_{l,u_l^*,2}^{(n)} + \Delta H_{u_l,l}^{(n)} g_{l,u_l^*,2}^{(n)} \right) S_{u_l,l}^{(n)} \leq I_{th,2}^{(n)}, \quad \forall n \tag{5.9}$$

$$\sum_{\forall u_j \in \mathcal{U}_j, j \neq l, j \in \mathcal{L}} |\Delta F_{u_l,u_j,l}^{(n)}|^2 \leq \left(\xi_{1_{u_l}}^{(n)}\right)^2, \forall u_l, n \tag{5.10}$$

$$\sum_{u_l \in \mathcal{U}_l} \sum_{n=1}^{N} |\Delta H_{u_l,l}^{(n)}|^2 \leq (\xi_{2l})^2 \tag{5.11}$$

$$\sum_{u_l \in \mathcal{U}_l} |\Delta g_{u_l^*,l,1}^{(n)}|^2 \leq \left(\xi_{3_{u_l}}^{(n)}\right)^2, \ \forall n \tag{5.12}$$

$$\sum_{u_l \in \mathcal{U}_l} |\Delta H_{u_l,l}^{(n)} g_{l,u_l^*,2}^{(n)}|^2 \leq \left(\xi_{4_{u_l}}^{(n)}\right)^2, \ \forall n \tag{5.13}$$

where for any parameter y, $\bar{y}$ denotes the nominal value and Δy represents the corresponding deviation part; ξ_{2l}, $\xi_{3_{u_l}}^{(n)}, and\ \xi_{4_{u_l}}^{(n)}$ are the maximum deviations (e.g.,

uncertainty bounds) of corresponding entries in CQI values. In **P3**, R_{u_l} is given by

$$R_{u_l} = \sum_{n=1}^{N} \tfrac{1}{2} x_{u_l}^{(n)} B_{RB} \times \log_2 \left(1 + \frac{\frac{S_{u_l,l}^{(n)}}{x_{u_l}^{(n)}}}{\sum\limits_{\substack{\forall u_j \in \mathcal{U}_j, \\ j \neq l, j \in \mathcal{L}}} \left(\bar{F}_{u_l,u_j,l}^{(n)} + \Delta F_{u_l,u_j,l}^{(n)} \right) S_{u_j,j}^{(n)} + \tilde{\sigma}_{u_l}^{(n)}} \right). \tag{5.14}$$

The above optimization problem is subject to an infinite number of constraints with respect to the uncertainty sets and hence becomes a semi-infinite programming (SIP) problem [65]. In order to solve the SIP problem it is required to transform **P5.2** into an equivalent problem with finite number of constraints. Similar to [62, 63], I apply the Cauchy-Schwarz inequality [66] and transform the SIP problem. More specifically, utilizing Cauchy-Schwarz inequality, I obtain the following:

$$\begin{aligned} \sum_{\substack{\forall u_j \in \mathcal{U}_j, \\ j \neq l, j \in \mathcal{L}}} \Delta F_{u_l,u_j,l}^{(n)} S_{u_j,j}^{(n)} &\leq \sqrt{\sum_{\substack{\forall u_j \in \mathcal{U}_j, \\ j \neq l, j \in \mathcal{L}}} |\Delta F_{u_l,u_j,l}^{(n)}|^2 \sum_{\substack{\forall u_j \in \mathcal{U}_j, \\ j \neq l, j \in \mathcal{L}}} |S_{u_j,j}^{(n)}|^2} \\ &\leq \xi_{1_{u_l}}^{(n)} \sqrt{\sum_{\substack{\forall u_j \in \mathcal{U}_j, \\ j \neq l, j \in \mathcal{L}}} \left(S_{u_j,j}^{(n)} \right)^2}. \end{aligned} \tag{5.15}$$

Similarly,

$$\sum_{u_l \in \mathcal{U}_l} \sum_{n=1}^{N} \Delta H_{u_l,l}^{(n)} S_{u_l,l}^{(n)} \leq \xi_{2l} \sqrt{\sum_{u_l \in \mathcal{U}_l} \sum_{n=1}^{N} \left(S_{u_l,l}^{(n)} \right)^2} \tag{5.16}$$

$$\sum_{u_l \in \mathcal{U}_l} \Delta g_{u_l^*,l,1}^{(n)} S_{u_l,l}^{(n)} \leq \xi_{3_{u_l}}^{(n)} \sqrt{\sum_{u_l \in \mathcal{U}_l} \left(S_{u_l,l}^{(n)} \right)^2} \tag{5.17}$$

$$\sum_{u_l \in \mathcal{U}_l} \Delta H_{u_l,l}^{(n)} g_{l,u_l^*,2}^{(n)} S_{u_l,l}^{(n)} \leq \xi_{4_{u_l}}^{(n)} \sqrt{\sum_{u_l \in \mathcal{U}_l} \left(S_{u_l,l}^{(n)} \right)^2}. \tag{5.18}$$

Note that, as presented in Section 5.2.1, to tackle the uncertainty in channel gains, I have considered the worst-case approach, e.g., the estimation error is assumed to

be bounded by a closed set (uncertainty set). Hence, from (5.15)-(5.18), under the worst-case channel uncertainties, the optimization problem **P5.2** can be rewritten as follows

(**P5.3**)

$$\max_{x_{u_l}^{(n)}, S_{u_l,l}^{(n)}} \sum_{u_l \in \mathcal{U}_l} R_{u_l}$$

$$\text{subject to} \quad \text{(5.2a), (5.2f), (5.2b), (5.2g)} \quad \text{and}$$

$$\sum_{u_l \in \mathcal{U}_l} \sum_{n=1}^{N} \bar{H}_{u_l,l}^{(n)} S_{u_l,l}^{(n)} + \xi_{2l} \sqrt{\sum_{u_l \in \mathcal{U}_l} \sum_{n=1}^{N} \left(S_{u_l,l}^{(n)}\right)^2} \leq P_l^{max} \tag{5.19}$$

$$\sum_{u_l \in \mathcal{U}_l} \bar{g}_{u_l^*,l,1}^{(n)} S_{u_l,l}^{(n)} + \xi_{3_{u_l}}^{(n)} \sqrt{\sum_{u_l \in \mathcal{U}_l} \left(S_{u_l,l}^{(n)}\right)^2} \leq I_{th,1}^{(n)}, \quad \forall n \tag{5.20}$$

$$\sum_{u_l \in \mathcal{U}_l} \bar{H}_{u_l,l}^{(n)} \bar{g}_{l,u_l^*,2}^{(n)} S_{u_l,l}^{(n)} + \xi_{4_{u_l}}^{(n)} \sqrt{\sum_{u_l \in \mathcal{U}_l} \left(S_{u_l,l}^{(n)}\right)^2} \leq I_{th,2}^{(n)}, \quad \forall n. \tag{5.21}$$

where R_{u_l} is given by

$$\begin{aligned} R_{u_l} &= \sum_{n=1}^{N} \frac{1}{2} x_{u_l}^{(n)} B_{RB} \log_2 \left(1 + \frac{\frac{S_{u_l,l}^{(n)}}{x_{u_l}^{(n)}}}{\sum\limits_{\substack{\forall u_j \in \mathcal{U}_j, \\ j \neq l, j \in \mathcal{L}}} \bar{F}_{u_l,u_j,l}^{(n)} S_{u_j,j}^{(n)} + \xi_{1_{u_l}}^{(n)} \sqrt{\sum\limits_{\substack{\forall u_j \in \mathcal{U}_j, \\ j \neq l, j \in \mathcal{L}}} \left(S_{u_j,j}^{(n)}\right)^2 + \tilde{\sigma}_{u_l}^{(n)}}} \right) \\ &= \sum_{n=1}^{N} \frac{1}{2} x_{u_l}^{(n)} B_{RB} \log_2 \left(1 + \frac{\frac{S_{u_l,l}^{(n)}}{x_{u_l}^{(n)}} \bar{h}_{u_l,l,1}^{(n)}}{\sum\limits_{\substack{\forall u_j \in \mathcal{U}_j, \\ j \neq l, j \in \mathcal{L}}} \bar{g}_{u_j,l,1}^{(n)} S_{u_j,j}^{(n)} + \bar{h}_{u_l,l,1}^{(n)} \xi_{1_{u_l}}^{(n)} \sqrt{\sum\limits_{\substack{\forall u_j \in \mathcal{U}_j, \\ j \neq l, j \in \mathcal{L}}} \left(S_{u_j,j}^{(n)}\right)^2 + \sigma^2}} \right). \end{aligned} \tag{5.22}$$

The transformed problem is a second-order cone program (SOCP) [34, Chapter 4] and the convexity of **P5.3** is conserved as shown in the following proposition.

Proposition 5.1. P5.3 *is a convex optimization problem.*

Proof. Using an argument similar to that in footnote 5, the objective function in

(5.19) in **P5.3** is concave. The constraints in (5.2a), (5.2b), (5.2g) are affine and the constraint in (5.2f) is convex. In addition, the additional square root term in the left hand side of the constraints in (5.19), (5.20), and (5.21) is the linear norm of the vector of power variables $S_{u_l,l}^{(n)}$ with order 2, which is convex [34, Section 3.2.4]. Therefore, the optimization problem **P5.3** is convex. □

The optimization problem **P5.3** is solvable using standard centralized algorithms such as interior point method. The joint RB and power allocation can be performed similar to **Algorithm 1** (see Page 24) and an upper bound for the solution to the RAP can be obtained under channel uncertainty. It is worth noting that solving the above SOCP using interior point method incurs a complexity of $\mathcal{O}\left(\left(\overline{\overline{\mathbf{x_l}}} + \overline{\overline{\mathbf{P}_l}}\right)^3\right)$ at each relay node where $\overline{\overline{\mathbf{y}}}$ denotes the length of vector $\mathbf{y}$. Besides, the size of the optimization problem increases with the number of network nodes. Despite the fact that the solution from **Algorithm 1** outputs the optimal data rate, considering short (e.g., 1 millisecond) scheduling period of LTE-A network, it may not be feasible to solve the RAP centrally in practical networks. Therefore, in the following, I provide a low-complexity distributed solution based on matching theory. That is, without solving the RAP in a centralized manner using any relaxation technique (e.g., time-sharing strategy as described in the preceding section), I apply the method of two-sided stable many-to-one matching [67].

5.3 Distributed Solution Approach for the RAP Under Channel Uncertainty

The resource allocation approach using stable matching involves multiple decision-making agents, i.e., the available RBs and the UEs; and the solutions (i.e., matching

between UE and RB) are produced by individual actions of the agents. The actions, i.e., matching requests and confirmations or rejections are determined by the given *preference profiles*. That is, for both the RBs and the UEs, the lists of preferred matches over the opposite set are maintained. For each RB, the relay holds its preference list for the UEs. The matching outcome yields mutually beneficial assignments between RBs and UEs. *Stability* in matching implies that, with regard to their initial preferences, neither RBs nor UEs have an incentive to alter the allocation.

5.3.1 Concept of Matching

A *matching* (i.e., allocation) is given as an assignment of RBs to UEs forming the set of pairs $(u_l, n) \in \mathcal{U}_l \times \mathcal{N}$. Note that a UE can be allocated more than one RB to satisfy its data rate requirement; however, according to the constraint in (2.7), one RB can be assigned to only one UE. This scheme corresponds to a *many-to-one* matching in the theory of stable matching. More formally, I define the matching as follows [68].

Definition 5.1. *A matching μ_l for $\forall l \in \mathcal{L}$ is defined as a function, i.e., $\mu_l : \mathcal{U}_l \cup \mathcal{N} \rightarrow \mathcal{U}_l \cup \mathcal{N}$ such that*

1. $\mu_l(n) \in \mathcal{U}_l \cup \{\varnothing\}$ *and* $\overline{\overline{\mu_l(n)}} \in \{0, 1\}$
2. $\mu_l(u_l) \in \mathcal{N}$ *and* $\overline{\overline{\mu_l(u_l)}} \in \{1, 2, \ldots, \kappa_{u_l}\}$

where the integer $\kappa_{u_l} \leq N$, $\mu_l(u_l) = n \Leftrightarrow \mu(n) = u_l$ for $\forall n \in \mathcal{N}, \forall u_l \in \mathcal{U}_l$ and $\overline{\overline{\mu_j(\cdot)}}$ denotes the cardinality of matching outcome $\mu_j(\cdot)$.

The above definition implies that μ_l is a one-to-one matching if the input to the function is an RB. On the other hand, μ_l is a one-to-many function, i.e., $\mu_l(u_l)$ is not unique if the input to the function is a UE. In order to satisfy the data rate

requirement for each of the UEs, I introduce the parameter κ_{u_l}, which denotes the number RB(s) which are sufficient to satisfy the minimum rate requirement Q_{u_l}. Consequently, the constraint in (5.2f) is rewritten as $\sum_{n=1}^{N} x_{u_l}^{(n)} = \kappa_{u_l},\ \forall u_l$. Generally this parameter is referred to as *quota* in the theory of matching [61]. Each user u_l will be subject to an acceptance quota κ_{u_l} over RB(s) within the range $1 \leq \kappa_{u_l} \leq N$ and allowed for matching to at most κ_{u_l} RB(s). The outcome of the matching determines the RB allocation vector at each relay l, e.g., $\mu_l \equiv \mathbf{x_l}$.

5.3.2 Utility Matrix and Preference Profile

Let me consider the utility matrix $\mathfrak{U}_l$ under the worst-case uncertainty, which denotes the achievable data rate for the UEs in different RBs, defined as follows:

$$\mathfrak{U}_l = \begin{bmatrix} R_1^{(1)} & \cdots & R_1^{(N)} \\ \vdots & \ddots & \vdots \\ R_{U_l}^{(1)} & \cdots & R_{U_l}^{(N)} \end{bmatrix} \tag{5.23}$$

where $\mathfrak{U}_l[i,j]$ denotes the entry of i-th row and j-th column in $\mathfrak{U}_l$, and $R_{u_l}^{(n)}$ is given by

$$R_{u_l}^{(n)} = \frac{1}{2} B_{RB} \log_2 \left(1 + \frac{P_{u_l,l}^{(n)} \bar{h}_{u_l,l,1}^{(n)}}{\sum\limits_{\substack{\forall u_j \in \mathcal{U}_j, \\ j \neq l, j \in \mathcal{L}}} x_{u_j}^{(n)} \bar{g}_{u_j,l,1}^{(n)} P_{u_j,j}^{(n)} + \bar{h}_{u_l,l,1}^{(n)} \xi_{1_{u_l}}^{(n)} \sqrt{\sum\limits_{\substack{\forall u_j \in \mathcal{U}_j, \\ j \neq l, j \in \mathcal{L}}} \left(x_{u_j}^{(n)} P_{u_j,j}^{(n)} \right)^2 + \sigma^2}} \right). \tag{5.24}$$

Each of the UEs and RBs holds a list of preferred matches where a preference relation can be defined as follows [69, Chapter 2].

Definition 5.2. *Let $\succeq$ be a binary relation on any arbitrary set Ξ. The binary relation $\succeq$ is* ***complete*** *if for $\forall i, j \in \Xi$, either $i \succeq j$ or $j \succeq i$ or both. A binary relation is* ***transitive*** *if $i \succeq j$ and $j \succeq k$ implies that $i \succeq k$ for $\forall k \in \Xi$. The binary relation $\succeq$*

is a (weak) ***preference*** *relation if it is complete and transitive.*

The preference profile of a UE $u_l \in \mathcal{U}_l$ over the set of available RBs $\mathcal{N}$ is defined as a vector of linear order $\mathcal{P}_{u_l}(\mathcal{N}) = \mathfrak{U}_l[u_l, i]_{i\in\mathcal{N}}$. The UE u_l prefers RB n_1 to n_2 if $n_1 \succeq n_2$, and consequently, $\mathfrak{U}_l[u_l, n_1] > \mathfrak{U}_l[u_l, n_2]$. Likewise, the preference profile of an RB $n \in \mathcal{N}$ is given by $\mathcal{P}_n(\mathcal{U}_l) = \mathfrak{U}_l[j, n]_{j\in\mathcal{U}_l}$.

5.3.3 Algorithm for Resource Allocation

Based on the discussions in the previous section, I utilize an improved version of matching algorithm (adapted from [70, Chapter 1.2]) to allocate the RBs. The allocation subroutine, as illustrated in **Algorithm 4**, executes as follows. While an RB n is unmatched (i.e., unallocated) and has a non-empty preference list, the RB is temporarily assigned to its first preference over UEs, i.e., u_l. If the allocation does not exceed κ_{u_l}, the allocation will persist. Otherwise, the worst preferred RB from u_l's matching will be removed, even though it was previously allocated. The iterations are repeated until there are unallocated pairs of RB and UE. The iterative process dynamically updates the preference lists and hence leads to a stable matching.

Once the optimal RB allocation is obtained, the transmit power of the UEs on assigned RB(s) is obtained similar to that approach presented in Section 3.2.1 (see Page 40). To be specific, at each iteration t, the transmission power for each allocated RB is updated as follows:

$$P_{u_l,l}^{(n)}(t) = \begin{cases} \Lambda(t-1), & \text{if } \Lambda(t-1) \leq \hat{P}_{u_l}^{(n)^{max}} \\ \hat{P}_{u_l,l}^{(n)}, & \text{otherwise} \end{cases} \tag{5.25}$$

where

Algorithm 4 RB allocation using stable matching

Input: The preference profiles $\boldsymbol{\mathcal{P}}_{u_l}(\mathcal{N})$, $\boldsymbol{\mathcal{P}}_n(\mathcal{U}_l)$; $\forall u_l \in \mathcal{U}_l, n \in \mathcal{N}$.
Output: The RB allocation vector $\mathbf{x_l}$.

Initialize $\mathbf{x_l} := \mathbf{0}$.
while $\exists n$ with $x_{u_l}^{(n)} = 0, \forall u_l \in \mathcal{U}_l$ **and** $\boldsymbol{\mathcal{P}}_n(\mathcal{U}_l) \neq \varnothing$ **do**
  u_{mp} := most preferred UE from the profile $\boldsymbol{\mathcal{P}}_n(\mathcal{U}_l)$.
  Set $x_{u_{mp}}^{(n)} := 1$. */* Temporarily allocate the RB */*
  if $\sum_{j=1}^{N} x_{u_{mp}}^{(j)} > \kappa_{u_{mp}}$ **then**
    n_{lp} := least preferred resource allocated to u_{mp}.
    Set $x_{u_{mp}}^{(n_{lp})} := 0$. */* Revoke allocation due to quota violation */*
  end if
  if $\sum_{j=1}^{N} x_{u_{mp}}^{(j)} = \kappa_{u_{mp}}$ **then**
    n_{lp} := least preferred resource allocated to u_{mp}.
    / Update preference profiles */*
    for each successor $\hat{n}_{lp}$ of n_{lp} on profile $\boldsymbol{\mathcal{P}}_{u_{mp}}(\mathcal{N})$ **do**
      remove $\hat{n}_{lp}$ from $\boldsymbol{\mathcal{P}}_{u_{mp}}(\mathcal{N})$.
      remove u_{mp} from $\boldsymbol{\mathcal{P}}_{\hat{n}_{lp}}(\mathcal{U}_l)$.
    end for
  end if
end while

$$\Lambda(t-1) = \frac{2^{Q_{u_l}}-1}{2^{R_{u_l}(t-1)}-1} P_{u_l,l}^{(n)}(t-1) \tag{5.26}$$

$$\hat{P}_{u_l}^{(n)^{max}} = \min\left(\frac{P_{u_l}^{max}}{\sum_{n=1}^{N} x_{u_l}^{(n)}}, \frac{P_l^{max}}{\left(\bar{H}_{u_l,l}^{(n)} + \xi_{2_{u_l}}\right) \sum_{u_l \in \mathcal{U}_l} \sum_{n=1}^{N} x_{u_l}^{(n)}} \right) \tag{5.27}$$

and $\hat{P}_{u_l,l}^{(n)}$ is obtained as

$$\hat{P}_{u_l,l}^{(n)} = \min\left(\tilde{P}_{u_l,l}^{(n)}, \ \min\left(\hat{P}_{u_l}^{(n)^{max}}, \varpi_{u_l,l}^{(n)} \right) \right). \tag{5.28}$$

In (5.28), the parameter $\tilde{P}_{u_l,l}^{(n)}$ is chosen arbitrarily within the range of $0 \leq \tilde{P}_{u_l,l}^{(n)} \leq$

Algorithm 5 Joint RB and power allocation algorithm

Phase I: Initialization

1: Each relay $l \in \mathcal{L}$ estimates the nominal CQI values from previous time slot and determines reference gains $\bar{g}^{(n)}_{u_l^*,l,1}$ and $\bar{g}^{(n)}_{l,u_l^*,2}, \forall u_l, n$.

2: Initialize $t := 0$, $P^{(n)}_{u_l,l} := \frac{P^{max}_{u_l}}{N}$ $\forall u_l, n$ and $\mathfrak{U}_l$ based on CQI estimates.

Phase II: Update

3: **for each** relay $l \in \mathcal{L}$ **do**

4: **repeat**

5: Update $t := t + 1$.

6: Build the preference profile $\mathcal{P}_n(\mathcal{U}_l)$ for each RB $n \in \mathcal{N}$ based on utility matrix and inform corresponding entries of $\mathfrak{U}_l$ to UEs.

7: Each UE $u_l \in \mathcal{U}_l$ builds the preference profile $\mathcal{P}_{u_l}(\mathcal{N})$.

8: Obtain RB allocation vector using **Algorithm 4**.

9: Update the transmission power using (5.25) for $\forall u_l, n$ and update the utility matrix $\mathfrak{U}_l$.

10: Inform the allocation variables $\mathbf{x_l}$, $\mathbf{P_l}$ to each relay $j \neq l, j \in \mathcal{L}$ and calculate the achievable data rate based on current allocation as $R_l(t) := \sum_{u_l \in \mathcal{U}_l} R_{u_l}(t)$.

11: **until** data rate not maximized **or** $t = T_{max}$.

12: **end for**

Phase III: Allocation

13: For each relay, allocate resources (i.e., RB and transmit power) to the associated UEs.

$\hat{P}^{(n)^{max}}_{u_l}$ and $\varpi^{(n)}_{u_l,l}$ is given by

$$\varpi^{(n)}_{u_l,l} = \min\left(\frac{I^{(n)}_{th,1}}{\bar{g}^{(n)}_{u_l^*,l,1}+\xi^{(n)}_{3_{u_l}}}, \frac{I^{(n)}_{th,2}}{\bar{H}^{(n)}_{u_l,l}\bar{g}^{(n)}_{l,u_l^*,2}+\xi^{(n)}_{4_{u_l}}}\right). \tag{5.29}$$

Based on the RB allocation, the relay informs the parameter $\hat{P}^{(n)^{max}}_{u_l}$ and each UE updates its transmit power in a distributed manner using (5.25). Each relay independently performs resource allocation and allocates resources to corresponding associated UEs. The joint RB and power allocation algorithm is summarized in **Algorithm 5**.

5.3.4 Signalling Over Control Channels

Assuming that the relays obtain the CQI prior to resource allocation, the centralized approach (e.g., presented in Chapter 2) does not require any exchange of information between a relay node and the associated UEs to perform resource allocation. However, in the distributed approach, the relay node and the UEs need to exchange information to update the preference profiles and transmit power. In both the approaches, the relay nodes need to exchange the allocation variables among themselves (e.g., over X2 interface) in order to calculate the interference levels at the receiving nodes.

In the distributed approach, the exchange of information between a UE and the relay node during execution of the resource allocation algorithm can be mapped onto the standard LTE-A scheduling control messages. For scheduling in LTE-A networks, the exchanges of messages over control channels are as follows [71]. The UEs will periodically sense the physical uplink control channel (PUCCH) by transmitting known sequences as sounding reference signals (SRS). When data is available for uplink transmission, the UE sends the scheduling request (SR) over PUCCH. The relay, in turn, uses the scheduling grant (SG) over physical downlink control channel (PDCCH) to allocate the appropriate RB(s) to the UE. Once the allocation of RB(s) is received, the UE regularly sends buffer status report (BSR) using PUCCH in order to update the resource requirement, and in response, the relay sends the acknowledgment (ACK) over the physical hybrid-ARQ indicator channel (PHICH). Given the above scenario, the UEs may provide the preference profile $\boldsymbol{\mathcal{P}}_{u_l}(\mathcal{N})$ with the SR and BSR messages. The relays may provide the corresponding values in the utility matrix, e.g., $\hat{\mathbf{u}}_{\boldsymbol{u_l,l}} = \mathfrak{U}_l[u_l, j]_{j=1,\cdots,N}$ and inform the parameter $\hat{P}_{u_l}^{(n)^{max}}$ using SG and ACK messages. Once the RB and power allocation is performed, the relays multicast the allocation information over X2 interface.

5.4 Analysis of the Proposed Solution

In the following, I analyze the performance of my proposed distributed resource allocation approach under bounded channel uncertainty. More specifically, I analyze the stability, optimality, and uniqueness of the solution, and its computational complexity.

5.4.1 Stability

Definition 5.3. *(a) The pair of UE and RB (u_l, n) in $\mathcal{U}_l \times \mathcal{N}$ is **acceptable** if u_l and n prefer each other (to be matched) to being remain unmatched.*

*(b) A matching μ_l is called **individually rational** if no agent (i.e., UE or RB) $\tilde{\jmath}$ prefers to remain unmatched to $\mu(\tilde{\jmath})$.*

Definition 5.4. *A matching μ_l is **blocked** by a pair of agents (i, j) if they each prefer each other to the matching they obtain by μ_l, i.e., $i \succeq \mu_l(j)$ and $j \succeq \mu_l(i)$.*

From **Definition 5.3**, **5.4**, the matching μ_l is blocked by RB n and UE u_l if n prefers u_l to $\mu_l(n)$ and either *i*) u_l prefers n to some $\hat{n} \in \mu_l(u_l)$, or *ii*) $\overline{\overline{\mu_l(u_l)}} < \kappa_{u_l}$ and n is acceptable to u_l. Using the above definitions, the stability of matching can be defined as follows [72, Chapter 5].

Definition 5.5. *A matching μ_l is **stable** if it is individually rational and there is no pair (u_l, n) in the set of acceptable pairs such that u_l prefers n to $\mu_l(u_l)$ and n prefers u_l to $\mu_l(n)$, i.e., not blocked by any pair of agents.*

Proposition 5.2. *The assignment performed in* **Algorithm 4** *abides by the preferences of the UEs and RBs and it leads to a stable allocation.*

Proof. See **Appendix D.1**. □

Note that the allocation of RBs is stable at each iteration of **Algorithm 5**. Since after evaluation of the utility, the preference profile of UEs and RBs are updated and the routine for RB allocation is repeated, a stable allocation is obtained.

5.4.2 Uniqueness

Proposition 5.3. *If there are sufficient number of RBs (i.e., $N \geq U_l$), and the preference lists of all UEs and RBs are determined by the $U_l \times N$ utility matrix $\mathfrak{U}_l$ whose entries are all different and obtained from given uncertainty bound, then there is a unique stable matching.*

Proof. See **Appendix D.2**. □

5.4.3 Optimality and Performance Bound

Definition 5.6. *A matching μ_l is weak Pareto optimal if there is no other matching $\widehat{\mu}_l$ that can achieve a better sum-rate, i.e., $\widehat{\mu}_l(\cdot) \geq \mu_l(\cdot)$, where the inequality is component-wise and strict for one user.*

Proposition 5.4. *The proposed resource allocation algorithm is weak Pareto optimal under bounded channel uncertainty.*

Proof. See **Appendix D.3**. □

Corollary 5.1. *Since $\mathbf{x_l}^*$ satisfies the binary constraint in (2.2), and the optimal allocation $(\mathbf{x_l}^*, \mathbf{P_l}^*)$ satisfies all the constraints in the optimization problem* **P4**, *for a sufficient number of available RBs, the data rate obtained by* **Algorithm 5** *gives a lower bound on the solution of the RAP under channel uncertainty.*

5.4.4 Complexity

Proposition 5.5. *The subroutine for RB allocation terminates after some finite number of steps T'.*

Proof. Let the finite set $\tilde{\mathcal{X}}$ represent all possible combinations of UE-RB matching where each element $\tilde{x}_i^{(j)} \in \tilde{\mathcal{X}}$ denotes that RB j is allocated to UE i. Since no UE rejects the same RB more than once (see line 7 in **Algorithm 4**), the finiteness of the set $\tilde{\mathcal{X}}$ ensures the termination of RB allocation subroutine in finite number of steps. □

In line 6-7 of **Algorithm 5**, the complexity to output the ordered set of preference profiles for the RBs using any standard sorting algorithm is $\mathcal{O}\left(NU_l \log U_l\right)$ and for each UE, the complexity to build the preference profile is $\mathcal{O}\left(N \log N\right)$. Let $\beta = \sum_{u_l=1}^{U_l} \overline{\overline{\mathcal{P}_{u_l}(\mathcal{N})}} + \sum_{n=1}^{N} \overline{\overline{\mathcal{P}_n(\mathcal{U}_l)}} = 2NU_l$ be the total length of input preferences in **Algorithm 4**, where $\overline{\overline{\mathcal{P}_j(\cdot)}}$ denotes the length of the profile vector $\mathcal{P}_j(\cdot)$. From **Proposition 5.5** and [70, Chapter 1] it can be shown that, if implemented with suitable data structures, the time complexity of RB allocation subroutine is linear in the size of input preference profiles, i.e., $\mathcal{O}(\beta) \approx \mathcal{O}\left(NU_l\right)$. Since **Phase II** of **Algorithm 5** runs at most fixed T_{max} iterations, at each relay node l, the complexity of the proposed solution is linear in $\overline{\overline{\mathcal{N}}}$ and $\overline{\overline{\mathcal{U}_l}}$.

5.5 Results

In the following, I demonstrate the performance evaluation results for the proposed relay-aided D2D communication approach. Similar to Chapter 4, I measure the uncertainty in channel gains as percentages and assume similar uncertainty bounds in the CQI parameters for all the UEs. For example, uncertainty bound

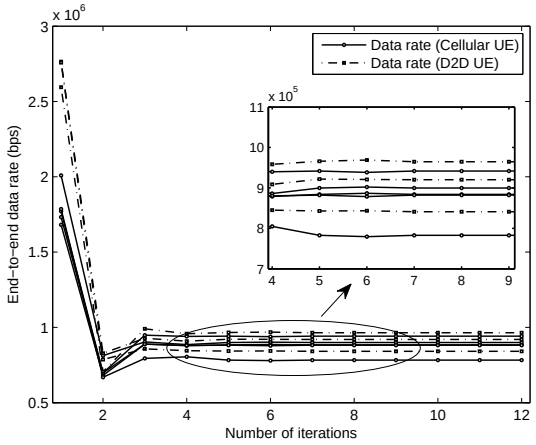

Figure 5.1: Convergence of the proposed solution where the number of CUEs and D2D UEs served by each relay node is 5 and 3, receptively (e.g., $|\mathcal{U}_l| = 8$). $D_{r,d}$ and $D_{d,d}$ are set to 50 m, and uncertainty in CQI parameters is assumed to be not more than 25%.

$\xi = \xi_{1_{u_l}}^{(n)} = \xi_{2_l} = \xi_{3_{u_l}}^{(n)} = \xi_{4_{u_l}}^{(n)} = 0.25$ refers that uncertainty (e.g., estimation error) in the CQI parameters for $\forall u_l, n, l$ is not more than 25% of their nominal values.

5.5.1 Convergence and Goodness of the Solution

In Fig. 5.1, I show the convergence behavior of my proposed distributed algorithm. In particular, I plot the average achievable data rate for the UEs in different network realizations versus the number of iterations. he algorithm starts with uniform power allocation over RBs, which provides a higher data rate at the first iteration; however, it may cause severe interference to other receiving nodes. As the algorithm executes, the allocations of RB and power are updated considering the interference threshold and data rate constraints. From this figure it can be observed that the solution converges to a stable data rate very quickly (e.g., in less than 10 iterations).

I compare the performance of my proposed scheme with a dual-decomposition based suboptimal resource allocation scheme proposed in [73]. I refer to this scheme

as *existing algorithm*. In this scheme, the relay node allocates RBs considering the data rate requirement and the transmit power is updated in an iterative manner by updating the Lagrange dual variables. For details refer to [73, Algorithm 2]. The complexity of this algorithm is of $\mathcal{O}\left(NU_l \log N + N \log U_l + \Delta\right)$, where Δ denotes the number of iterations it takes for the power allocation vector to converge [73].

In Fig. 5.2(a), I show the performances of the proposed distributed scheme and the existing algorithm, and the upper bound of the optimal solution which can be obtained in a centralized manner using **Algorithm 1**. I use the MATLAB optimization toolbox to obtain this upper bound. I plot the average achievable data rate for the UEs versus the total number of UEs. The average data rate is given by $R_{\text{avg}} = \frac{\sum_{u \in \{\mathcal{C} \cup \mathcal{D}\}} R_u^{\text{ach}}}{C+D}$, where R_u^{ach} is the achievable data rate for UE u. Note that, for a given number of RBs, increasing the number of UEs decreases the data rate. Recall that, the complexity of both the proposed and reference schemes is linear with the number of RBs and UEs; and for the optimal solution, the complexity is cubic to the number of RBs and UEs. As can be seen from this figure, the proposed approach outperforms the existing algorithm and performs close to the optimal solution.

In order to obtain more insights into the performance, in Fig 5.2(b), I plot the efficiency of the proposed scheme and existing algorithm for different number of UEs. Similar to [74, Chapter 3], I measure the efficiency as $\eta_{(\cdot)} = \frac{R_{(\cdot)}}{R_{\text{optm}}}$, where R_{optm} is the network sum-rate for optimal solution. The parameters R_{prop} and R_{exst} denote the data rate for the proposed and existing schemes, respectively, which are used to calculate the corresponding efficiency metric η_{prop} and η_{exst}. The closer the $\eta_{(\cdot)}$ to 1, the nearer the solution is to the optimal solution. Clearly, the efficiency of the existing algorithm is lower compared to the proposed scheme. From the figure I observe that even in a dense network scenario (i.e., $C + D = 15 + 18 = 33$) the

proposed scheme performs 80% close to the optimal solution (compared to 60% for the existing algorithm); however, with much less computational complexity.

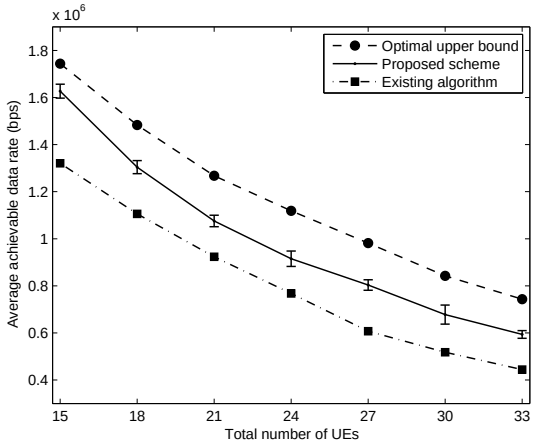

(a)

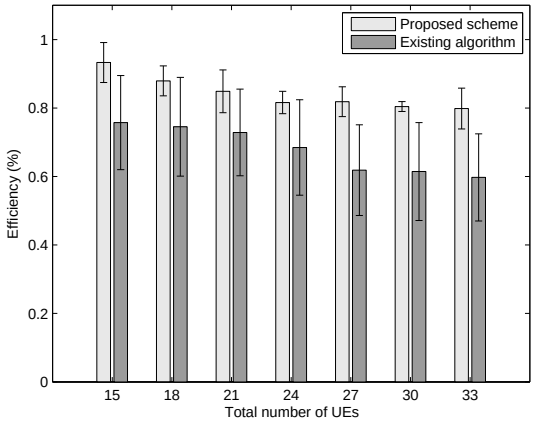

(b)

Figure 5.2: (a) Average achievable data rate for optimal upper bound, distributed stable matching and existing algorithm. (b) Efficiency of the proposed solution and the existing algorithm. Total number of UEs (i.e., $C + D$) are varied from $9 + 6 = 15$ to $15 + 18 = 33$. $D_{r,d}$ and $D_{d,d}$ are assumed to be 50 m.

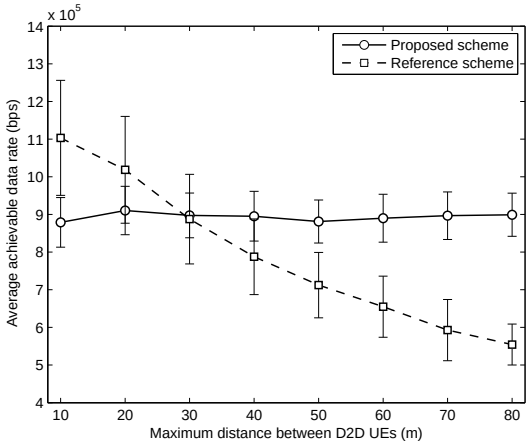

Figure 5.3: Gain in average achievable data rate with varying distance between D2D peers using a setup similar to that for Fig. 5.1. The reference scheme is an underlay D2D communication approach proposed in [17].

5.5.2 Impact of Relaying

Average achievable data rate vs. distance between D2D UEs:

The average achievable data rates of D2D UEs for both the proposed and reference schemes are illustrated in Fig. 5.3. I find the trends in the performance evaluation results are similar to those in earlier chapters. Although the reference scheme outperforms when the distance between the D2D UEs is small (i.e., $d < 40$ m), my proposed relay-aided communication approach, can greatly improve the data rate especially when the distance increases.

Gain in aggregate achievable data rate vs. varying distance between D2D UEs:

The gain in terms of aggregate achievable data rate under both uncertain and perfect CQI is shown in Fig. 5.4. The figure shows that, compared to direct communication, with the increasing distance between D2D UEs, relaying provides considerable gain

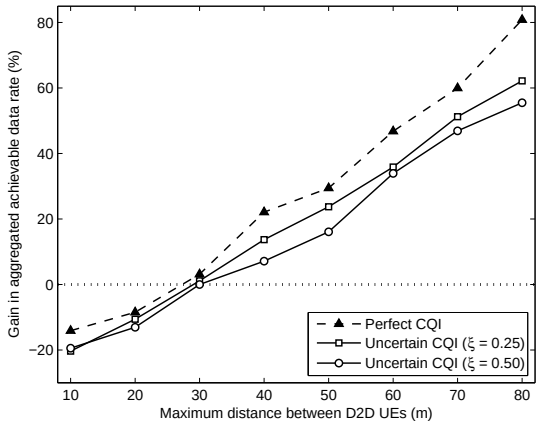

Figure 5.4: Gain in aggregate achievable data rate for both perfect and uncertain CQI parameters. For uncertain CQI, uncertainty bound $\xi = 0.25$ and $\xi = 0.50$ refer that uncertainty in CQI parameters is not more than 25% and 50%, respectively. For both the perfect and uncertain cases, there is a critical distance, beyond which relaying of D2D traffic provides significant performance gain.

in terms of achievable data rate and hence spectrum utilization. As expected, the gain reduces under channel uncertainty since the algorithm becomes cautious against channel fluctuations and allocates RBs and power accordingly to protect the receiving nodes in the network. Note that there is a trade-off between performance gain and robustness against channel uncertainty. For example, when the distance $D_{r,d} = 50$ m, the performance gain of relaying under perfect CQI is 30%. In the case of uncertain CQI, the gain reduces to 24% and 16% for the uncertainty bound parameter $\xi = 0.25$ and $\xi = 0.50$, respectively. As the uncertainty bounds increase, the system becomes more roust against uncertainty; however, the achievable data rate degrades.

Effect of relay-UE distance and distance between D2D UEs on rate gain:

The performance gain in terms of the achievable aggregate data rate under different relay-D2D UE distances is shown in Fig. 5.5. It is clear from the figure that, even for relatively large relay-D2D UE distances, e.g., $D_{r,d} > 60$ m, relaying D2D traffic provides considerable rate gain for distant D2D UEs.

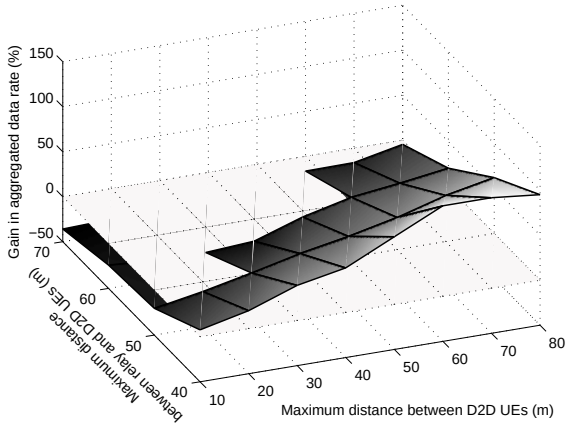

Figure 5.5: Effect of relay distance on rate gain: $|\mathcal{C}| = 15$, $|\mathcal{D}| = 9$. Uncertainty in CQI parameters is assumed to be not more than 25%. For every $D_{r,d}$, there is a distance threshold (i.e., upper position of the light-shaded surface) beyond which relaying provides significant gain in terms of aggregate achievable rate.

5.6 Summary and Discussions

I have provided a comprehensive resource allocation framework for relay-assisted D2D communication considering uncertainties in wireless channels and propose an iterative distributed solution using stable matching. I have analyzed the stability, uniqueness, and optimality of the proposed solution. I have also analyzed the complexity of the proposed approach. Numerical results have shown that the distributed solution is

close to the centralized optimal solution with significantly lower computational complexity. I have also compared the proposed relay-aided D2D communication scheme with an underlay D2D communication scheme. Through extensive simulations I have observed that, in comparison with a direct D2D communication scheme, beyond a distance threshold, relaying of D2D traffic for distant D2D UEs significantly improves the network performance.

Chapter 6

Conclusion and Future Directions

6.1 Concluding Remarks

Relay-aided D2D communication approach could be an effective solution for many next generation (e.g., 5G) cellular wireless applications, especially when the distance between D2D link is far and/or the link quality is not favorable. Considering a multi-relay multi-user environment in a multi-channel OFDMA system, in this work I have presented a radio resource allocation framework for relay-aided D2D communication networks. In Chapter 2, I have developed a RB and power allocation algorithm where the relays are able to perform resource allocation centrally. Since the complexity of the centralized scheme is cubic to the available resources and the number of UEs, in Chapter 3 I have developed a low complexity distributed solution. In Chapter 4 and Chapter 5, I have extended the mathematical formulations considering the uncertainties in wireless link using robust optimization techniques. To be specific, in Chapter 4 I have presented a gradient-based distributed solution considering the uncertainties in the interference links. I have also discussed the trade-off between robustness and optimality of the solution. Considering the uncertainties in both the

direct and interference links, in Chapter 5 I have developed a distributed resource allocation algorithm utilizing the concept of stable matching. In Chapter 3 and Chapter 5, I have also briefly discussed the possible implementation approaches of my proposed distributed solutions in practical LTE-A systems. From the numerical results I can conclude that, there is a distance margin beyond which relaying of D2D traffic improves the data rate without increasing the end-to-end delay significantly.

6.2 Future Research Directions

This work can be extended in two major directions to provide a comprehensive radio resource management framework. Similar to most of the literature, in this work I also assume that the potential D2D peers are already discovered. However, for a relay-aided D2D communication approach, the D2D peers may wish to dynamically select/discover the potential peers based on network dynamics. Furthermore, due to large number of devices and and their frequent access in the radio channel, existing medium access control (MAC) protocols need to be redesigned considering the relay-aided communication paradigm. A brief discussion on these research directions is provided below.

6.2.1 Device Discovery Schemes for Relay-Aided D2D Communication

Peer discovery methods for a D2D communication scenario is relatively under-explored area of research. Most of the existing mechanisms (e.g., a-priori/a-posteriori [28], beacon-based [75] etc.) are mainly centralized (e.g., operator/network controlled); and therefore, may suffer from scalability issues for future dense deployment scenarios. In addition since the D2D traffic could be assisted by relays, D2D UEs

can opportunistically select/update their potential peers based on network dynamics (e.g., link condition, network load, interference dynamics, application level requirements etc.). To the best of my knowledge, there is no prior work that considers link uncertainties in peer discovery method for a relay-aided D2D communication scenarios. The performance of existing D2D peer discovery mechanisms in a practical multi-user LTE-A scenario still remains unknown, and therefore, opens up new research opportunities.

6.2.2 Design and Analysis of MAC Protocols

It is anticipated that future generation of mobile network will be a *muti-tier heterogeneous* architecture to improve the overall end-user quality of experience [76], [77]. In addition to conventional macrocell-tier (e.g., an eNB with corresponding CUEs), these heterogeneous network tiers may include low power nodes (e.g., small cells, relays etc.) as well as wireless P2P nodes (e.g., D2D and M2M UEs, sensors etc.). The network-controlled P2P communications (e.g., similar to those approaches presented in this work) in 5G systems will allow other nodes (such as relay or M2M gateway), rather than the macro eNB, to control the communications among P2P nodes. It is also expected that the deployments of heterogeneous nodes in 5G systems will significantly have much higher density than present single-tier networks [78]. However, due to large number of devices and their frequent access in the wireless channels, network congestion will occur [16], and therefore, require an efficient radio access mechanism (e.g., MAC protocol). Design and analysis of a unified MAC protocol incorporating mode selection, device discovery, and such relay-aided D2D communication in the context of 5G LTE-A heterogeneous networks will be an interesting area of research.

Bibliography

[1] Y.-D. Lin and Y.-C. Hsu, "Multihop cellular: a new architecture for wireless communications," in *IEEE INFOCOM*, vol. 3, 2000, pp. 1273–1282.

[2] L. Lei, Z. Zhong, C. Lin, and X. Shen, "Operator controlled device-to-device communications in LTE-advanced networks," *IEEE Wireless Communications*, vol. 19, no. 3, pp. 96–104, 2012.

[3] M. Corson, R. Laroia, J. Li, V. Park, T. Richardson, and G. Tsirtsis, "Toward proximity-aware internetworking," *IEEE Wireless Communications*, vol. 17, no. 6, pp. 26–33, 2010.

[4] "Technical specification group services and system aspects; Feasibility study for proximity services (ProSe), release 12," 3rd Generation Partnership Project, Tech. Rep. 3GPP TR 22.803 V12.2.0, June 2013.

[5] J. Du, W. Zhu, J. Xu, Z. Li, and H. Wang, "A compressed HARQ feedback for device-to-device multicast communications," in *IEEE Vehicular Technology Conference (VTC Fall)*, 2012, pp. 1–5.

[6] B. Zhou, H. Hu, S.-Q. Huang, and H.-H. Chen, "Intracluster device-to-device relay algorithm with optimal resource utilization," *IEEE Transactions on Vehicular Technology*, vol. 62, no. 5, pp. 2315–2326, 2013.

[7] K. Doppler, M. Rinne, C. Wijting, C. Ribeiro, and K. Hugl, "Device-to-device communication as an underlay to LTE-advanced networks," *IEEE Communications Magazine*, vol. 47, no. 12, pp. 42–49, 2009.

[8] N. Golrezaei, A. Molisch, and A. Dimakis, "Base-station assisted device-to-device communications for high-throughput wireless video networks," in *IEEE International Conference on Communications (ICC)*, 2012, pp. 7077–7081.

[9] J. Li, M. Lei, and F. Gao, "Device-to-device (D2D) communication in MU-MIMO cellular networks," in *IEEE Global Communications Conference (GLOBECOM)*, 2012, pp. 3583–3587.

[10] N. K. Pratas and P. Popovski, "Low-rate machine-type communication via wireless device-to-device (D2D) links," *Submitted to JSAC "Device-to-Device Communications in Cellular Networks"*, 2013, arXiv preprint, http://arxiv.org/abs/1305.6783.

[11] X. Bao, U. Lee, I. Rimac, and R. R. Choudhury, "Dataspotting: offloading cellular traffic via managed device-to-device data transfer at data spots," *ACM SIGMOBILE Mobile Computing and Communications Review*, vol. 14, no. 3, pp. 37–39, Dec. 2010.

[12] F. Wang, C. Xu, L. Song, Z. Han, and B. Zhang, "Energy-efficient radio resource and power allocation for device-to-device communication underlaying cellular networks," in *International Conference on Wireless Communications Signal Processing (WCSP)*, 2012, pp. 1–6.

[13] P. Phunchongharn, E. Hossain, and D. Kim, "Resource allocation for device-to-device communications underlaying LTE-advanced networks," *IEEE Wireless Communications*, vol. 20, no. 4, pp. 91–100, 2013.

[14] L. Su, Y. Ji, P. Wang, and F. Liu, "Resource allocation using particle swarm optimization for D2D communication underlay of cellular networks," in *IEEE Wireless Communications and Networking Conference (WCNC)*, 2013, pp. 129–133.

[15] D. I. Kim, W. Choi, H. Seo, and B.-H. Kim, "Partial information relaying and relaying in 3GPP LTE," in *Cooperative Cellular Wireless Networks*. Cambridge University Press, 2011.

[16] M. Hasan, E. Hossain, and D. Niyato, "Random access for machine-to-machine communication in LTE-advanced networks: issues and approaches," *IEEE Communications Magazine*, vol. 51, no. 6, pp. 86–93, 2013.

[17] M. Zulhasnine, C. Huang, and A. Srinivasan, "Efficient resource allocation for device-to-device communication underlaying LTE network," in *IEEE 6th International Conference on Wireless and Mobile Computing, Networking and Communications (WiMob)*, 2010, pp. 368–375.

[18] Y. Pei and Y.-C. Liang, "Resource allocation for device-to-device communications overlaying two-way cellular networks," *IEEE Transactions on Wireless Communications*, vol. 12, no. 7, pp. 3611–3621, 2013.

[19] R. Zhang, X. Cheng, L. Yang, and B. Jiao, "Interference-aware graph based resource sharing for device-to-device communications underlaying cellu-

lar networks," in *IEEE Wireless Communications and Networking Conference (WCNC)*, 2013, pp. 140–145.

[20] L. B. Le, "Fair resource allocation for device-to-device communications in wireless cellular networks," in *IEEE Global Communications Conference (GLOBECOM)*, 2012, pp. 5451–5456.

[21] X. Ma, R. Yin, G. Yu, and Z. Zhang, "A distributed relay selection method for relay assisted device-to-device communication system," in *IEEE 23rd International Symposium on Personal Indoor and Mobile Radio Communications (PIMRC)*, 2012, pp. 1020–1024.

[22] L. Wang, T. Peng, Y. Yang, and W. Wang, "Interference constrained relay selection of D2D communication for relay purpose underlaying cellular networks," in *8th International Conference on Wireless Communications, Networking and Mobile Computing (WiCOM)*, 2012, pp. 1–5.

[23] D. Lee, S.-I. Kim, J. Lee, and J. Heo, "Performance of multihop decode-and-forward relaying assisted device-to-device communication underlaying cellular networks," in *International Symposium on Information Theory and its Applications (ISITA)*, 2012, pp. 455–459.

[24] K. Vanganuru, S. Ferrante, and G. Sternberg, "System capacity and coverage of a cellular network with D2D mobile relays," in *Military Communications Conference (MILCOM)*, 2012, pp. 1–6.

[25] M. Belleschi, G. Fodor, and A. Abrardo, "Performance analysis of a distributed resource allocation scheme for D2D communications," in *2011 IEEE GLOBECOM Workshops (GC Wkshps)*, 2011, pp. 358–362.

[26] M. Alam, J. W. Mark, and X. Shen, "Relay selection and resource allocation for multi-user cooperative LTE-A uplink," in *IEEE International Conference on Communications (ICC)*, 2012, pp. 5092–5096.

[27] A. Ghosh, J. Zhang, J. G. Andrews, and R. Muhamed, *Fundamentals of LTE*, 1st ed. Prentice Hall Press, 2010.

[28] G. Fodor, E. Dahlman, G. Mildh, S. Parkvall, N. Reider, G. Miklós, and Z. Turányi, "Design aspects of network assisted device-to-device communications," *IEEE Communications Magazine*, vol. 50, no. 3, pp. 170–177, March 2012.

[29] M. Sikora, J. Laneman, M. Haenggi, D. Costello, and T. Fuja, "Bandwidth- and power-efficient routing in linear wireless networks," *IEEE Transactions on Information Theory*, vol. 52, no. 6, pp. 2624–2633, 2006.

[30] Alcatel-Lucent, "The LTE network architecture," December 2009, White Paper.

[31] A. Abdelnasser and E. Hossain, "Joint subchannel and power allocation in two-tier OFDMA HetNets with clustered femtocells," in *IEEE International Conference on Communications (ICC)*, June 2013, pp. 6002–6007.

[32] Z. Shen, J. Andrews, and B. Evans, "Adaptive resource allocation in multiuser OFDM systems with proportional rate constraints," *IEEE Transactions on Wireless Communications*, vol. 4, no. 6, pp. 2726–2737, 2005.

[33] M. Tao, Y.-C. Liang, and F. Zhang, "Resource allocation for delay differentiated traffic in multiuser OFDM systems," *IEEE Transactions on Wireless Communications*, vol. 7, no. 6, pp. 2190–2201, 2008.

[34] S. Boyd and L. Vandenberghe, *Convex Optimization*. New York, NY, USA: Cambridge University Press, 2004.

[35] W. Yu and R. Lui, "Dual methods for nonconvex spectrum optimization of multicarrier systems," *IEEE Transactions on Communications*, vol. 54, no. 7, pp. 1310–1322, 2006.

[36] D. Bharadia, G. Bansal, P. Kaligineedi, and V. Bhargava, "Relay and power allocation schemes for OFDM-based cognitive radio systems," *IEEE Transactions on Wireless Communications*, vol. 10, no. 9, pp. 2812–2817, 2011.

[37] A. Rogers, A. Farinelli, R. Stranders, and N. R. Jennings, "Bounded approximate decentralised coordination via the max-sum algorithm," *Artificial Intelligence*, vol. 175, no. 2, pp. 730–759, 2011.

[38] J. S. Yedidia, W. T. Freeman, and Y. Weiss, "Understanding belief propagation and its generalizations," in *Exploring artificial intelligence in the new millennium*, G. Lakemeyer and B. Nebel, Eds. San Francisco, CA, USA: Morgan Kaufmann Publishers Inc., 2003, pp. 239–269.

[39] S. Aji and R. McEliece, "The generalized distributive law," *IEEE Transactions on Information Theory*, vol. 46, no. 2, pp. 325–343, 2000.

[40] A. Abrardo, M. Belleschi, P. Detti, and M. Moretti, "Message passing resource allocation for the uplink of multi-carrier multi-format systems," *IEEE Transactions on Wireless Communications*, vol. 11, no. 1, pp. 130–141, 2012.

[41] ——, "A min-sum approach for resource allocation in communication systems," in *IEEE International Conference on Communications (ICC)*, 2011, pp. 1–6.

[42] F. Berggren, R. Jantti, and S.-L. Kim, "A generalized algorithm for constrained power control with capability of temporary removal," *IEEE Transactions on Vehicular Technology*, vol. 50, no. 6, pp. 1604–1612, 2001.

[43] S. Im, H. Jeon, and H. Lee, "Autonomous distributed power control for cognitive radio networks," in *IEEE 68th Vehicular Technology Conference (VTC-Fall)*, 2008, pp. 1–5.

[44] K. Yang, N. Prasad, and X. Wang, "A message-passing approach to distributed resource allocation in uplink DFT-Spread-OFDMA systems," *IEEE Transactions on Communications*, vol. 59, no. 4, pp. 1099–1113, 2011.

[45] D. Schultz, R. Pabst, and B. Walke, "Analytical estimation of packet delays in relay-based imt-advanced networks," in *IEEE Vehicular Technology Conference (VTC Spring)*, 2008, pp. 2411–2415.

[46] A. Ben-tal and A. Nemirovski, "Robust solutions of uncertain linear programs," *Operations Research Letters*, vol. 25, pp. 1–13, 1999.

[47] X. Zhang, D. Palomar, and B. Ottersten, "Statistically robust design of linear MIMO transceivers," *IEEE Transactions on Signal Processing*, vol. 56, no. 8, pp. 3678–3689, 2008.

[48] S. Zhou and G. Giannakis, "Optimal transmitter eigen-beamforming and space-time block coding based on channel mean feedback," *IEEE Transactions on Signal Processing*, vol. 50, no. 10, pp. 2599–2613, 2002.

[49] A. Ben-Tal and A. Nemirovski, "Selected topics in robust convex optimization," *Mathematical Programming*, vol. 112, no. 1, pp. 125–158, 2008.

[50] S.-J. Kim, N. Soltani, and G. Giannakis, "Resource allocation for OFDMA cognitive radios under channel uncertainty," *IEEE Transactions on Wireless Communications*, vol. 12, no. 7, pp. 3578–3587, 2013.

[51] S. Mallick, R. Devarajan, M. Rashid, and V. Bhargava, "Robust power allocation designs for cognitive radio networks with cooperative relays," in *IEEE International Conference on Communications (ICC)*, 2012, pp. 1677–1682.

[52] S. Parsaeefard and A.-R. Sharafat, "Robust worst-case interference control in underlay cognitive radio networks," *IEEE Transactions on Vehicular Technology*, vol. 61, no. 8, pp. 3731–3745, 2012.

[53] M. Mdard, "The effect upon channel capacity in wireless communications of perfect and imperfect knowledge of the channel." *IEEE Transactions on Information Theory*, vol. 46, no. 3, pp. 933–946, 2000.

[54] D. Bertsimas, D. Pachamanova, and M. Sim, "Robust linear optimization under general norms," *Operations Research Letters*, vol. 32, no. 6, pp. 510–516, Nov. 2004.

[55] K. Fazel and S. Kaiser, *Multi-Carrier and Spread Spectrum Systems*. New York, NY, USA: John Wiley & Sons, Inc., 2003.

[56] K. Son, B. C. Jung, S. Chong, and D. K. Sung, "Power allocation for OFDM-based cognitive radio systems under outage constraints," in *IEEE International Conference on Communications (ICC)*, 2010, pp. 1–5.

[57] A. J. G. Anandkumar, A. Anandkumar, S. Lambotharan, and J. Chambers, "Robust rate maximization game under bounded channel uncertainty," *IEEE Transactions on Vehicular Technology*, vol. 60, no. 9, pp. 4471–4486, 2011.

[58] A. Pascual-Iserte, D. Palomar, A. Perez-Neira, and M.-A. Lagunas, "A robust maximin approach for MIMO communications with imperfect channel state information based on convex optimization," *IEEE Transactions on Signal Processing*, vol. 54, no. 1, pp. 346–360, 2006.

[59] A. Ben-Tal and A. S. Nemirovskiaei, "Conic quadratic programming," in *Lectures on Modern Convex Optimization: Analysis, Algorithms, and Engineering Applications (MPS-SIAM Series on Optimization)*. Philadelphia, PA, USA: Society for Industrial and Applied Mathematics, 2001.

[60] Y. Gu, W. Saad, M. Bennis, M. Debbah, and Z. Han, "Matching theory for future wireless networks: fundamentals and applications," *arXiv preprint arXiv:1410.6513*, 2014.

[61] E. Jorswieck, "Stable matchings for resource allocation in wireless networks," in *17th International Conference on Digital Signal Processing (DSP)*, July 2011, pp. 1–8.

[62] K. Yang, Y. Wu, J. Huang, X. Wang, and S. Verdu, "Distributed robust optimization for communication networks," in *IEEE Conference on Computer Communications (INFOCOM)*, April 2008.

[63] S. Sun, W. Ni, and Y. Zhu, "Robust power control in cognitive radio networks: A distributed way," in *Communications (ICC), 2011 IEEE International Conference on*, June 2011, pp. 1–6.

[64] A. J. G. Anandkumar, A. Anandkumar, S. Lambotharan, and J. Chambers, "Robust rate-maximization game under bounded channel uncertainty," in *IEEE*

International Conference on Acoustics Speech and Signal Processing (ICASSP), March 2010, pp. 3158–3161.

[65] R. Hettich and K. O. Kortanek, "Semi-infinite programming: theory, methods, and applications," *SIAM review*, vol. 35, no. 3, pp. 380–429, 1993.

[66] S. S. Dragomir, "A survey on Cauchy-Bunyakovsky-Schwarz type discrete inequalities," *Journal of Inequalities in Pure and Applied Mathematics*, vol. 4, no. 3, pp. 1–142, 2003.

[67] D. Gale and L. S. Shapley, "College admissions and the stability of marriage," *American Mathematical Monthly*, pp. 9–15, 1962.

[68] B. Rastegari, A. Condon, N. Immorlica, and K. Leyton-Brown, "Two-sided matching with partial information," in *14th ACM Conference on Electronic Commerce*. New York, NY, USA: ACM, 2013, pp. 733–750.

[69] A. B. MacKenzie and L. A. DaSilva, "Game theory for wireless engineers," *Synthesis Lectures on Communications*, vol. 1, no. 1, pp. 1–86, 2006.

[70] G. O'Malley, "Algorithmic aspects of stable matching problems," Ph.D. dissertation, University of Glasgow, 2007.

[71] 3GPP TS 36.321 V12.1.0, "Medium Access Control (MAC) protocol specification (release 12)," 3rd Generation Partnership Project (3GPP), Tech. Rep., March 2014.

[72] A. E. Roth and M. A. O. Sotomayor, *Two-sided matching: a study in game-theoretic modeling and analysis*. Cambridge University Press, 1992, no. 18.

[73] H. Zhang, C. Jiang, N. Beaulieu, X. Chu, X. Wen, and M. Tao, "Resource allocation in spectrum-sharing OFDMA femtocells with heterogeneous services," *IEEE Transactions on Communications*, vol. 62, no. 7, pp. 2366–2377, July 2014.

[74] L. Song, Z. Han, and C. Xu, *Resource Management for Device-to-Device Underlay Communication*. Springer, 2013.

[75] K. Doppler, C. Ribeiro, and J. Kneckt, "Advances in D2D communications: Energy efficient service and device discovery radio," in *2nd International Conference on Wireless Communication, Vehicular Technology, Information Theory and Aerospace Electronic Systems Technology (Wireless VITAE)*, Feb 2011, pp. 1–6.

[76] W. H. Chin, Z. Fan, and R. Haines, "Emerging technologies and research challenges for 5G wireless networks," *IEEE Wireless Communications*, vol. 21, no. 2, pp. 106–112, April 2014.

[77] E. Hossain, M. Rasti, H. Tabassum, and A. Abdelnasser, "Evolution toward 5G multi-tier cellular wireless networks: An interference management perspective," *IEEE Wireless Communications*, vol. 21, no. 3, pp. 118–127, June 2014.

[78] N. Bhushan, J. Li, D. Malladi, R. Gilmore, D. Brenner, A. Damnjanovic, R. Sukhavasi, C. Patel, and S. Geirhofer, "Network densification: The dominant theme for wireless evolution into 5G," *IEEE Communications Magazine*, vol. 52, no. 2, pp. 82–89, February 2014.

[79] Y. Yuan, "LTE-A relay scenarios and evaluation methodology," in *LTE-Advanced Relay Technology and Standardization*. Springer, 2013, pp. 9–38.

[80] B. Kaufman and B. Aazhang, "Cellular networks with an overlaid device to device network," in *42nd Asilomar Conference on Signals, Systems and Computers*, Oct 2008, pp. 1537–1541.

[81] L. B. Le, D. Niyato, E. Hossain, D. I. Kim, and D. T. Hoang, "QoS-aware and energy-efficient resource management in OFDMA femtocells," *IEEE Transactions on Wireless Communications*, vol. 12, no. 1, pp. 180–194, 2013.

[82] A. M. d. Turkmani, "Probability of error for M-branch macroscopic selection diversity," *IEE Proceedings I Communications, Speech and Vision*, vol. 139, no. 1, pp. 71–78, 1992.

[83] H. Fu and D. I. Kim, "Analysis of throughput and fairness with downlink scheduling in WCDMA networks," *IEEE Transactions on Wireless Communications*, vol. 5, no. 8, pp. 2164–2174, 2006.

[84] N. Mehta, J. Wu, A. Molisch, and J. Zhang, "Approximating a sum of random variables with a lognormal," *IEEE Transactions on Wireless Communications*, vol. 6, no. 7, pp. 2690–2699, 2007.

[85] D. P. Bertsekas, *Nonlinear Programming*, 2nd ed. Athena Scientific, 1999.

[86] K. Yang, N. Prasad, and X. Wang, "An auction approach to resource allocation in uplink OFDMA systems," *IEEE Transactions on Signal Processing*, vol. 57, no. 11, pp. 4482–4496, 2009.

[87] S. Boyd and A. Mutapcic, "Subgradient methods," [Online], www.stanford.edu/class/ee364b/notes/subgrad_method_notes.pdf, lecture notes for EE364b, Stanford University.

[88] D. G. Cacuci, *Sensitivity and Uncertainty Analysis. Vol. 1: Theory.* Boca Raton, FL: Chapman and Hall/CRC, 2003.

Appendix A

A.1 Radio Propagation Model

For modeling the propagation channel, I consider distance-dependent path-loss and shadow fading; furthermore, the channel is assumed to experience Rayleigh fading. In particular, I consider realistic 3GPP propagation environment[1] presented in [79]. For example, UE-relay (and relay-D2D) link follows the following path-loss equation:

$$PL_{u_l,l}(\ell)_{[dB]} = 103.8 + 20.9\log(\ell) + L_{su} + 10\log(\varsigma) \tag{A.1}$$

where ℓ is the distance between UE and relay in kilometer, L_{su} accounts for shadow fading and is modelled as a log-normal random variable, and ς is an exponentially distributed random variable which represents the Rayleigh fading channel power gain. Similarly, the path-loss equation for relay-eNB link is expressed as

$$PL_{l,eNB}(\ell)_{[dB]} = 100.7 + 23.5\log(\ell) + L_{sr} + 10\log(\varsigma) \tag{A.2}$$

[1]Any other propagation model for D2D communication can be used for the proposed resource allocation method.

where L_{sr} is a log-normal random variable accounting for shadow fading. Hence given the distance ℓ, the link gain between any pair of network nodes i, j can be calculated as $10^{-\frac{PL_{i,j}(\ell)}{10}}$.

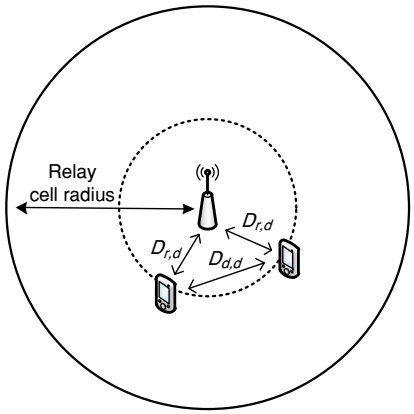

Figure A.1: D2D UEs are uniformly distributed within radius $D_{r,d}$ and maintain distance $D_{d,d}$ between peers.

A.2 Simulation Setup

I develop a discrete-time simulator in MATLAB and evaluate the performance of my proposed solution. I simulate a single three-sectored cell in a rectangular area of 700 m $\times$ 700 m, where the eNB is located in the center of the cell and three relays are deployed, i.e., one relay in each sector. The CUEs are uniformly distributed within the relay cell. The D2D UEs are located according to the clustered distribution model [80]. In particular, as shown in Fig. A.1, the D2D transmitters are uniformly distributed over a radius $D_{r,d}$; and the D2D receivers are distributed uniformly in the perimeter of the circle with radius $D_{d,d}$ centered at the corresponding D2D transmitter. Both $D_{r,d}$ and $D_{d,d}$ are varied as simulation parameters and the values are specified in the corresponding figures. The simulation results are averaged over different network realizations of user locations and link gains. I consider a snapshot model and all the

Table A.1: Simulation Parameters

Parameter	**Values**
Cell layout	Isolated cell, hexagonal grid, 3-sector sites
Carrier frequency	2.35 GHz
System bandwidth	2.5 MHz
Total number of available RBs	13
MAC frame duration	10 msec
Scheduling time	0.10 msec
Packet size	1500 bytes
Relay cell radius	200 meter
Distance between eNB and relays	125 meter
Minimum distance between UE and relay	10 meter
Total power available at each relay	30 dBm
Total power available at UE	23 dBm
Rate requirement for cellular UEs	128 Kbps
Rate requirement for D2D UEs	256 Kbps
Interference threshold	-70 dBm
Standard deviation of shadow fading:	
for relay-eNB links	6 dB
for UE-relay links	10 dB
Noise power spectral density	-174 dBm/Hz

network parameters are assumed to remain unchanged during a simulation run.

A.3 Parameters

The parameter values used in the simulation are summarized in Table A.1.

Appendix B

B.1 Required Number of RB(s) for a Given QoS Requirement

Let $\gamma_{u_l,l,1}^{(n)}$ and $\bar{\gamma}_{u_l,l,1}^{(n)}$ denote the instantaneous and average SINR for the UE u_l over RB n. In order to determine the required number of RB(s) for a given data rate requirement for any UE, I need to derive the probability distribution of $\frac{\gamma_{u_l,l,1}^{(n)}}{\bar{\gamma}_{u_l,l,1}^{(n)}}$ [81]. Note that, the channel gain due to Rayleigh fading and log-normal shadowing can be approximated by a single log-normal distribution [82, 83]. In addition, the sum of random variables having log-normal distribution can be represented by a single log-normal distribution [84]. Therefore, $\Gamma_{u_l,l,1}^{(n)} = \frac{\gamma_{u_l,l,1}^{(n)}}{\bar{\gamma}_{u_l,l,1}^{(n)}}$ can be approximated by a log-normal random variable whose mean and standard deviation can be calculated as shown in [83]. Hence the average rate achieved by UE u_l over RB n can be written as (B.1) where $F_{\Gamma_{u_l,l,1}^{(n)}}(\vartheta)$ and $f_{\Gamma_{u_l,l,1}^{(n)}}(\vartheta)$ are the probability density function and probability distribution function of $\Gamma_{u_l,l,1}^{(n)}$, respectively.

$$\bar{r}_{u_l,l}^{(n)} = \frac{1}{2} B_{RB} \int_0^{\infty} \log_2\left(1 + P_{u_l,l}^{(n)} \Gamma_{u_l,l,1}^{(n)} \bar{\gamma}_{u_l,l,1}^{(n)}\right) \left[\prod_{\substack{j \in \mathcal{U}_l, \\ j \neq u_l}} F_{\Gamma_{j,l,1}^{(n)}}(\vartheta)\right] f_{\Gamma_{u_l,l,1}^{(n)}}(\vartheta) d\vartheta. \quad \text{(B.1)}$$

Now, let $\underline{R}_{u_l,l}$ be the minimum rate achieved by UE u_l. In order to maintain the data rate requirement, I can derive the following inequality[1]:

$$Q_{u_l} \leq \kappa_{u_l} \leq \underline{R}_{u_l,l}\left(|\mathcal{U}_l|\right) \tag{B.2}$$

where by $\underline{R}_{u_l,l}\left(|\mathcal{U}_l|\right)$ I explicitly describe the dependence of the minimum achievable rate $\underline{R}_{u_l,l}$ on the number of UEs $|\mathcal{U}_l|$. Therefore, the minimum number of required RBs is given by

$$\kappa_{u_l} \geq \left\lceil \frac{Q_{u_l}}{\underline{R}_{u_l,l}\left(|\mathcal{U}_l|\right)} \right\rceil. \tag{B.3}$$

B.2 Proof of Proposition 3.1

$$\begin{aligned}\mathbb{L}_l = &\sum_{u_l\in\mathcal{U}_l}\sum_{n=1}^{N} \tfrac{1}{2} x_{u_l}^{(n)} R_{u_l}^{(n)} + \sum_{n=1}^{N} \ddot{a}_n \left(1 - \sum_{u_l\in\mathcal{U}_l} x_{u_l}^{(n)}\right) + \sum_{u_l\in\mathcal{U}_l} \ddot{b}_{u_l} \left(P_{u_l}^{max} - \sum_{n=1}^{N} x_{u_l}^{(n)} P_{u_l,l}^{(n)}\right) \\ &+ \ddot{c}_l \left(P_l^{max} - \sum_{u_l\in\mathcal{U}_l}\sum_{n=1}^{N} \frac{\gamma_{u_l,l,1}^{(n)}}{\gamma_{l,u_l,2}^{(n)}} x_{u_l}^{(n)} P_{u_l,l}^{(n)}\right) + \sum_{n=1}^{N} \ddot{d}_n \left(I_{th,1}^{(n)} - \sum_{u_l\in\mathcal{U}_l} x_{u_l}^{(n)} P_{u_l,l}^{(n)} g_{u_l^*,l,1}^{(n)}\right) \\ &+ \sum_{n=1}^{N} \ddot{e}_n \left(I_{th,2}^{(n)} - \sum_{u_l\in\mathcal{U}_l} \frac{\gamma_{u_l,l,1}^{(n)}}{\gamma_{l,u_l,2}^{(n)}} x_{u_l}^{(n)} P_{u_l,l}^{(n)} g_{l,u_l^*,2}^{(n)}\right) + \sum_{u_l\in\mathcal{U}_l} \ddot{f}_{u_l} \left(\sum_{n=1}^{N} \tfrac{1}{2} x_{u_l}^{(n)} R_{u_l}^{(n)} - Q_{u_l}\right).\end{aligned} \tag{B.4}$$

[1]Similar to [81], I assume that the long-term channel gains on different RBs are same, and hence, the average rates achieved by a particular UE on different RBs are the same.

Let me rearrange the Lagrangian of **P2.1** defined by (B.4) as follows:

$$\begin{aligned}\mathbb{L}_l = &\sum_{u_l\in\mathcal{U}_l}\sum_{n=1}^{N}\tfrac{1}{2}x_{u_l}^{(n)}R_{u_l}^{(n)} - \sum_{n=1}^{N}\ddot{a}_n\sum_{u_l\in\mathcal{U}_l}x_{u_l}^{(n)}\\ &- \sum_{u_l\in\mathcal{U}_l}\ddot{b}_{u_l}\sum_{n=1}^{N}x_{u_l}^{(n)}P_{u_l,l}^{(n)} - \ddot{c}_l\sum_{u_l\in\mathcal{U}_l}\sum_{n=1}^{N}\frac{\gamma_{u_l,l,1}^{(n)}}{\gamma_{l,u_l,2}^{(n)}}x_{u_l}^{(n)}P_{u_l,l}^{(n)}\\ &- \sum_{n=1}^{N}\ddot{d}_n\sum_{u_l\in\mathcal{U}_l}x_{u_l}^{(n)}P_{u_l,l}^{(n)}g_{u_l^*,l,1}^{(n)}\\ &- \sum_{n=1}^{N}\ddot{e}_n\sum_{u_l\in\mathcal{U}_l}\frac{\gamma_{u_l,l,1}^{(n)}}{\gamma_{l,u_l,2}^{(n)}}x_{u_l}^{(n)}P_{u_l,l}^{(n)}g_{l,u_l^*,2}^{(n)}\\ &- \sum_{u_l\in\mathcal{U}_l}\ddot{f}_{u_l}\sum_{n=1}^{N}\tfrac{1}{2}x_{u_l}^{(n)}R_{u_l}^{(n)} + \widetilde{O}. \end{aligned} \tag{B.5}$$

where $\widetilde{O}$ denote the leftover terms involving Lagrange multipliers, i.e., $\ddot{\boldsymbol{a}}, \ddot{\boldsymbol{b}}, \ddot{\boldsymbol{c}}, \ddot{\boldsymbol{d}}, \ddot{\boldsymbol{e}}, \ddot{\boldsymbol{f}}$. From above I can derive the following lemma:

Lemma B.2.1. *The slackness conditions for* **P2.1** *are*

$$\widehat{R}_{u_l}^{(n)} - \ddot{\lambda}_{u_l}^{(n)^*} = \max_{1\le j\le N}\left(\widehat{R}_{u_l}^{(j)} - \ddot{\lambda}_{u_l}^{(j)^*}\right) \tag{B.6}$$

where $\ddot{\lambda}_{u_l}^{(n)}$ *involves the terms with Lagrange multipliers for* $\forall u_l, n$.

Proof. By Weierstrass' theorem (Appendix A.2, Proposition A.8 in [85]), the dual function can be calculated by (B.7).

$$
\begin{aligned}
\mathcal{D}_l &= \inf_{\boldsymbol{x_l}} \mathbb{L}_l \\
&= \inf_{\boldsymbol{x_l}} \sum_{u_l \in \mathcal{U}_l} \left(\sum_{n=1}^{N} \left(\tfrac{1}{2} R_{u_l}^{(n)} - \ddot{a}_n - \ddot{b}_{u_l} P_{u_l,l}^{(n)} - \ddot{c}_l \tfrac{\gamma_{u_l,l,1}^{(n)}}{\gamma_{l,u_l,2}^{(n)}} P_{u_l,l}^{(n)} - \ddot{d}_n P_{u_l,l}^{(n)} g_{u_l^*,l,1}^{(n)} \right. \right. \\
&\qquad \left. \left. - \ddot{e}_n \tfrac{\gamma_{u_l,l,1}^{(n)}}{\gamma_{l,u_l,2}^{(n)}} P_{u_l,l}^{(n)} g_{l,u_l^*,2}^{(n)} + \ddot{f}_{u_l} \tfrac{1}{2} R_{u_l}^{(n)} \right) x_{u_l}^{(n)} \right) + \widetilde{O} \\
&= \sum_{u_l \in \mathcal{U}_l} \left(\sum_{n=1}^{N} \inf_{\boldsymbol{x_l}} \left(\tfrac{1}{2} R_{u_l}^{(n)} (1 + \ddot{f}_{u_l}) - \ddot{\lambda}_{u_l}^{(n)} \right) x_{u_l}^{(n)} \right) + \widetilde{O} \\
&= \sum_{u_l \in \mathcal{U}_l} \max_{1 \le n \le N} \left(\widehat{R}_{u_l}^{(n)} - \ddot{\lambda}_{u_l}^{(n)} \right) \kappa_{u_l} + \widetilde{O}. \qquad \text{(B.7)}
\end{aligned}
$$

Therefore, if **P2.1** has an optimal solution, its dual has an optimal solution, i.e.,

$$
\mathcal{D}_l{}^* = \sum_{u_l \in \mathcal{U}_l} \sum_{n=1}^{N} \widehat{R}_{u_l}^{(n)} x_{u_l}^{(n)*}. \qquad \text{(B.8)}
$$

Hence,

$$
\sum_{u_l \in \mathcal{U}_l} \max_{1 \le n \le N} \left(\widehat{R}_{u_l}^{(n)} - \ddot{\lambda}_{u_l}^{(n)^*} \right) \kappa_{u_l} + \widetilde{O} = \sum_{u_l \in \mathcal{U}_l} \sum_{n=1}^{N} \widehat{R}_{u_l}^{(n)} x_{u_l}^{(n)*}. \qquad \text{(B.9)}
$$

Since $\boldsymbol{x_l}^*$ is an optimal allocation, from (B.9) I obtain

$$
\sum_{u_l \in \mathcal{U}_l} \max_{1 \le n \le N} \left(\widehat{R}_{u_l}^{(n)} - \ddot{\lambda}_{u_l}^{(n)^*} \right) \kappa_{u_l} = \sum_{u_l \in \mathcal{U}_l} \sum_{n=1}^{N} \left(\widehat{R}_{u_l}^{(n)} - \ddot{\lambda}_{u_l}^{(n)^*} \right) x_{u_l}^{(n)*}. \qquad \text{(B.10)}
$$

In addition, since $\sum_{n=1}^{N} x_{u_l}^{(n)} = \kappa_{u_l}$, (B.10) becomes

$$\sum_{u_l \in \mathcal{U}_l} \sum_{n=1}^{N} \left(\widehat{R}_{u_l}^{(n)} - \ddot{\lambda}_{u_l}^{(n)^*} - \max_{1 \leq n \leq N} \left(\widehat{R}_{u_l}^{(n)} - \ddot{\lambda}_{u_l}^{(n)^*} \right) \right) x_{u_l}^{(n)^*} = 0. \tag{B.11}$$

Now, if $x_{u_l}^{(n)^*} > 0$, I have $\widehat{R}_{u_l}^{(n)} - \ddot{\lambda}_{u_l}^{(n)^*} = \max_{1 \leq j \leq N} \left(\widehat{R}_{u_l}^{(j)} - \ddot{\lambda}_{u_l}^{(j)^*} \right)$. □

From (3.24), at each iteration, each UE u_l can distinguish between two different subsets of RBs by sorting the marginals in an increasing order. Let me define the first subset $\dot{\mathcal{N}}_{u_l} \in \mathcal{N}$ given by the first $\kappa_{u_l} \leq N$ RBs in the ordered list of marginals where the second subset $\ddot{\mathcal{N}}_{u_l} \in \mathcal{N}$ is given by the last $N - \kappa_{u_l}$ of the list. Accordingly, I can have the following lemma:

Lemma B.2.2. *At convergence,* $\widehat{R}_{u_l}^{(\dot{n})} + \tilde{\psi}_{u_l,l}^{(\dot{n})} < \widehat{R}_{u_l}^{(\ddot{n})} + \tilde{\psi}_{u_l,l}^{(\ddot{n})}$ *for* $\forall u_l, \dot{n} \in \dot{\mathcal{N}}_{u_l}, \ddot{n} \in \ddot{\mathcal{N}}_{u_l}$.

Proof. See [41]. □

From **Lemma B.2.1** and **B.2.2**, it can be noted that, the inequality $\widehat{R}_{u_l}^{(\dot{n})} - \ddot{\lambda}_{u_l}^{(\dot{n})^*} < \widehat{R}_{u_l}^{(\ddot{n})} - \ddot{\lambda}_{u_l}^{(\ddot{n})^*}$ implies the slackness condition (B.6) by imposing $\ddot{\lambda}_{u_l}^{(\dot{n})^*} = -\tilde{\psi}_{u_l,l}^{(\dot{n})}$ and $\ddot{\lambda}_{u_l}^{(\ddot{n})^*} = -\tilde{\psi}_{u_l,l}^{(\ddot{n})}$; hence, the proof of **Proposition 3.1** follows.

B.3 Proof of Proposition 3.2

From [35] and Proposition 4 of [86], there must exist a non-overlapping binary valued feasible allocation even after relaxation when the number of RBs tends to infinity. Since in my problem the number of RBs is sufficiently large, the messages converge to a fixed point and I can conclude that the LP relaxation of **P2.1**, i.e., $x_{u_l}^{(n)} \in (0, 1]$ achieves the same optimal objective value. Thus, directly following the theorem of integer programming duality (i.e., if the primal problem has an optimal solution, then

the dual also has an optimal one) for any finite N, the optimal objective value of $\mathcal{D}_l$ lies between **P2.1** and its LP relaxation.

Appendix C

C.1 Power and RB Allocation for Nominal Problem

To observe the nature of power allocation for a UE, I use Karush-Kuhn-Tucker (KKT) optimality conditions and define the Lagrangian function as follows

$$\begin{aligned}\mathbb{L}_l(\mathbf{x},\mathbf{S},\boldsymbol{\omega},\boldsymbol{\mu},\boldsymbol{\rho},\nu_l,\boldsymbol{\psi},\boldsymbol{\varphi},\boldsymbol{\lambda},\boldsymbol{\varrho}) = &-\sum_{u_l\in\mathcal{U}_l}\sum_{n=1}^{N}\tfrac{1}{2}x_{u_l}^{(n)}B_{RB}\log_2\left(1+\tfrac{S_{u_l,l}^{(n)}h_{u_l,l,1}^{(n)}}{x_{u_l}^{(n)}\omega_{u_l}^{(n)}}\right)\\
&+\sum_{n=1}^{N}\mu_n\left(\sum_{u_l\in\mathcal{U}_l}x_{u_l}^{(n)}-1\right)+\sum_{u_l\in\mathcal{U}_l}\rho_{u_l}\left(\sum_{n=1}^{N}S_{u_l,l}^{(n)}-P_{u_l}^{max}\right)\\
&+\nu_l\left(\sum_{u_l\in\mathcal{U}_l}\sum_{n=1}^{N}\tfrac{h_{u_l,l,1}^{(n)}}{h_{l,u_l,2}^{(n)}}S_{u_l,l}^{(n)}-P_l^{max}\right)\\
&+\sum_{n=1}^{N}\psi_n\left(\sum_{u_l\in\mathcal{U}_l}S_{u_l,l}^{(n)}g_{u_l^*,l,1}^{(n)}\ -I_{th,1}^{(n)}\right)\\
&+\sum_{n=1}^{N}\varphi_n\left(\sum_{u_l\in\mathcal{U}_l}\tfrac{h_{u_l,l,1}^{(n)}}{h_{l,u_l,2}^{(n)}}S_{u_l,l}^{(n)}g_{l,u_l^*,2}^{(n)}-I_{th,2}^{(n)}\right)\\
&+\sum_{u_l\in\mathcal{U}_l}\lambda_{u_l}\left(Q_{u_l}-\sum_{n=1}^{N}\tfrac{1}{2}x_{u_l}^{(n)}B_{RB}\log_2\left(1+\tfrac{S_{u_l,l}^{(n)}h_{u_l,l,1}^{(n)}}{x_{u_l}^{(n)}\omega_{u_l}^{(n)}}\right)\right)\\
&+\sum_{u_l\in\mathcal{U}_l}\sum_{n=1}^{N}\varrho_{u_l}^{n}\left(I_{u_l,l}^{(n)}+\sigma^2-\omega_{u_l}^{(n)}\right). \qquad \text{(C.1)}\end{aligned}$$

where $\boldsymbol{\lambda}$ is the vector of Lagrange multipliers associated with individual QoS requirements for cellular and D2D UEs. Similarly, $\boldsymbol{\mu}, \boldsymbol{\rho}, \nu_l, \boldsymbol{\psi}, \boldsymbol{\varphi}$ are the Lagrange multipliers for the constraints in (4.6a)–(4.6e). Differentiating (C.1) with respect to $S_{u_l,l}^{(n)}$, I obtain (4.7) for power allocation for the link u_l over RB n. Similarly, differentiating (C.1) with respect to $x_{u_l}^{(n)}$ gives the condition for RB allocation.

C.2 Proof of Proposition 4.1

The uncertainty constraints in (4.6d), (4.6e), and (4.6h) are satisfied if and only if

$$\max_{\mathbf{g}_{l,1}^{(n)} \in \Re_{g_{l,1}}^{(n)}} \sum_{u_l \in \mathcal{U}_l} S_{u_l,l}^{(n)} g_{u_l^*,l,1}^{(n)} \leq I_{th,1}^{(n)}, \quad \forall n$$

$$\max_{\mathbf{g}_{l,2}^{(n)} \in \Re_{g_{l,2}}^{(n)}} \sum_{u_l \in \mathcal{U}_l} \frac{h_{u_l,l,1}^{(n)}}{h_{l,u_l,2}^{(n)}} S_{u_l,l}^{(n)} g_{l,u_l^*,2}^{(n)} \leq I_{th,2}^{(n)}, \quad \forall n$$

$$\max_{I_{u_l,l}^{(n)} \in \Re_{I_{u_l,l}}^{(n)}} I_{u_l,l}^{(n)} + \sigma^2 \leq \omega_{u_l}^{(n)}, \quad \forall n, u_l$$

which is equivalent to

$$\sum_{u_l \in \mathcal{U}_l} S_{u_l,l}^{(n)} \bar{g}_{u_l^*,l,1}^{(n)} + \max_{\mathbf{g}_{l,1}^{(n)} \in \Re_{g_{l,1}}^{(n)}} \sum_{u_l \in \mathcal{U}_l} S_{u_l,l}^{(n)} \left(g_{u_l^*,l,1}^{(n)} - \bar{g}_{u_l^*,l,1}^{(n)} \right) \leq I_{th,1}^{(n)}, \ \forall n$$

$$\sum_{u_l \in \mathcal{U}_l} \frac{h_{u_l,l,1}^{(n)}}{h_{l,u_l,2}^{(n)}} S_{u_l,l}^{(n)} \bar{g}_{l,u_l^*,2}^{(n)} + \max_{\mathbf{g}_{l,2}^{(n)} \in \Re_{g_{l,2}}^{(n)}} \sum_{u_l \in \mathcal{U}_l} \frac{h_{u_l,l,1}^{(n)}}{h_{l,u_l,2}^{(n)}} S_{u_l,l}^{(n)} \left(g_{l,u_l^*,2}^{(n)} - \bar{g}_{l,u_l^*,2}^{(n)} \right) \leq I_{th,2}^{(n)}, \ \forall n$$

$$\bar{I}_{u_l,l}^{(n)} + \max_{I_{u_l,l}^{(n)} \in \Re_{I_{u_l,l}^{(n)}}} \left(I_{u_l,l}^{(n)} - \bar{I}_{u_l,l}^{(n)} \right) + \sigma^2 \leq \omega_{u_l}^{(n)}, \ \forall n, u_l.$$

Since the max function over a convex set is a convex function (Section 3.2.4 in [34]), convexity of the problem **P4.2** is conserved.

C.3 Proof of Proposition 4.2

Using the expression $\mathbf{w}_{l,1}^{(n)} = \frac{\mathbf{M}_{g_{l,1}}^{(n)} \cdot \left(\bar{\mathbf{g}}_{l,1}^{(n)} - \mathbf{g}_{l,1}^{(n)}\right)^{\mathsf{T}}}{\Psi_{l,1}^{(n)}}$, the uncertainty set (4.11a) becomes

$$\Re_{g_l,1}^{(n)} = \left\{ \mathbf{w}_{l,1}^{(n)} | \parallel \bar{\mathbf{w}}_{l,1}^{(n)} - \mathbf{w}_{l,1}^{(n)} \parallel \leq 1 \right\}, \quad \forall n. \tag{C.2}$$

Besides, the protection function (4.13a) can be rewritten as

$$\begin{aligned} &\max_{\mathbf{g}_{l,1}^{(n)} \in \Re_{g_{l,1}}^{(n)}} \sum_{u_l \in \mathcal{U}_l} S_{u_l,l}^{(n)} \left(g_{u_l^*,l,1}^{(n)} - \bar{g}_{u_l^*,l,1}^{(n)} \right) \\ &= \max_{\mathbf{g}_{l,1}^{(n)} \in \Re_{g_{l,1}}^{(n)}} \mathbf{S}_{l,1}^{(n)} \cdot \left(\mathbf{g}_{l,1}^{(n)} - \bar{\mathbf{g}}_{l,1}^{(n)} \right)^{\mathsf{T}} \\ &= \max_{\mathbf{g}_{l,1}^{(n)} \in \Re_{g_{l,1}}^{(n)}} \mathbf{S}_{l,1}^{(n)} \cdot \left(\mathbf{M}_{g_{l,1}}^{(n)\,-1} \cdot \mathbf{w}_{l,1}^{(n)} \right). \end{aligned} \tag{C.3}$$

Note that, given a norm $\parallel \mathbf{y} \parallel$ for a vector $\mathbf{y}$, its dual norm induced over the dual space of linear functionals $\mathbf{z}$ is $\parallel \mathbf{z} \parallel^* = \max_{\|\mathbf{y}\| \leq 1} \mathbf{z}^{\mathsf{T}}\mathbf{y}$ [54]. Since the protection function in (C.3) is the dual norm of uncertainty region in (4.11a), the proof follows. The protection functions for the uncertainity sets in (4.11b) and (4.12) are obtained in a similar way.

C.4 Power and RB Allocation for Robust Problem

To obtain a more tractable formula, for any vector $\mathbf{y}$ I use the inequality $\parallel \mathbf{y} \parallel_2 \leq \parallel \mathbf{y} \parallel_1$ and rewrite the constraints (4.16d) and (4.16e), respectively as follows

$$\sum_{u_l \in \mathcal{U}_l} S_{u_l,l}^{(n)} \bar{g}_{u_l^*,l,1}^{(n)} + \Psi_{l,1}^{(n)} \sum_{u_l \in \mathcal{U}_l} m_{u_l u_{l g_{l,1}}}^{(n)} S_{u_l,l}^{(n)} \leq I_{th,1}^{(n)}, \quad \forall n \tag{C.4a}$$

$$\sum_{u_l \in \mathcal{U}_l} \frac{h_{u_l,l,1}^{(n)}}{h_{l,u_l,2}^{(n)}} S_{u_l,l}^{(n)} \bar{g}_{l,u_l^*,2}^{(n)} + \Psi_{l,2}^{(n)} \sum_{u_l \in \mathcal{U}_l} m_{u_l u_{l g_{l,2}}}^{(n)} \frac{h_{u_l,l,1}^{(n)}}{h_{l,u_l,2}^{(n)}} S_{u_l,l}^{(n)} \leq I_{th,2}^{(n)}, \quad \forall n \tag{C.4b}$$

$$
\begin{aligned}
&\mathbb{L}_{\Delta l}(\mathbf{x},\mathbf{S},\boldsymbol{\omega\mu},\boldsymbol{\rho},\nu_l,\boldsymbol{\psi},\boldsymbol{\varphi},\boldsymbol{\lambda},\boldsymbol{\varrho}) = \\
&\quad - \sum_{u_l\in\mathcal{U}_l}\sum_{n=1}^{N} \tfrac{1}{2} x_{u_l}^{(n)} B_{RB}\log_2\left(1+\tfrac{S_{u_l,l}^{(n)} h_{u_l,l,1}^{(n)}}{x_{u_l}^{(n)}\omega_{u_l}^{(n)}}\right) + \sum_{n=1}^{N}\mu_n\left(\sum_{u_l\in\mathcal{U}_l} x_{u_l}^{(n)} - 1\right) \\
&\quad + \sum_{u_l\in\mathcal{U}_l}\rho_{u_l}\left(\sum_{n=1}^{N} S_{u_l,l}^{(n)} - P_{u_l}^{max}\right) + \nu_l\left(\sum_{u_l\in\mathcal{U}_l}\sum_{n=1}^{N}\tfrac{h_{u_l,l,1}^{(n)}}{h_{l,u_l,2}^{(n)}} S_{u_l,l}^{(n)} - P_l^{max}\right) \\
&\quad + \sum_{n=1}^{N}\psi_n\left(\sum_{u_l\in\mathcal{U}_l} S_{u_l,l}^{(n)}\bar{g}_{u_l^*,l,1}^{(n)} + \Psi_{l,1}^{(n)}\sum_{u_l=1}^{|\mathcal{U}_l|}\left(m_{u_l u_{l_{g_{l,1}}}}^{(n)} S_{u_l,l}^{(n)}\right) - I_{th,1}^{(n)}\right) \\
&\quad + \sum_{n=1}^{N}\varphi_n\left(\sum_{u_l\in\mathcal{U}_l}\tfrac{h_{u_l,l,1}^{(n)}}{h_{l,u_l,2}^{(n)}} S_{u_l,l}^{(n)}\bar{g}_{l,u_l^*,2}^{(n)} + \Psi_{l,2}^{(n)}\sum_{u_l=1}^{|\mathcal{U}_l|}\left(m_{u_l u_{l_{g_{l,2}}}}^{(n)}\tfrac{h_{u_l,l,1}^{(n)}}{h_{l,u_l,2}^{(n)}} S_{u_l,l}^{(n)}\right) - I_{th,2}^{(n)}\right) \\
&\quad + \sum_{u_l\in\mathcal{U}_l}\lambda_{u_l}\left(Q_{u_l} - \sum_{n=1}^{N}\tfrac{1}{2} x_{u_l}^{(n)} B_{RB}\log_2\left(1+\tfrac{S_{u_l,l}^{(n)}\gamma_{u_l,l,1}^{(n)}}{x_{u_l}^{(n)}\omega_{u_l}^{(n)}}\right)\right) \\
&\quad + \sum_{u_l\in\mathcal{U}_l}\sum_{n=1}^{N}\varrho_{u_l}^{n}\left(\bar{I}_{u_l,l}^{(n)} + \Delta_{I_{u_l,l}}^{(n)} + \sigma^2 - \omega_{u_l}^{(n)}\right). \qquad \text{(C.5)}
\end{aligned}
$$

where for any diagonal matrix $\mathbf{A}$, m_{jj} represents the j-th element of $\mathbf{A}^{-1}(j,:)$. Considering the convexity of **P4.4**, the Lagrange dual function can be obtained by (C.5) in which $\boldsymbol{\mu},\boldsymbol{\rho},\nu_l,\boldsymbol{\psi},\boldsymbol{\varphi},\boldsymbol{\lambda},\boldsymbol{\varrho}$ are the corresponding Lagrange multipliers. Differentiating (C.5) with respect to $S_{u_l,l}^{(n)}$ and $x_{u_l}^{(n)}$ gives (4.17) and (4.8) for power and RB allocation, respectively.

C.5 Update of Variables and Lagrange Multipliers

After finding the optimal solution, i.e., $P_{u_l,l}^{(n)^*}$ and $x_{u_l}^{(n)^*}$, the primal and dual variables at the $(t+1)$-th iteration are updated using (C.7a)–(C.7h), where $\Lambda_\kappa^{(t)}$ is the small step size for variable κ at iteration t and the partial derivative of the Lagrange dual

$$\omega_{u_l}^{(n)}(t+1) = \left[\omega_{u_l}^{(n)}(t) - \Lambda_{\omega_{u_l}^{(n)}}^{(t)} \frac{\partial \mathbb{L}_{\boldsymbol{l}}}{\partial \omega_{u_l}^{(n)}}\bigg|_t\right]^+ \tag{C.7a}$$

$$\mu_n(t+1) = \left[\mu_n(t) + \Lambda_{\mu_n}^{(t)} \left(\sum_{u_l \in \mathcal{U}_l} x_{u_l}^{(n)} - 1\right)\right]^+ \tag{C.7b}$$

$$\rho_{u_l}(t+1) = \left[\rho_{u_l}(t) + \Lambda_{\rho_{u_l}}^{(t)} \left(\sum_{n=1}^{N} S_{u_l,l}^{(n)} - P_{u_l}^{max}\right)\right]^+ \tag{C.7c}$$

$$\nu_l(t+1) = \left[\nu_l(t) + \Lambda_{\nu_l}^{(t)} \left(\sum_{u_l \in \mathcal{U}_l} \sum_{n=1}^{N} \frac{h_{u_l,l,1}^{(n)}}{h_{l,u_l,2}^{(n)}} S_{u_l,l}^{(n)} - P_l^{max}\right)\right]^+ \tag{C.7d}$$

$$\psi_n(t+1) = \left[\psi_n(t) + \Lambda_{\psi_n}^{(t)} \left(\sum_{u_l \in \mathcal{U}_l} S_{u_l,l}^{(n)} \bar{g}_{u_l^*,l,1}^{(n)} + \Psi_{l,1}^{(n)} \sum_{u_l=1}^{|\mathcal{U}_l|} \left(m_{u_l u_{l g_{l,1}}}^{(n)} S_{u_l,l}^{(n)}\right) - I_{th,1}^{(n)}\right)\right]^+ \tag{C.7e}$$

$$\varphi_n(t+1) = \left[\varphi_n(t) + \Lambda_{\varphi_n}^{(t)} \left(\sum_{u_l \in \mathcal{U}_l} \frac{h_{u_l,l,1}^{(n)}}{h_{l,u_l,2}^{(n)}} S_{u_l,l}^{(n)} \bar{g}_{l,u_l^*,2}^{(n)} + \Psi_{l,2}^{(n)} \sum_{u_l=1}^{|\mathcal{U}_l|} \left(m_{u_l u_{l g_{l,2}}}^{(n)} \frac{h_{u_l,l,1}^{(n)}}{h_{l,u_l,2}^{(n)}} S_{u_l,l}^{(n)}\right) - I_{th,2}^{(n)}\right)\right]^+ \tag{C.7f}$$

$$\lambda_{u_l}(t+1) = \left[\lambda_{u_l}(t) + \Lambda_{\lambda_{u_l}}^{(t)} \left(Q_{u_l} - \sum_{n=1}^{N} \tfrac{1}{2} x_{u_l}^{(n)} B_{RB} \log_2\left(1 + \frac{S_{u_l,l}^{(n)} \gamma_{u_l,l,1}^{(n)}}{x_{u_l}^{(n)} \omega_{u_l}^{(n)}}\right)\right)\right]^+ \tag{C.7g}$$

$$\varrho_{u_l}^n(t+1) = \left[\varrho_{u_l}^n(t) + \Lambda_{\varrho_{u_l}^n}^{(t)} \left(\bar{I}_{u_l,l}^{(n)} + \Delta_{I_{u_l,l}}^{(n)} + \sigma^2 - \omega_{u_l}^{(n)}\right)\right]^+. \tag{C.7h}$$

function with respect to $\omega_{u_l}^{(n)}$ is

$$\frac{\partial \mathbb{L}_{\Delta l}}{\partial \omega_{u_l}^{(n)}} = \tfrac{1}{2} B_{RB} \frac{(\lambda_{u_l} + 1)\, x_{u_l}^{(n)} S_{u_l,l}^{(n)} h_{u_l,l,1}^{(n)}}{\omega_{u_l}^{(n)} \left(x_{u_l}^{(n)} \omega_{u_l}^{(n)} + S_{u_l,l}^{(n)} h_{u_l,l,1}^{(n)}\right) \ln 2} - \varrho_{u_l}^n. \tag{C.6}$$

C.6 Proof of Proposition 4.3

It is easy to verify that the computational complexity at each iteration of variable updating in (C.7a)–(C.7h) is polynomial in $|\mathcal{U}_l|$ and N. There are $|\mathcal{U}_l|N$ computations

$$\mathcal{R}^*(\mathbf{a},\mathbf{b},\mathbf{c}) = \inf\Bigg\{ \max_{x_{u_l}^{(n)},S_{u_l,l}^{(n)},\omega_{u_l}^{(n)}} \sum_{u_l\in\mathcal{U}_l}\sum_{n=1}^{N} \frac{1}{2}x_{u_l}^{(n)} B_{RB}\log_2\left(1+\frac{S_{u_l,l}^{(n)}h_{u_l,l,1}^{(n)}}{x_{u_l}^{(n)}\omega_{u_l}^{(n)}}\right)\Bigg|,$$

$$\sum_{u_l\in\mathcal{U}_l} x_{u_l}^{(n)} \le 1, \quad \sum_{n=1}^{N} S_{u_l,l}^{(n)} \le P_{u_l}^{max}, \quad \sum_{u_l\in\mathcal{U}_l}\sum_{n=1}^{N} \frac{h_{u_l,l,1}^{(n)}}{h_{l,u_l,2}^{(n)}} S_{u_l,l}^{(n)} \le P_l^{max},$$

$$\sum_{u_l\in\mathcal{U}_l} S_{u_l,l}^{(n)}\bar{g}_{u_l^*,l,1}^{(n)} + \Delta_{g_{l,1}}^{(n)} \le I_{th,1}^{(n)}, \quad \sum_{u_l\in\mathcal{U}_l} \frac{h_{u_l,l,1}^{(n)}}{h_{l,u_l,2}^{(n)}} S_{u_l,l}^{(n)}\bar{g}_{l,u_l^*,2}^{(n)} + \Delta_{g_{l,2}}^{(n)} \le I_{th,2}^{(n)},$$

$$\sum_{n=1}^{N} \frac{1}{2}x_{u_l}^{(n)} B_{RB}\log_2\left(1+\frac{S_{u_l,l}^{(n)}h_{u_l,l,1}^{(n)}}{x_{u_l}^{(n)}\omega_{u_l}^{(n)}}\right) \ge Q_{u_l}, \quad S_{u_l,l}^{(n)} \ge 0, \quad \bar{I}_{u_l,l}^{(n)} + \Delta_{I_{u_l,l}}^{(n)} + \sigma^2 \le \omega_{u_l}^{(n)}\Bigg\} \tag{C.8}$$

which are required to obtain the reference gains and if T iterations are required for convergence, the overall complexity of the algorithm is $\mathcal{O}\left(|\mathcal{U}_l|N + T|\mathcal{U}_l|N\right)$.

For any Lagrange multiplier κ, if I choose $\kappa(0)$ in the interval $[0, \kappa_{max}]$, the distance between $\kappa(0)$ and κ^* is upper bounded by κ_{max}. Then it can be shown that at iteration t, the distance between the current best objective and the optimum objective is upper bounded by $\frac{\kappa_{max}^2+\kappa(t)^2\sum_{i=i}^{t}{\Lambda_\kappa^{(i)}}^2}{2\sum_{i=i}^{t}\Lambda_\kappa^{(i)}}$. If I take the step size $\Lambda_\kappa^{(i)} = \frac{a}{\sqrt{i}}$, where a is a small constant, there are $\mathcal{O}\left(\frac{1}{\varepsilon^2}\right)$ iterations required for convergence to have the bound less than ε [87]. Hence, the complexity of the proposed algorithm is $\mathcal{O}\left(\left(1+\frac{1}{\varepsilon^2}\right)|\mathcal{U}_l|N\right)$.

C.7 Proof of Proposition 4.4

Since **P4.3** is a perturbed version of **P4.1** with protection functions in the constraints (4.6d), (4.6e), and (4.6h), to obtain (4.19), I use local sensitivity analysis of **P4.3** by perturbing its constraints [88, Chapter IV], [34, Section 5.6]. Let the elements of $\mathbf{a},\mathbf{b},\mathbf{c}$ contain $\Delta_{g_{l,1}}^{(n)}, \Delta_{g_{l,2}}^{(n)}$ $\forall n$, and $\Delta_{I_{u_l,l}}^{(n)}$ $\forall u_l, n$, where $\mathcal{R}^*(\mathbf{a},\mathbf{b},\mathbf{c})$ is given by (C.8).

When $\Delta_{g_{l,1}}^{(n)}, \Delta_{g_{l,2}}^{(n)}$, and $\Delta_{I_{u_l,l}}^{(n)}$ are small, $\mathcal{R}^*(\mathbf{a},\mathbf{b},\mathbf{c})$ is differentiable with respect to the perturbation vectors $\mathbf{a},\mathbf{b}$, and $\mathbf{c}$ [88, Chapter IV]. Using Taylor series, (C.8) can be written as

$$\mathcal{R}^*(\mathbf{a},\mathbf{b},\mathbf{c}) = \mathcal{R}^*(\mathbf{0},\mathbf{0},\mathbf{0}) + \sum_{n=1}^{N} a_n \frac{\partial \mathcal{R}^*(\mathbf{0},\mathbf{b},\mathbf{c})}{\partial a_n} + \sum_{n=1}^{N} b_n \frac{\partial \mathcal{R}^*(\mathbf{a},\mathbf{0},\mathbf{c})}{\partial b_n} + \sum_{u_l \in \mathcal{U}_l} \sum_{n=1}^{N} c_{u_l}^n \frac{\partial \mathcal{R}^*(\mathbf{a},\mathbf{b},\mathbf{c})}{\partial c_{u_l}^n} + o \tag{C.9}$$

where $\mathcal{R}^*(\mathbf{0},\mathbf{0},\mathbf{0})$ is the optimal value for **P4.1**, $\mathbf{0}$ is the zero vector, and o is the truncation error in the Taylor series expansion. Note that $\mathcal{R}^*(\mathbf{0},\mathbf{0},\mathbf{0})$ and $\mathcal{R}^*(\mathbf{a},\mathbf{b},\mathbf{c})$ are equal to R^* and R_Δ^*, respectively. Since **P4.1** is convex, $\mathcal{R}^*(\mathbf{a},\mathbf{b},\mathbf{c})$ is obtained from the Lagrange dual function [i.e., (C.1)] of **P4.1**; and using the sensitivity analysis (Chapter IV in [88]), I have $\frac{\partial \mathcal{R}^*(\mathbf{0},\mathbf{b},\mathbf{c})}{\partial a_n} \approx -\psi_n^*$, $\frac{\partial \mathcal{R}^*(\mathbf{a},\mathbf{0},\mathbf{c})}{\partial b_n} \approx -\varphi_n^*$ and $\frac{\partial \mathcal{R}^*(\mathbf{a},\mathbf{b},\mathbf{0})}{\partial c_{u_l}^n} \approx -\varrho_{u_l}^{n*}$. Rearranging (C.9) I obtain

$$R_\Delta^* - R^* \approx -\sum_{n=1}^{N} \psi_n^* \Delta_{g_{l,1}}^{(n)} - \sum_{n=1}^{N} \varphi_n^* \Delta_{g_{l,2}}^{(n)} - \sum_{u_l \in \mathcal{U}_l} \sum_{n=1}^{N} \varrho_{u_l}^{n*} \Delta_{I_{u_l,l}}^{(n)}. \tag{C.10}$$

Since $\psi_n^*, \varphi_n^*, \varrho_{u_l}^{n*}$ are non-negative Lagrange multipliers, the achievable sum-rate is reduced compared to the case in which perfect channel information is available.

C.8 Parameters used for Approximations in the Chance Constraint Approach

In order to balance the robustness and optimality, the parameters used for safe approximations of the chance constraints (obtained from [49]) are given in Table C.1.

Table C.1: Values of $\eta^{+}_{\mathcal{P}_j}$ and $\tau_{\mathcal{P}_j}$ for Typical Families of Probability Distribution $\mathcal{P}_j$

$\mathcal{P}_j$	$\eta^{+}_{\mathcal{P}_j}$	$\tau_{\mathcal{P}_j}$
$\sup\{\mathcal{P}_j\} \in [-1,+1]$	1	0
$\sup\{\mathcal{P}_j\}$ is unimodal and $\sup\{\mathcal{P}_j\} \in [-1,+1]$	$\frac{1}{2}$	$\frac{1}{\sqrt{12}}$
$\sup\{\mathcal{P}_j\}$ is unimodal and symmetric	0	$\frac{1}{\sqrt{3}}$

Appendix D

D.1 Proof of Proposition 5.2

Note that any arbitrary matching is not necessarily stable. In the following, I show that for any given preference profiles, each iteration of **Algorithm 5** ends up with a stable matching (i.e., there is no blocking pair). I prove the proposition by contradiction. Let μ_l be a matching obtained by **Algorithm 4** at any step t of **Algorithm 5**. Let me assume that RB n is not allocated to UE u_l, but it has a higher order in the preference list. According to this assumption, the (u_l, n) pair will block μ_l.

Since the position of u_l in the preference profile of n is higher compared to the user $\hat{u}_l$ that is matched by μ_l, i.e., $u_l \succeq \mu_l(n)$, RB n must select u_l before the algorithm terminates. However, the pair (u_l, n) does not match each other in the matching outcome μ_l. This implies that u_l rejects n (e.g., line 7 in **Algorithm 4**) and $(\hat{u}_l, n)$ is a better assignment. As a result, the pair (u_l, n) will not block μ_l, which contradicts my assumption. Consequently, the matching outcome μ_l leads to a stable matching since no blocking pair exists and the proof concludes.

D.2 Proof of Proposition 5.3

The proof is followed by the induction of number of users U_l, that are supported by relay l. For instance, let $\kappa_{u_l} = 1,\ \forall u_l \in \mathcal{U}_l$ (the proof for $\kappa_{u_l} > 1$ can be done analogously introducing dummy rows [i.e., UEs] in the utility matrix). The basis (i.e., $U_l = 1$) is trivial, since the only user definitely gets the best RBs according to her preference. When $U_l \geq 2$, let me consider $R_i^{(j)}$ to be the maximal entity of the utility matrix $\mathfrak{U}_l$. For instance, let the matrix $\widehat{\mathfrak{U}}_l$ be obtained by removing the i-th row and j-th column from the utility matrix $\mathfrak{U}_l$. If μ_l is a stable matching for $\mathfrak{U}_l$, then by definition $\mu_l(i) = j$ and hence $\mu_l \setminus \{(i,j)\}$ must be a stable matching for $\widehat{\mathfrak{U}}_l$. By induction, there exists a unique stable matching $\widehat{\mu}_l$ for the smaller matrix $\widehat{\mathfrak{U}}_l$. Therefore, the proof is concluded due to the fact that $\mu_l = \widehat{\mu}_l \cup \{(i,j)\}$ is the unique stable matching for the utility matrix $\mathfrak{U}_l$.

D.3 Proof of Proposition 5.4

Without loss of generality, let $\mathfrak{R}_{u_l,l}(\mu_l)$ denote the data rate achieved by UE u_l for any matching μ_l for given uncertainty bounds and $\mathfrak{R}_l(\mu_l) = \sum_{u_l \in \mathcal{U}_l} \mathfrak{R}_{u_l,l}(\mu_l)$ is the sum-rate of all UEs. On the contrary, let $\widehat{\mu}_l$ denote an arbitrary unstable outcome better than μ_l, i.e., $\widehat{\mu}_l$ can achieve a better sum-rate. There are two cases that make $\widehat{\mu}_l$ unstable: *1*) lack of individual rationality, and/or *2*) blocked by a UE-RB pair [61]. I analyze both the cases below.

Case 1 (lack of individual rationality): If RB n is not individually rational, then the utility of n can be improved by removing user $\widehat{\mu}_l(n)$ with any arbitrarily user $u_l = \mu_l(n)$. Hence, the utility of u_l increases and $\mathfrak{R}_{u_l,l}(\widehat{\mu}_l) < \mathfrak{R}_{u_l,l}(\mu_l)$.

Case 2 ($\widehat{\mu}_l$ is blocked): When $\widehat{\mu}_l$ is blocked by any UE-RB pair (u_l, n), RB n

strictly prefers UE u_l to $\widehat{\mu}_l(n)$ and one of the following conditions must be true:

(i) u_l strictly prefers n to some $\hat{n} \in \widehat{\mu}_l(u_l)$, or

(ii) $\overline{\overline{\widehat{\mu}_l(u_l)}} < \kappa_{u_l}$ and n is acceptable to u_l.

If condition *(i)* is true, I can obtain a stable matching μ_l by interchanging n and $\hat{n}$ for u_l as follows:

$$\mu_l(u_l) = \{\widehat{\mu}_l(u_l) \setminus \hat{n}\} \cup n. \tag{D.1}$$

Hence, the new data rate of UE u_l is

$$\begin{aligned}\mathfrak{R}_{u_l,l}(\mu_l) &= \sum_{j \in \mu_l(u_l)} R_{u_l}^{(j)} = R_{u_l}^{(n)} + \sum_{\substack{j \in \mu_l(u_l),\\ j \neq n}} R_{u_l}^{(j)} \\ &> R_{u_l}^{(\hat{n})} + \sum_{\substack{j \in \widehat{\mu}_l(u_l),\\ j \neq n}} R_{u_l}^{(j)} = \sum_{j \in \widehat{\mu}_l(u_l)} R_{u_l}^{(j)} = \mathfrak{R}_{u_l,l}(\widehat{\mu}_l)\end{aligned} \tag{D.2}$$

where $R_{u_l}^{(n)}$ is given by (5.24). Since u_l strictly prefers RB n to $\hat{n}$ and the data rates for other UEs remain unchanged, for condition *(i)*, it can be shown that $\mathfrak{R}_l(\mu_l) \geq \mathfrak{R}_l(\widehat{\mu}_l)$.

When condition *(ii)* is true,

$$\begin{aligned}\mathfrak{R}_{u_l,l}(\mu_l) &= \sum_{j \in \widehat{\mu}_l(u_l)} R_{u_l}^{(j)} + R_{u_l}^{(n)} \\ &> \sum_{j \in \widehat{\mu}_l(u_l)} R_{u_l}^{(j)} = \mathfrak{R}_{u_l,l}(\widehat{\mu}_l).\end{aligned} \tag{D.3}$$

Let $\hat{u}_l = \widehat{\mu}_l(n)$ with data rate $R_{\hat{u}_l}^{(n)}$. Then

$$\begin{aligned}\mathfrak{R}_{\hat{u}_l,l}(\mu_l) &= \sum_{j \in \widehat{\mu}_l(\hat{u}_l)} R_{\hat{u}_l}^{(j)} - R_{\hat{u}_l}^{(n)} \\ &< \sum_{j \in \widehat{\mu}_l(\hat{u}_l)} R_{\hat{u}_l}^{(j)} = \mathfrak{R}_{\hat{u}_l,l}(\widehat{\mu}_l).\end{aligned} \tag{D.4}$$

From (D.3) and (D.4), neither $\mathfrak{R}_l(\mu_l) > \mathfrak{R}_l(\widehat{\mu}_l)$ nor $\mathfrak{R}_l(\widehat{\mu}_l) > \mathfrak{R}_l(\mu_l)$. Since for both cases *1*) and *2*) there is no outcome $\widehat{\mu}_l$ better than μ_l, by **Definition 5.6**, μ_l is an optimal allocation and the proof follows.